DESIGNING AGRIVOLTAIC SYSTEMS TO OPTIMIZE CROP PRODUCTIVITY AND ENERGY GENERATION

SIM YANG HONG

UNIVERSITI TUNKU ABDUL RAHMAN

DESIGNING AGRIVOLTAIC SYSTEMS TO OPTIMIZE CROP PRODUCTIVITY AND ENERGY GENERATION

SIM YANG HONG

A project report submitted in partial fulfilment of the requirements for the award of Bachelor of Mechanical Engineering with Honours

Lee Kong Chian Faculty of Engineering and Science
Universiti Tunku Abdul Rahman

September 2025

DECLARATION

I hereby declare that this project report is based on my original work except for citations and quotations which have been duly acknowledged. I also declare that it has not been previously and concurrently submitted for any other degree or award at UTAR or other institutions.

Name : Sim Yang Hong

ID No. : 2002468

Date : 15 September 2025

COPYRIGHT STATEMENT

This final year project report is submitted in partial fulfilment of the requirements for the degree of Mechanical Engineering at Universiti Tunku Abdul Rahman (UTAR). This final year project report represents the work of the author, except where due acknowledgement has been made in the text. No part of this final year project report may be reproduced, stored, or transmitted in any form or by any means, whether electronic, mechanical, photocopying, recording, or otherwise, without the prior written permission of the author or UTAR, in accordance with UTAR's Intellectual Property Policy.

ACKNOWLEDGEMENTS

I would like to express my gratitude to Assistant Professor Ir Dr. Ting Chen Hunt as my research supervisor for his invaluable advice, guidance and enormous patience throughout the development of the research.

I would also like to thank the faculty and the departmental members from Lee Kong Chian Faculty of Engineering and Science and Department of Mechanical and Materials Engineering, for creating a pleasant working environment throughout my years in UTAR.

Besides, I am grateful for the owner of Hami EcoFarms, Mr Aw for allowing his farms to become subject of this research. Apart from that, he also provided constructive feedback and suggestions to resolve the issues encountered.

Lastly, to my dearest families and friends for their help, friendship, and support throughout the research which has been instrumental to the success of this research project.

ABSTRACT

Agrivoltaics integrates agricultural production with photovoltaic (PV) energy generation, offering a potential solution to the increasing competition for land between food and energy sectors. This study focuses on the design and optimisation of an agrivoltaic system to maximise both crop yield and solar power generation. The implementation of PV panels, however, introduces shading effects that can alter crop's growth performance. To address this, different PV layouts were designed and evaluated through PVsyst simulations and controlled experimental trials. Crop growth performance under varying shading levels was assessed alongside energy yields to determine the most efficient system configuration. Results indicate that a tilt angle of 15° is optimal for Malaysian conditions, as it minimises thermal losses while balancing energy output and crop productivity. A full-density solar configuration achieved the highest annual electricity generation (702.93 MWh) but significantly reduced crop growth performance. Conversely, a half-density solar configuration provided more favourable growing conditions, with partially shaded crops recording the highest growth performance index (0.60), followed by open-field crops (0.50) and heavily shaded crops (0.19) by recorded the variables such as number of fruits, average fruit diameter, height and number of new leaves per week and conducted Multi Criteria Analysis. The integration scenario combining half-density PV arrays with partially shaded crops produced the highest Land Equivalent Ratio (LER) of 1.64, highlighting superior land-use efficiency compared to full-density arrays (LER = 1.38). For the case study of Hami EcoFarm, prioritising agricultural productivity while maintaining sustainable energy output suggests that the half-density configuration represents the most suitable implementation strategy.

Keywords: Agrivoltaic, Solar Energy, Crop, Land Equivalent Ratio, land use efficiency, PVsyst.

Subject Area: TJ807-830

TABLE OF CONTENTS

LIST OF TABLES

LIST OF FIGURES

LIST OF SYMBOLS / ABBREVIATIONS

C_p	specific heat at constant pressure, $kg^{-1}{}^{\circ}C^{-1}$
E_b	beam irradiance,W/m^2
E_d	diffuse irradiance, W/m^2
E_g	ground reflected irradiance, W/m^2
T	temperature, K
v_j	junction voltage, V
I_{ph}	photon current, eV
I_{ph}	load current, A
I_{sc}	maximum current produced by solar cell, A
I_o	solar constant, W/m^2
V_{oc}	maximum voltage of cell produced, V
P	atmospheric pressure, kPa
P_{max}	maximum power output of panel, W
$Y_{crop-apv}$	yield of crops under agrivoltaics system, kg/m^2
Y_{crop}	yield of crops under agriculture farm alone, kg/m^2
Y_{pv-apv}	yield of electricity power under agrivoltaics system, Wh/m^2
Y_{pv}	yield of electricity power under photovoltaic farm alone, Wh/m^2
β	tilt angle
ρ	Albedo coefficient
θ_z	azimuth angle
γ	psychrometric constant
λ	latent heat vaporization
ε	ratio molecular weight of water vapour or dry air
Δ	slope of saturation vapour pressure curve at air temperature
AC	alterating current
CC	green canopy cover
CDC	canopy decline coefficient

CGC	canopy growth coefficient
CGx	maximum canopy cover
DC	direct current
ETo	standard evapotrasnpiration
GCR	ground coverage ratio
GHG	green house gases
GHI	global horizontal irradiance
LER	land equipvalent ratio
MPPT	maximum power point tracking
PAR	photosynthetically active radiation
POA	plane-of-array irradiance
PV	photovoltanic
RCP	representive concentration pathway
SDG	sustainable development goals
STC	standard test condition
SWOT	strength, weakness, opputurnities and threat
THD	total harmonic distortion

LIST OF APPENDICES

CHAPTER 1

INTRODUCTION

1.1 General Introduction

Climate change, or global warming, has emerged as the paramount worldwide obstacles, with harsh climatic scenarios and rising temperatures which have been adversely affect the environment, especially in agriculture issues. The results from global warming significantly affecting agriculture through increased carbon emissions, thereby leading to potential yield decrement. Consequently, the world has shifted to exploring sustainable energy instead of utilizing fossil fuels to generate electricity. Nowadays, solar power has achieved a greater degree of maturity, which makes it ready for widespread implementation. Solar energy, being as a renewable energy which is deriving from the sunlight and converted into electricity. As a renewable energy source, solar energy has been diminished the need of fossil fuels, hence minimises greenhouse gas emissions.

Agrivoltaics technology has come into view in sustainable agriculture, combining photovoltaic panels with crop yielding. (U.S.Department of energy, n.d.). This new approach allows the generation of solar energy and crop cultivation simultaneously, which tends to be optimised land use. Strategically arranged photovoltaic panels above the crop, agrivoltaic systems could provide a shading effect that avoids the microclimate effect. Most importantly, solar energy tends to reduce the dependency of using fossil fuels and contributes to preserving the natural environment while attenuating environmental degradation. Therefore, this study aims to optimise an agrivoltaics system in a passion fruit farm. The study's direction is focused on maximising the electrical power generated by solar power and passion fruit cultivation within the farm. However, due to time constraints for this research, passion fruits has been replaced by calamansi plants as experiment models, which having similar tropical fruits's characteristics and faster growth rate which can reflect the similar growth conditions of passion fruits under photovoltaics panels.

1.2 Importance of the Study

Nowadays, land scarcity has been an issue for demanding food and clean energy. Traditional solar farms and agriculture farms are highly demanding of space. The implementation of agrivoltaic systems creates a solution by combining agriculture activities and solar energy generation on the same land. This study is dedicated to explore the optimisation of such systems which help to solve land-use conflicts without compromising energy efficiency and food security. Next, implementation of agrivoltaics helps in improving agricultural productivity, as it provides a shading effect which reduces heat stress and microclimate issues. Eventually, it helps to create more desirable conditions for plant growth.

The use of agrivoltaics systems in agricultural realm has enhanced the production of sustainable energy, thereby contributing to long term energy sustainability. Thus, it can reduce the dependence on fossil fuels and reduce green house gases (GHGs). Lastly, this study also has the potential to save costs and increase income for crop production and reduce electricity bill usage. Launching of an agrivoltaic system creates a win-win situation, enabling electricity generation while simultaneously getting crop yields.

1.3 Problem Statement

When applying the agrivoltaics system, it is necessary to consider the land use issues. Since agriculture farms and photovoltaic farms necessitate extensive land expanses to produce remarkable results. For example, if the photovoltaic portion is larger than the agricultural area, it would lead to under-yielding for passion fruits. Therefore, it is needed to provide a solution to balance the land use of agriculture and photovoltaics. In addition, the installation of the photovoltaic panels would also cause shading effects on the final yields of passion fruits, such as temperature and humidity changes. The issue here is to address whether the microclimate changes have a significant impact on the crop yield. Ultimately, economic profitability and the requirements of the farm would be the primarly considerations in deciding the necessity for the implementation of agrivoltaics.

1.4 Aim and Objectives

This research seeks to design an agrivoltaics which is simultaneously produce both agriculture and photovoltaic yields. This study also focusses on integrating a photovoltaic system with agricultural realm to balance crop and solar energy yielding. For example, the research would be based on the configuration of PV panels, the characteristics of the tropical fruits, and the optimal area usage for plantation passion fruits and PV panels. In this experiment, the tropical fruits models would be calamansi as having similar characteristic when compared with passion fruits. Eventually the purpose is to propose a sustainable solution that supports environmental conservation while also providing food security and economic income for local farmers. In addition, the objective based on the aims of this study would be:

(i) To design photovoltaics panels layout which optimize electrical power yielding

(ii) To identify the impact of photovoltaics layout that affects crop productivity

(iii) To identify best agrivoltaic configuration to maximize the Land Equivalent Ratio

(iv) To evaluate the monetary revenue for different agrivoltaics configurations

1.5 Scope and Limitation of the Study

Firstly, the project needs to identify the best photovoltaics layout to optimise the electrical power yield. Next, the project's second objective is to examine and study the growth characteristics of crops under different shading conditions. Under the research based on characteristics of passion fruits, it can be simulated and predict the yielding outcome under microclimate, which is affected by the PV panels. In addition, the last scope is needed to suggest the best agrivoltaics configuration, which optimises the Land Equivalent Ratio and fulfils the requirements of the farm.

The limitation would be the physical testing of actual yielding values, as it requires a large land area and money investment for PV panels. Therefore, this research can only be conducted on a small scale to examine the shading effects on the crops and observe their yielding conditions. In addition, the

limitation is lack of fundamental knowledge about the agricultural realm.Therefore, instead of using passion fruit as crop model, calamansi would be replace with passion fruits due to more ease of monitoring.

1.6 Contribution of the Study

This research has been focuses on maximizing land use efficiency of the agrivoltaics system. Utilizing the usage of photovoltaics modules and crop plantation within a same piece of land has been increase land use efficiency and reduce the dependence on fossil fuels. Besides, this study also provides insights into the process of developing the agrivoltaics system and results which allowing reference for future potential agrivoltaics projects. Therefore, this research support in sustainability for environment and reveals agrivoltaics design reference.

1.7 Outline of the Report

Chapter 2 would discuss the literature review of the study which consider as 3 part. The first part is photovoltaics characteristics, followed by crop growing conditions and agrivoltaics infomations. In addition, chapter 3 revelas the methodology to conduct the research. It consists of simulations approaches which categorize into photovoltaic simulations and crop yielding simulations. Besides, a small scale experiment about the affect of photovoltaic shading has also been planned to be determined. Other than that, chapter 4 presents the simulated yielding for different solar density scenario and growth performance index for crops in different shaded conditions. After that, Land Equivalent Ratio (LER) has been determined to explained the land use efficiency. Lastly, chapter 5 would conclude the findings and suggests recommendations for future work.

CHAPTER 2

LITERATURE REVIEW

2.1 Introduction

An agrivoltaic system is the combination of photovoltaics with agricultural practice which eliminates land-use conflicts and ensures food & energy security. In this chapter, the key aspects of agrivoltaics would discuss solar panel configuration, which includes optimising tilt angle, azimuth and pitch. On the other hand, there are also environmental issues affecting the photovoltaics (PV) panel, such as wind load, temperature and dust. Various PV cooling methods, panel types and purposes of inverters are also discussed in this chapter, along with the role of PVsyst software. On the agricultural side, the review highlights the impact of agrivoltaics on crop growth, explaining the characteristics of passion fruit and calamansi plants as an experiment model. Besides, this research has also been introducing AquaCrop as crop simulation software. Lastly, the economic viability and system efficiency of agrivoltaics would be mentioned in this chapter. Sustainable Development Goals and SWOT also discussed the strategic potential and challenges of implementing agrivoltaic systems.

2.2 Photovoltanic

Solar panels are the critical components in the agrivoltaics system, functioning as generators of photovoltaic power, which converts the sunlight into electrical power. In this section, the configuration of the solar panels would be discussed in terms of the method of optimising its output by studying the optimal tilt angle, azimuth angle and pitch.

Besides, the study of the temperature-raising effect and dust accumulation would also be important, as these are the factors that affect the overall output performance of the photovoltaic panels. In addition, the study of wind load effect would also enhance the rigidity of the structure support of the panel rack to avoid support failure.

In addition, according to Gross (2023), the simulation software, PVsyst, is used to evaluate the performance of PV panels in terms of total

energy output, specific energy, different losses and shading conditions. Lastly, the parameters of the solar panels and inverters are also important to investigate to fill in as the input parameters in the PVsyst software and as a reference.

2.2.1 Configuration of Solar Panel

Before installing the solar panel, it is crucial to determine its configuration. The optimisation of the solar panel depends on the amount of irradiation it receives. Therefore, addressing the placement of solar panels would affect the optimisation of power generated by the solar panels. The placement of the solar panels is related to their tilt angle, azimuth angle, and pitch. According to Rooji (n.d.), the solar panel tilt angle depends on where the user is in the world. The sun would move across the sky, and it would be in different positions depending on the time of day and the season. Ideally, the ideal angle should never be fixed and needs to follow the direction of the sun to get most of the irradiation. The tilt angle refers to the angle between the panel surface and the mounting ground.

According to Selvaraj *et al.* (2022), a photovoltaic (PV) module has been tested for its performance at different tilt angles in an experiment carried out at UM Power Energy Dedicated Advanced Center (UMPEDAC), University of Malaya, Kuala Lumpur, Malaysia. To be more specific about the exact location, it is at latitude 3.1169 N and longitude 101.6669 E. The PV module has been facing the south direction and tilted to the horizontal from 0 to 80 degrees with an increment step of 5 degrees. The result found out that when the tilt angle increases, the solar cell temperature would get lower. For example, when compared between 15 and 60 ° of tilt angle, the solar cell temperature has decreased 11.11%. Besides, the bottom surface temperature and top surface temperature had also decreased 10% and 12.5%. For the output power results, for every 5° increment in the tilt angle of PV panels, the efficiency would drop by 0.76%. The temperature coefficient of power output is related to module tilt. If the temperature increases, the power output value at an optimised tilt angle would also decrease. Based on Figure 2.1, it is shown that for outdoor performance results, it may conclude that 15° would be the

optimum tilt angle to maintain the tradeoff between the PV panel's temperature, power output and efficiency.

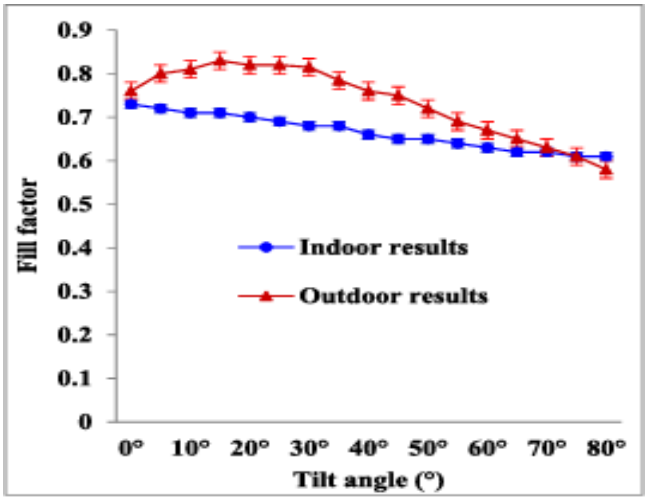

Figure 2. 1: Fill factor (efficiency) of PV panel (Selvaraj *et al*., 2022)

In addition, azimuth angle is also considered an important parameter that affects the performance of the PV panels. The azimuth angle is a horizontal angle, which is measured clockwise from the north (0 degrees). It tends to explain the direction of the object relative to an observer. (Pveducation, 2019). In addition, the numbers 90 denote the east, 180 the south, and 270 the west. According to the research by Poobalan et al. (2020), the research has been conducted at Chennai, India, with the coordinates 13.0827°N and 80.2707°E. The experiment has been tested with 8 azimuth angles to determine the respective PV panel performance. The experiment also tests various tilt angles. Based on the result in Figure 2.2, Chennai has the maximum net inverter power, which is 7700 kWh at an azimuth angle of 180° (South) and a tilt angle of 18°.

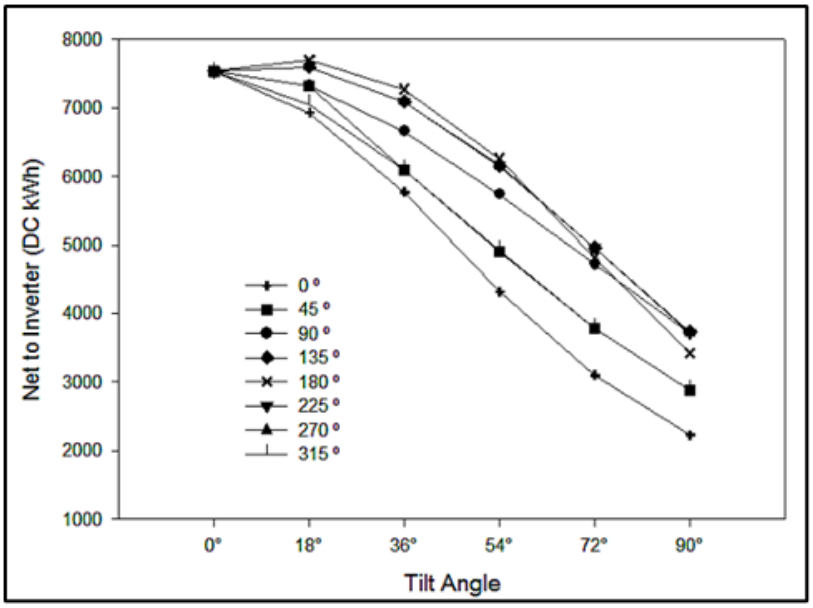

Figure 2. 2: Net to Inverter (DC kWh) versus tilt angle and azimuth angle (Poobalen *et al.*, 2020)

The ideal tilt angle is close to the result done by Selvaraj *et al*. (2022), which is around 15 to 20 from the horizontal surface. When the tilt angle is set to zero degrees, the PV panel can receive maximum irradiation and ideally would generate maximum solar power yield. However, the temperature would be the highest among other tilt angles due to all the surface of the PV panel being easily covered by sunlight. The higher temperature would lead to decreases in efficiency because more electrons have been excited and lead to recombination states. It reduced the number of free electrons to pass through the circuit, which leads to decreased voltage and power output. In addition, when the tilt angle is 0°, dust and rainwater can be easily accumulated on the surface because there is no inclined gravity acceleration. However, when the tilt angles are too high, less irradiation can be received by the solar panel due to less area covered by the sunlight. Although the temperature would be lower, the overall efficiency difference would be more than 20% when comparison between 150° tilt angle and more than a 60° tilt angle. In addition, the performance of PV panels would be optimised when set to 180° (South). This is because the sun's apparent path across the sky is a daily routine from east to west due to the earth rotating on its axis from west to east. Therefore, let the PV panels facing south optimise the receiver of irradiation during the daytime.

Lastly, pitch distance refers to the spacing between rows of solar panels as shown in Figure 2.3. When the PV modules are arranged in row per row, it is expected that the front row would cause a shading effect on the back row. Too little pitch distance would lead to more shading effect, which would reduce the receiver of irradiance from the sun to the PV panels. On the other hand, too much pitch distance would lead to land not being optimised for use. Besides, the optimal pitch distance depends on the tilt angle and size of the panels. Pitch distance also directly affects the ground coverage ratio (GCR), which is defined as the portion of ground area covered by the solar panels. GCR dedicates itself to optimising the layout of solar arrays to balance the land usage.

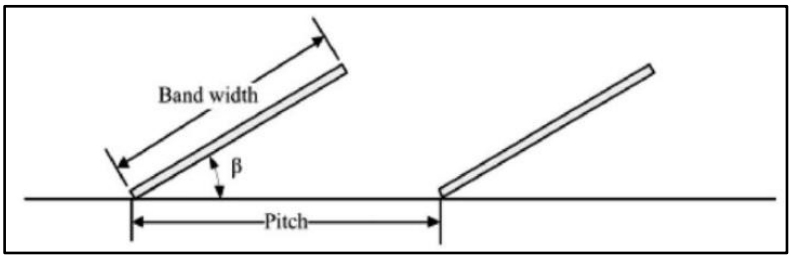

Figure 2. 3: Pitch between the PV panels

According to Alsulaiman & Mohammadi (2020), the array of PV modules has been arranged as in Figure 2.4 below, at different pitch distances with a fixed 15 degrees tilt angle. The result has been found that when the spacing arrangement is 3m, the loss is the most among other pitch distances such as 4m, 5m and 6m. Firstly, the shading effect for 3 m pitch is 9.2%, while other pitch distances are less than 2%. On the other hand, the electricity yield (MWh/year) for 3m pitch is at least 7% lower. The difference in yielding amount is mostly due to the shading effect. After 3 m of pitch distance, the yield increases due to decreasing the loss of irradiation, which is up to 2%. However, when pitch distance increases, the area of solar panels would also increase in the range of 29.03% to 83.87%.

Therefore, from the result obtained, the pitch distance should be more than 3m. However, the pitch distance should also depend on the available land area. If having enough land area, a higher pitch is preferable, as it can reduce the shading effect and increase the yield.

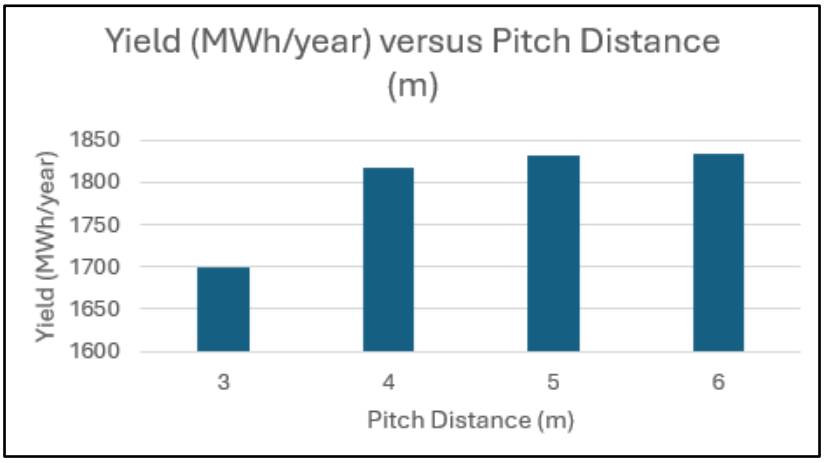

Figure 2. 4: Yield of photovoltaic power versus pitch distance

2.2.2 Wind Load

Wind load would be having a significant impact on the PV structure, as most of them are exposed to the outdoor environment. Having a wind load analysis could prevent potential damage or failure, especially for a floating PV structure. In Malaysia, typically in the site location (Ipoh), the wind speed is typically lower than in other locations. This is due to the fact that Malaysia lacks extensive open plains or large elevated areas, which limited the overall wind speeds. (Koons, 2023). Figure 2.5 shows the range of wind speed at different locations in Malaysia. As in the site location, the wind speed is lower than 2 m/s.

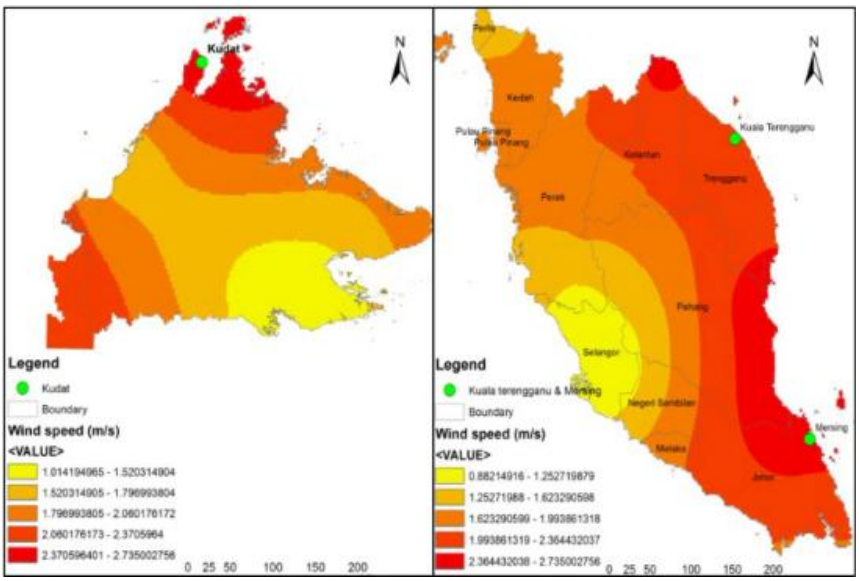

Figure 2. 5: Average wind speed in Malaysia (EnergyTrackerAsia, n.d.)

Wind direction is also considered an important parameter that needs to be investigated. Different wind directions would have an impact on different rows of the PV panels.

Based on the research done by Liu *et al. (2023*), a structure for the flexible PV support has been built for the study. The height of the column is 6 m, and the pitch distance for the PV is 3.5 m. On the other hand, the length of the PV support is 33m, which is expected to fit 28 PV modules, each weighing 32.3kg for 11 rows. In addition, the PV structure is built within a wind tunnel, which would simulate different wind directions and speeds. From the result obtained, the vertical and torsional displacement of the PV modules increases exponentially when the wind speed increases. For each wind speed, the first row would always have higher average vertical and torsional displacement when the direction of wind is 0°. Additionally, when the wind direction changes to 180°, the last row experiences a higher force impact. The first and last rows block the wind, so the middle row would be less affected. As referred to in Figure 2.6 and Figure 2.7, the wind speed started from 4 m/s, which is quite high when compared to Malaysia wind speed; therefore, in this case, the deflection would be relatively lower than the result obtained.

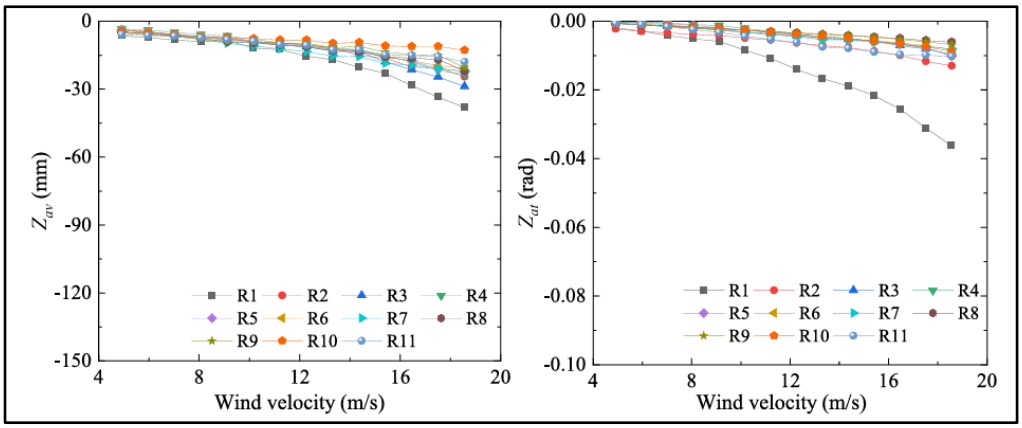

Figure 2. 6: Average vertical and torsional displacement at different wind speed. (Liu *et al.*, 2023). Reprinted with permission from Copyright 2023 Elsevier.

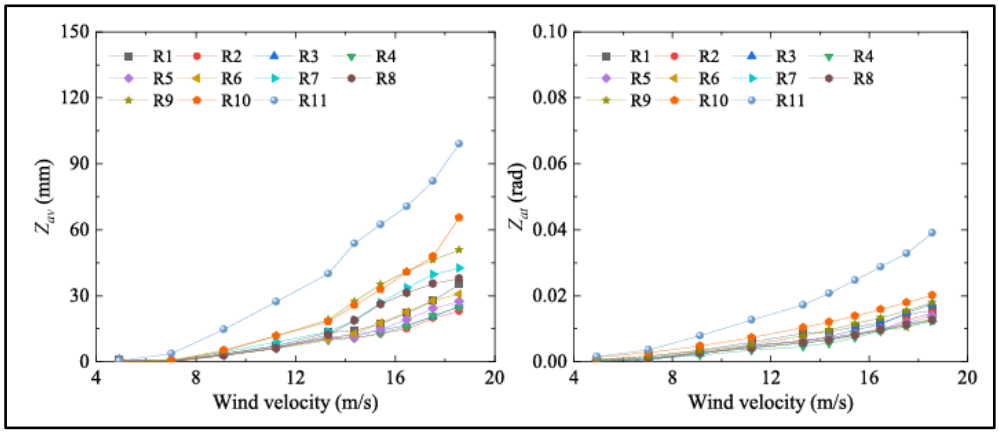

Figure 2. 7: Average vertical and torsional displacement with different wind speed when wind direction equal to 180° (Liu *et al.*, 2023). Reprinted with permission from Copyright 2023 Elsevier.

2.2.3 Temperature and Dust Effect

Malaysia has a tropical climate which has an annual temperature of 25.4 ℃. Other than that, there is a typical range from a low of around 23℃ to 33℃ with the hottest months being in April, May and June. (Climate Change Knowledge Portal, 2021). In other words, Malaysia is located at the equator of the earth. Therefore, the temperature would be slightly hotter compared with other European countries and North America. It is quite important to determine the effect of higher and lower temperatures acting on the performance of the photovoltaic panels. In addition, the temperature is also related to the irradiation from the sun. The higher the irradiation, the higher the temperature on the photovoltaic panels. As Malaysia is located near the equator, it can receive large amounts of solar radiation over the year. As a result, the annual solar irradiation has been estimated to be approximately more than 1700 kWh/m² with annual daily irradiation ranging from 5.0 to 5.8 kWh/m² from the research by Solargis, (2021).

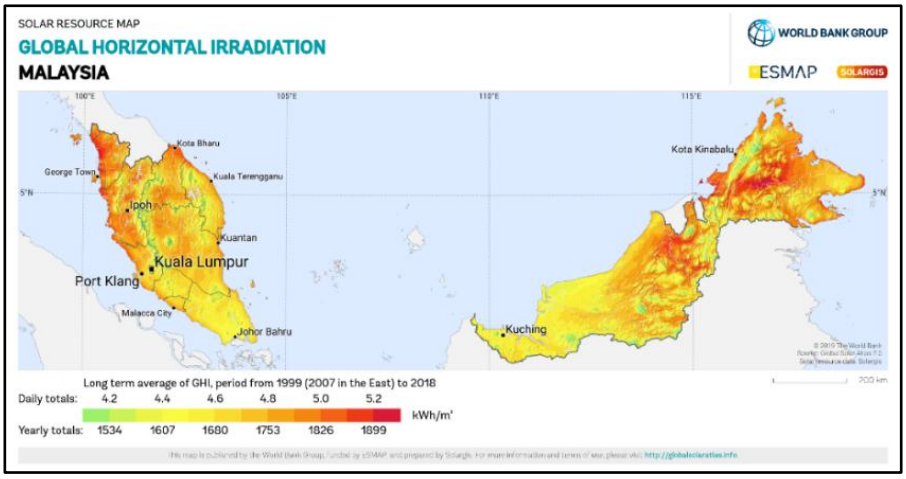

Figure 2. 8: Irradiation in Malaysia (Maity *et al.*, 2024)

Solar irradiation has a significant impact on the photovoltaics' s photon current (I_{ph}). In the solar cells, photons would generate the energy to excite the electrons in the semiconductor by creating a PN junction such as the component in the diode. The PN junction refers to the electron-hole pairs, as the movement of the electron is referring to the photon current. The photon current is the source of current that flows through the load while the current (I_L) is the actual current that flows to the real-life application when photovoltaic panels cell is output to an external circuit. (EIA, 2023). Therefore, when the photon current increases, the load current would increase. According to Suman *et al* (2021), when solar light irradiation increases from 200 W/m^2 to 1000 W/m^2, the load current has an average increment of 57.40% per 200 W/m^2. In addition, Figure 2.9 also shown the current increase also would lead to an increment in the output power (W) of about 54.76% per 200 W/m^2.

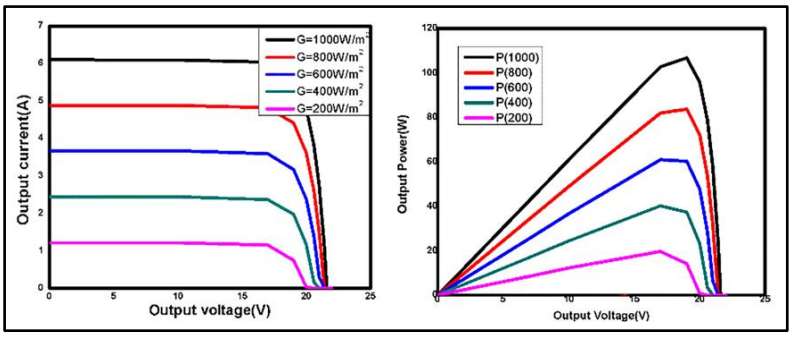

Figure 2. 9: Load Current and output power at different irradiance (Sumen *et al.*, 2021). Reprinted with permission from Copyright 2021 Elsevier.

On the other hand, the solar radiance is also related to the temperature. The higher the irradiance (W/m²), the higher the ambient temperature as well as the PV panel temperature. Higher solar irradiance has the possibility to increase the output power, but the output power would also be counterbalanced by the PV temperature. According to Amelia *et al.* (2016), an experiment has been conducted in Kuala Lumpur, Malaysia, about the PV power output in relation to the ambient temperature. To be more specific, the testing location lies at 6.43° N latitude and 100.19° E longitude. Besides, there were 4 units of sensors that have been attached to the PV panel, and data was measured from 9.00 a.m. to 5.00 p.m. with 10 minutes interval. From Figure 2.10, afternoon (12.40 p.m.) has the highest solar irradiance at around 899.49 W/m², while the lowest irradiance is 155.50 W/m² at 9am. Based on the irradiance values, the ambient temperature is 28℃ at 155.50 W/m² (9.00 am) and 38.99℃ when 899.49 W/m². Therefore, the maximum solar temperature recorded at 63.20 ℃ while the minimum was 34.90℃.

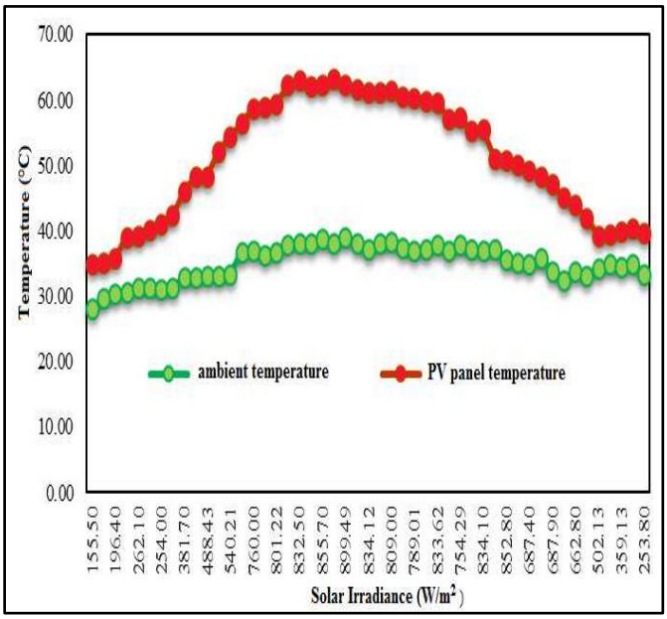

Figure 2. 10: PV panel temperature and ambient temperature on experiment day (Amelia *et al.*, 2016)

Besides, after gathering the data, the results found out that the maximum power output was 61.76 W when PV temperature was at 59.03℃ while the minimum power was 12.65 W when PV temperature was at

34.90℃ . From the result, it means the highest irradiance does not give the highest power output; it is also affected by the PV temperature. The output power cannot perform at its expected rate, which is due to an increase in PV temperature. Elevated temperatures lead to decreased voltage while slightly increasingthe output current. The drastically decreased output voltage has led to lower electrical efficiency. Figure 2.11 shows that the optimal PV temperature to produce the highest power output is around 59℃ with the irradiance of 760 W/m².

Figure 2. 11: Power versus PV panel temperature (Amelia *et al.*, 2016)

In addition, dust would also affect the performance of the PV panels. This is because the dust acts as a barrier for blocking the radiation received by the PV panel. According to Shen et al. (2024), dust accumulation is an incremental progression at the increases by random times. The number of dust accumulation N(t) can be written as equation 2.1.

$$N\,(t) = \sum_{i=1}^{\infty} 1_{\{T_i \le t\}} \tag{2.1}$$

Next, the X_j can be the increase of dust thickness with time which follows an exponential distribution. The total dust accumulated at time would be defined as:

$$x\,(t) = \sum_{j=1}^{N(t)} X_j, t \geq 0 \qquad (2.2)$$

By following the amount of dust accumulation X(t), the reduction of PV panel power generation D(t) can be calculated as

$$D(t) = \frac{-0.521}{1+\left[\frac{x(t)}{12.653}\right]^{1.74}} + 0.532 \qquad (2.3)$$

On the other hand, based on Rajput & Sudhakar (2013) research, Figure 2.12 shown there was an experiment has been carried out to investigate the effect of dust on the performance of the PV panel. The PV panel has been setup at outdoors with the manipulation variable of dust. The result found out that the PV panel having maximum efficiency of 6.38% and minimum efficiency of 2.29% without dust. On the other hand, the maximum efficiency of 0.64% and minimum efficiency of 0.33% with dust. The result shows quite significantly that the PV panel without having more performance.

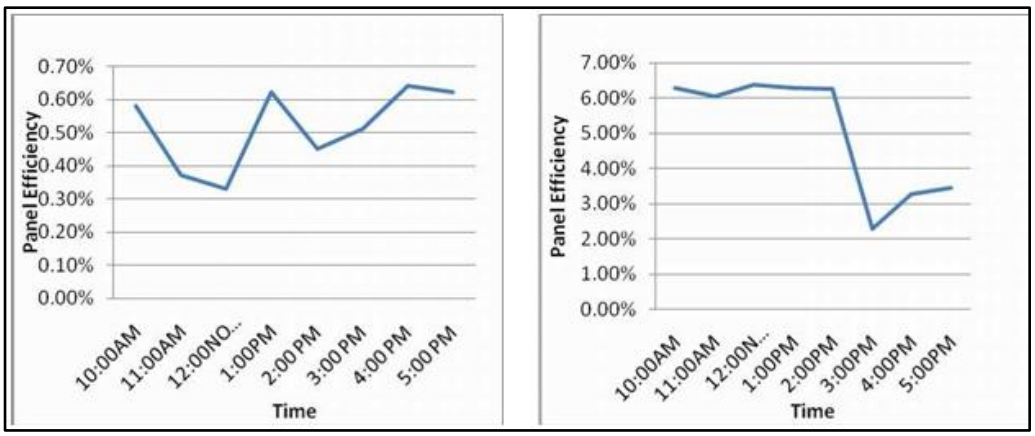

Figure 2.12: With dust (left) and without dust (right) (Rajput & Sudhakar ,2013)

2.2.4 Cooling Method

Cooling PV panels is also important because high temperatures could reduce efficiency. This is because heat would wear out the material as overheating and directly. The power output of photovoltaic (PV) panels would decrease as the temperature within the PV panels increases. For Southeast East Asia

temperature, the PV panels would rise at most to 70℃ thus causing more than 20% power loss during the test condition. Therefore, the implementation of PV cooling would be essential to avoid additional loss in terms of performance and durability of the PV panels. The cooling methods are generally categorized into 2 groups which are passive air cooling and active air cooling. Whereas the passive air cooling is using natural air flow or installing fins to dissipate heat. On the other hand, the active air cooling is using pump power or motor power. For example, water cooling is an active cooling method using a pump to deliver water flows over and behind the panels to absorb heat. In addition, air cooling can also install fans to blow air across the PV panel, which also achieves active cooling methods.

From research by Mah *et al.* (2018), four solar panels have been tested at 770 W/m^2 of the solar irradiance and a tilt angle set at 10° by facing the south direction. They are using water cooling by attaching a pipe to the top of the solar panels and using a 135 W water pump to transfer water to the surface of the PV panels. The pump can supply cooling water for four solar panels at the flow rate of 6 L/min. During the experiment, one solar panel acted as the reference panel without any water cooling while the remaining panels were water-cooled with different flow rates. Besides, the effect of wind blowing is no longer effective because the cooling water removed the heat from the solar panels at a higher rate due to the higher heat capacity possessed by water. The result shows that, when measured at the center point of the solar panels, the temperature difference is 27.9 ℃ with 44.5% decrease in temperature decrease after water cooling. Therefore, the thermal stress was also reduced which was expected to prolong the lifespan of the solar panels. In addition, water flow also would affect the power gain of solar panels. Power gain refers to the increment of power output when applied water-cooled as compared to without water cooling conditions. The maximum power gain occurs at 20L/min flowrate which has achieved 32.4 W. However, the results in Figure 2.13 also show that the improvement of the power output remains idle when the cooling water flow rate is 6 L/min or above. At 6 L/min flowrate, the power gain has already reached 32 W which is negligible effect when compared to 20 L/min flowrate. Therefore, further increase of the cooling water flow rate would become a burden to the system because of an

insignificant amount of power gain. In a nutshell, water cooling mainly reduces the thermal stress of the solar panels and 6 L/min of water flow rate is the optimal solution to reach of performance improvement of 15 %.

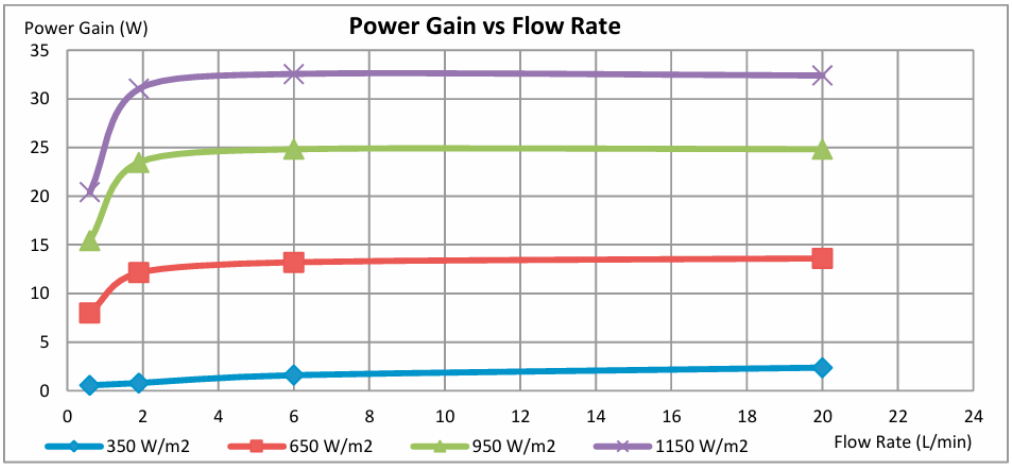

Figure 2.13: Power gain against cooling water flow rate at various solar irradiances (Mah *et al.*, 2018)

In addition, air cooling also shows some cooling effect on the solar panels. Based on research by Patil *et al* (2023), experiments have been carried out for active and passive cooling by using air to investigate the performance of PV panels under these 2 conditions. The experiment has been carried in India with tile angle 30° and facing south. In addition, it is an outdoor experiment which is conducted from 9am to 5pm on a full sunny day. During the experimentation, the average wind speed was found to be 2.44m/s and average ambient temperature is at 34.41℃. The maximum temperature of solar panels was ranging between 60.3℃ and 63℃ during noon when no cooling applied. On the other hand, when air cooling applies, the temperature can decrease 10%. In addition, the different mass flow rates of air also have different effects. Output power has been having increment of 11%, 11.8% and 12.6% with the flow rates of 0.04kg/s, 0.06kg/s and 0.08kg/s. The detailed output is shown below Figure 2.14.

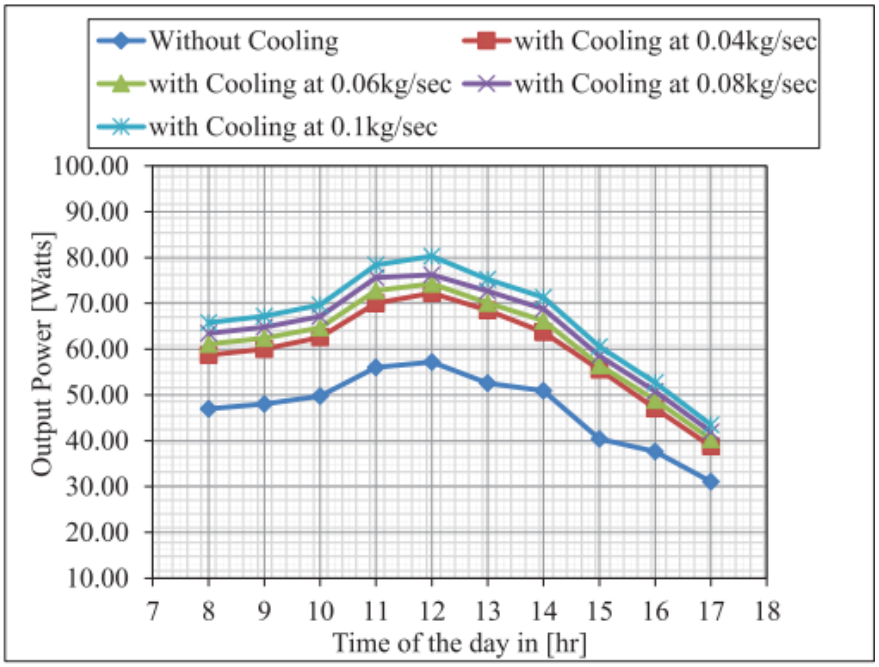

Figure 2.14: Output power versus time of day at various mass flow rate (Patil *et al.*, 2023). Reprinted with permission from Copyright 2023 Elsevier.

For the cooling system, water cooling would be more efficient and have significant increment. However, it is more complicated to set up the water-cooling system when compared to active air cooling which only requires an air blower and valve. The cooling system would also need to depend on the layout design of the agrivoltaics system and decide which cooling method would optimize the output.

2.2.5 Photovoltanics output simulation software

PVsyst, a photovoltaic system simulation software, was developed in Switzerland by André Mermoud in 1992. It helps in designing the configuration of the PV system and simulates the amount of electrical energy generated. In more detailed explanation, PVsyst helps to model different brands of solar panel's performance while accounting for system loss, energy yield and partial shading.

Based on the studies by Baqir & Channi (2022), they are using PVsyst software to analyze and design the solar PV system in Afghanistan. Some rural area in Afghanistan is facing electrical shortage although the

country spending 280 million dollars to buy electricity from neighboring country. Therefore, the government plans to cover 30% of electrical demand by using PV system by 2032. Based on this research, a 700KWp grid-connected solar power has been designed to be ground mounted with the coordinate of 33.2 N and 66.15 E. The configuration of PV system highly depends on the location and solar irradiation. While the quality, orientation and inclination of solar panels would affect the configuration. By selecting the proper configuration and layout of the PV panels, the simulation results would be the main concern for this part. Firstly, the Arghanistan study has achieved a performance ratio (PR) of 0.797 and annual production of 1266MWh which shown in Table 2.1. The losses are mainly due to array losses that are 14.3%, which is temperature losses and system losses such as inverter inefficiencies. In addition, based on the Figure 2.15, it evaluates the sun path and angle which is useful for the agrivoltaics to ensure crop light availability. In addition, PV syst also calculated this Afghanistan system having payback period of 4.7 years.

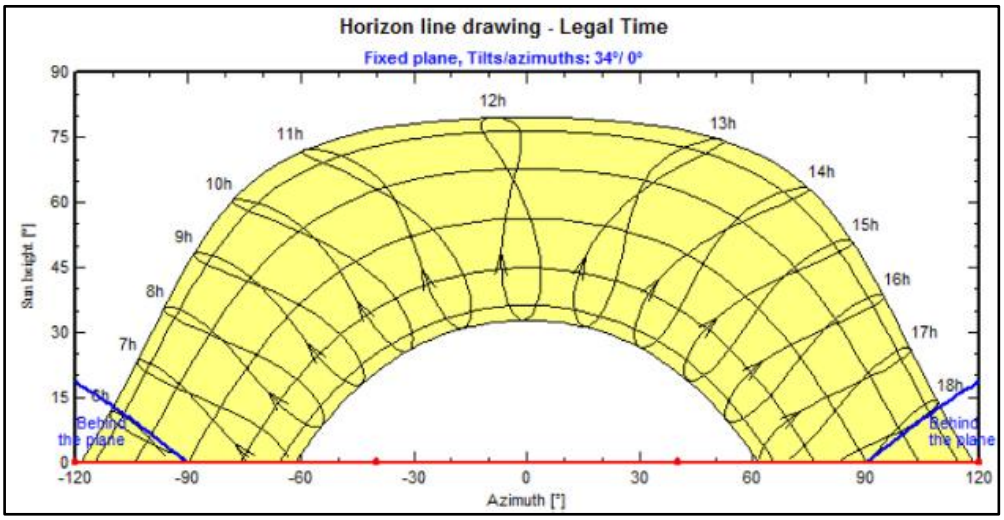

Figure 2.15: Sun Path in Arghanistan (Baqir & Channi, 2022). Reprinted with permission from Copyright 2022 Elsevier

Table 2.1: Solar Irradiation and power output data (Baqir & Channi, 2022). Reprinted with permission from Copyright 2022 Elsevier.

Month	GlobHor kWh/m^2	DiffHor kWh/m^2	T_Amb °C	GlobInc kWh/m^2	GlobEff kWh/m^2	EArray MWh	E_Grid MWh	PR Ratio
January	87.8	33.23	1.98	136.0	127.3	83.7	81.9	0.859
February	105.3	39.69	5.04	145.0	136.2	88.6	86.8	0.853
March	141.6	54.60	10.34	167.5	156.6	98.4	96.4	0.820
April	170.6	63.69	15.41	177.7	165.3	101.5	99.5	0.798
May	217.8	62.30	20.76	202.3	187.9	111.8	109.6	0.772
June	242.8	56.28	22.83	212.6	197.2	116.2	113.9	0.763
July	249.4	53.29	22.93	224.5	208.6	122.6	120.1	0.762
August	219.1	52.81	21.81	218.2	203.4	119.8	117.5	0.767
September	201.2	43.87	18.88	231.6	217.1	127.5	125.1	0.769
October	160.5	34.48	14.18	221.4	209.1	126.0	123.6	0.796
November	108.0	30.06	7.55	169.2	159.0	100.0	98.1	0.826
December	93.7	25.50	3.44	158.3	148.3	95.3	93.4	0.840
Year	1997.8	549.80	13.81	2264.1	2116.0	1291.4	1266.1	0.797

In addition, Kumar *et al*. (2021) designed a standalone solar PV system for powering up the office in India and using PV syst to evaluate the performance and losses. Based on the system designed, the office's daily energy demand is met by using monocrystalline panels which are 230 Wp and battery storage of 6kWh capacity. There is an average performance ratio is 0.728% and peak during December with 0.86 due to lower temperatures. However, for hot weather such as April, the performance ratio would fluctuate and drop to 64%. The solar fraction is calculated as 98.3% which means it is near-complete energy self-sufficiency. In addition, the annual energy loss is combined with 20% array losses and 4.3% system losses. The Figure 2.16 shows a more comprehensive loss result that is simulated from the software.

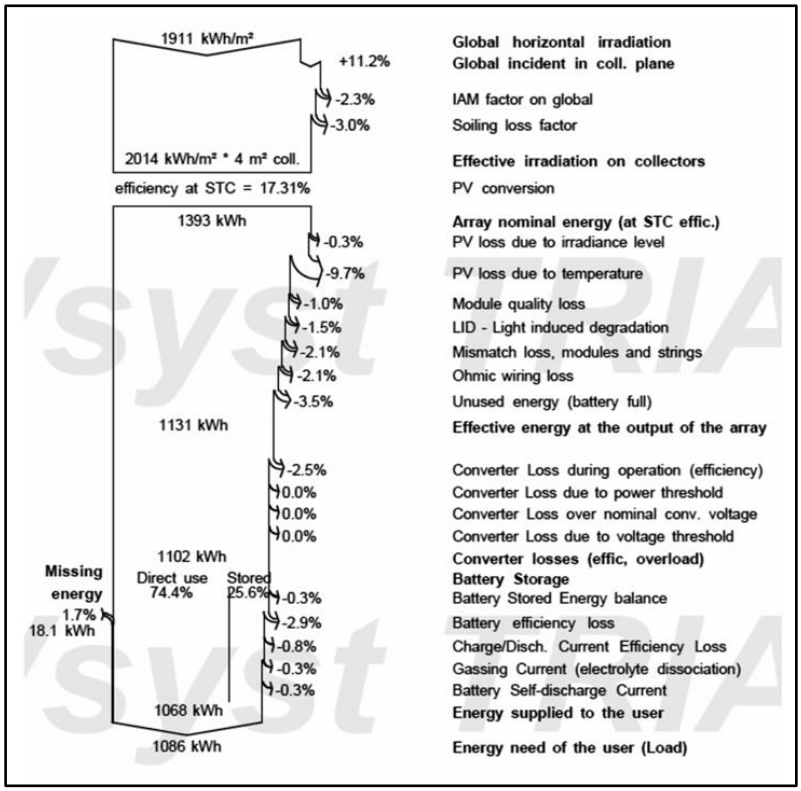

Figure 2.16: Loss Diagram (Kumar *et al.,* 2021). Reprinted with permission from Copyright 2021 Elsevier

From the research done in Afghanistan and India, PV syst could simulate the model based on grid-connected or standalone PV system. Both systems account for solar irradiance, temperature, shading effects and system losses. For geographical customization, PV syst supports specific meteorological data such as Baqir & Channi (2022) used Afghanistan meteorological data (4.5 – 7 kWh/m^2/day). Next, it simulated the performance ratio, specific and loss diagram that can be a guidance for modifying the PV system to reach desire designed output. Lastly, evaluation of financial metric would be important for project viability. However, PV syst doesn't build templates for agrivoltaics systems as it only focuses on photovoltaic system. Therefore, it cannot predict the crop yield impacts under PV arrays.

2.2.6 Solar Panel Type

The coated silicon semiconductor is the main material to design solar cells or photovoltaic cells. Different types of solar panels have been developed to meet different needs, from rooftops house-hold application to photovoltaic farm.

Each type of solar panel has its pros and cons. Understanding the type of solar panel helps to decide the most suitable solar solution for specific use.

According to Dhilipan *et al.* (2022), mono-crystalline and poly-crystalline silicon solar cells are formed of a cylindrical alloy of silicon developed method as same as semiconductor. They belong to the 1st generation of solar panels. Mostly they are in black color which makes them have higher light absorption. The advantages of mono-crystalline cells are higher efficiency but high cost. On the other hand, poly-crystalline is lower in price but has lower efficiency. In addition, based on Binns & Reeves (2024), silicon thin-film solar cells use thin layer of amorphous silicon (a-Si) which can adapted to a wide range of construction needs which make them more accessible. The efficiency of the thin film is based on the selected semiconductor. However, they have lower rates of energy efficiency which need more of them to provide desire power output. For the third generation of solar panels, it is not common to use in real life applications when compared to first and second generation. For example, organic solar made up of carbon-based organic compounds which are used in thin layer which make the difference for silicon solar cells. Organic solar cells are easy to integrate into property but have a shorter life span and lower efficiency than first generation. In a nutshell, mono-crystalline or poly crystalline are more suitable to be installed in agrivoltaics system as provide higher efficiency.

In addition, there are few electrical parameters that are important to evaluate performance which shown in Table 2.2.

Table 2.2: Electrical Parameters of photovoltanics panels (Suman *et al.* 2021)

Electrical Parameters	Description
Short Circuit Current (I_{SC})	Maximum current produced by the solar cell when the output terminals are shorted. The value is measured in ampere (A)
Open Circuit Voltage (V_{OC})	Maximum voltage that the cell produced under open circuit conditions is measured in volts (V)
Rated Maximum power (P_{max})	Maximum electrical power that the panel can produce under standard test conditions. The equation is formed by multiple of maximum power voltage (V_{mp}) and maximum power current (I_{mp}). It is measured in Watts (W)
Efficiency	Maximum output power is divided by the input power. The value is measured in % which indicates the percentage of input sunlight power converted to electrical power

2.2.7 Inverter

Another important components in the PV system are the inverter which converts the direct current (DC) which is what yields from solar panel and converts to the alternating current (AC). The alternating currents are suitable for agricultural electrical applications, storage batteries and grid connection. The efficiency of the inverter impact heavily total solar power yielding from the agrivoltaics system. As mentioned by Zainol *et al.* (2021), the Maximum Power Point Tracking (MPPT) system in the inverter reduces the power losses due to inconsistent irradiance which enhances the stability of energy output. It enables continuous optimization of power output although there is fluctuating solar condition in agrivoltaics system. Higher-performance inverters typically obtain an efficiency level of 98%, for example Solis Inverter. Besides, high quality inverters would further enhance system integration by offering low total harmonic distortion (THD) which is lower than 2%. THD would measure

the waveform distortion caused by harmonics and lower THD reduces the equipment stress therefore minimizing THD would improve the inverter's performance. In addition, Othman *et al.* (2021) highlights that in large-scale farms, the inverters would rate output voltage power rating from 5kW to 100kW depending on the system size and energy demand. Other than that, the Pnom ratio is defined as the DC/AC ratio representing the ratio of the nominal power of the PV array. A proper Pnom ration ensures the inverter operates efficiently near its ability. According to PVsyst (n.d.), when Pnom ratio ranges from 1.25 to 1.3 for a well-oriented systems. This has been indicated that the solar panels can generate 25% or 30% more power than the inverter rated output. For example, if the inverter rated at 20kW and the Pnom ratio is 1.3, the solar panel would have a total rated power of 26kW which are oversized compared to the inverter. Therefore, if the ratio is too high, power clipping might occur as DC input exceeds the limit of inverter. Thus, by considering the electrical parameters such as MPPT range, output rated AC power and Pnom ratio, the inverter becomes a significant factor in development of agrivoltaics.

2.3 Crop

Crop would be another component in the agrivoltaics system. In this research, passion fruits would be the crop type to be planted under the photovoltanics system. Therefore, the study of passion fruit characteristic would be important to utilize the plnating technique and crop characteristic to enchance the productivity. In addition, analyze of passion fruit market would helps in calculating the economic profitability.

Other than that, this subtopic also revela the effects of crop under the agrivoltaics system. As the shading effect and microclimates issues, the growth of the crop would be expected to have different conditions when compared to the normal growing method. Lastly, Aquacrop would be the simulation software to simulate the growth conditions of crop.

2.3.1 Passion Fruit Characteristics

Passion fruit or granadilla is a vine plant from the Passiforaceae family which named scientific as Passiflora edulis Sims. (Ghada *et al*). In general, there are

2 main types of passion fruits which are yellow and purple passion fruits. In Malaysia, both color of the passion fruits called as “Markisa”. Purple and yellow passion fruits can be distinguished by their plant’s growth condition and fruits characteristics. According to Md Nor *et al* (2022), yellow passion fruit plant having less chilling resistant to a more vigorous vine. Yellow passion fruits are highly remanufactured in the food industry due to more acidic juice. On the other hand, purple passion fruit is more resistant to chilling temperature while lesser acidic juice and superior in aroma.

In addition, for purple passion fruits, vines are grown at higher elevations. The weight would be around 35-45g, the diameter is average at 4.5cm. On the other hand, the yellow passion fruits are suitable to grow in lower elevations area. The fruit size would be bigger than purple passion fruits and heavier than purple passion fruits. In addition, passion fruit is a high acid food due to high in citric acid and malic acid. Based on its nature characteristic, passion fruits provided vitamin A, B2 and C and important minerals such as K, P, CA, Fe, Na, Mg, S, CI and protein. (Thokchom & Mandal. 2017). On the other hand, for the economic value of passion fruits, passion fruit having high potential crop yielding and income increment especially plantation in big farming area. This is due to the higher market value, which is an average USD400-600 per metric ton. According to Uchoa et al (2021), the benefit/cost ratio is calculated as more than 2 which means it having double return of investment and net revenue could reached up to USD8958 per hectare.

For the requirement of passion fruit, it is suitable to be frown in low-elevation tropical zones and therefore yellow passion fruits is suitable to be grown in Malaysia which it is more sensitive to cold weather. The purple passion fruits are grown in condition of highland climate with cooler weather but not frost. For both passion characteristics, they should be grown at around 29^{o}c average temperatures and require rainfall of 1500mm per year. Besides, passion vines prefer slightly acid soil and should set up a windbreaks system to provide protection for the crops. For the planting density, it is suggested that 625 plants/hectare would be given the highest yield due to sufficient sunlight and water has been evenly distributed to all crops. (Didier, C. 2001). Besides, for a fruit grown in tropical country, setting a calendar date that depends on days from flowering to fruit would be useful guidelines to reach the optimal

yielding stages. Since passion fruits cannot grow in too hot conditions, the implementation of agrivoltaics has avoided microclimate issues which reduce extreme sunlight and protect from excessive heat which also maintain the moisture level needed by the passion fruits. Therefore, planting passion fruits would be a remarkable investment and suitable to be grown in agrivoltaics system.

2.3.2 Calamansi Plant Charateristics

For actual experiment purposes, calamansi, which is also known as 'limau kasturi' in the Malaysian language, is planned to be used as a crop experiment model. This is due to the fact that calamansi plants are more suitable for amateurs to plant. On the other hand, passion fruits required more experienced farmers to monitor the planting conditions. In addition, both calamansi and passion fruits have similar characteristics, as both plants are categorised as tropical plants. Therefore, it can be assumed the effect on both crops under the agrivoltaics system would become similar.

Calamansi, which also has the scientific name *Citrus mitis*, is an evergreen tree that yields in tropical hot countries (25 ℃). According to Taitano *et al*. (2023), the preferred soil type for calamansi is sandy loam soil or clay loam soil with a pH range of 5.5 to 7. In addition, the calamansi is expected to yield in around 0.19 m to 1 m in height when growing in a pot. However, when the plants are grown in soil ground, the height can reach around 1.5 m. Other than that, calamansi fruits are green to orange when turning mature. The fruits are very low in pH value, which is around 2 to 2.8.

In terms of growth cycle, the calamansi takes about 2 to 3 weeks from seed conditions to germination. After that, when the seedling has grown to 0.15 m, it can be transferred into the ground or bigger pots. In addition, once a flower bud forms, the crops require 3 to 4 months for the calamansi fruits to reach commercial maturity. Lastly, the calamansi begins to bear fruit much faster, which is within 6 months to 1 year.

In addition, as calamansi are consider easy maintenance, therefore only light pruning would be needed. There are 3 objective when purning the trees which are increasing the total area, improve air flow and increasing the amount of sunlight received by the plants. In addition, around 0.25 litre of

water would be needed to keep the moisture of the soil for a medium size of the calamansi plants. For a commercial production, installing a drip irrigation system would be highly recommended as it always maintains moisture of a tropical plants.

Other than that, approximately 75 grams of urea can be used as fertiliser during the plantation of calamansi. For a suggestion by an experienced farmer, the fertilisation process only needed to be done once for a week. As the tree gets older, the amount of the fertiliser should increase as well. Lastly, the calamansi flowers are generally pure white in colour and rich in sweet fragrance. Calamansi flowers and fruits produce throughout the year and are expected to have 4–5 periods of new growth in each year. A single harvest would last for 3 months, and fruits take approximately 5 months to get mature after flowering.

2.3.3 Effect of crop under agrivoltaics system

The effect of crop yielding when combined with a photovoltaic system depends on the solar panel layout, shading effect and crop species when it applies in Malaysia. Firstly, solar panels provide shading effects as installed in the upper direction of the crops. Therefore, it would effectively reduce crop exposure to the sunlight. The shading effects would have a positive effect, especially during the hot season in Malaysia. In addition, shading effects maintain the soil moisture and need less irrigation. When applying the agrivoltaics system, the structure would be similar to the screenhouse structure. As shading screenhouses could control plant growth by controlling the light intensity and create other micro-environmental conditions such as air and soil temperature, air velocity and humidity. (Xu, G. *et al*., 2017).

According to the study by Jamil & Pearce (2025), it focuses on the impact of shading effects on strawberries. The study has been carried out in the Western University Biotron in a controlled environment room. For these studies, they are using the transparency level of the PV modules instead of the shading effect on the crops. As the transparency level decreases, the shading effect would increase. The transparency level has been set from 10 % to 80 %, and Cd-Te PV modules have been chosen due to their semitransparency and ease of installation. The studies were carried out on February 20, 2024, with a

duration of 112 days. From the result obtained in Figure 2.17, when the transparency level is 10 % (high shading effect), the maximum weight of the strawberry range is 16 grams. When getting more transparent (40 %), the weight increases to 92 g. As the transparency increases linearly, the weight of the crops would also increase. However, when the transparency increases to 70 %, it would reach the maximum weight of the strawberry, which is 155 g. On the other hand, during unshaded conditions, the maximum weight was only achieved at 110 g. The relationship between the transparency level and strawberry yields shows a positive relationship which peaks under the 70 % transparency level. It can also be noticed that the average yield for 100 % transparency was lower than the maximum yield of 70 % transparency. This is because 70 % transparency (30 % shading effect) allowed for sufficient light intensity and having a lower temperature surround the crops. When the transparency level is lower, it leads to excessive shading. The finding of these studies also shows that when creating a shading effect of less than 40 %, it would be advantageous for use in agrivoltaic systems.

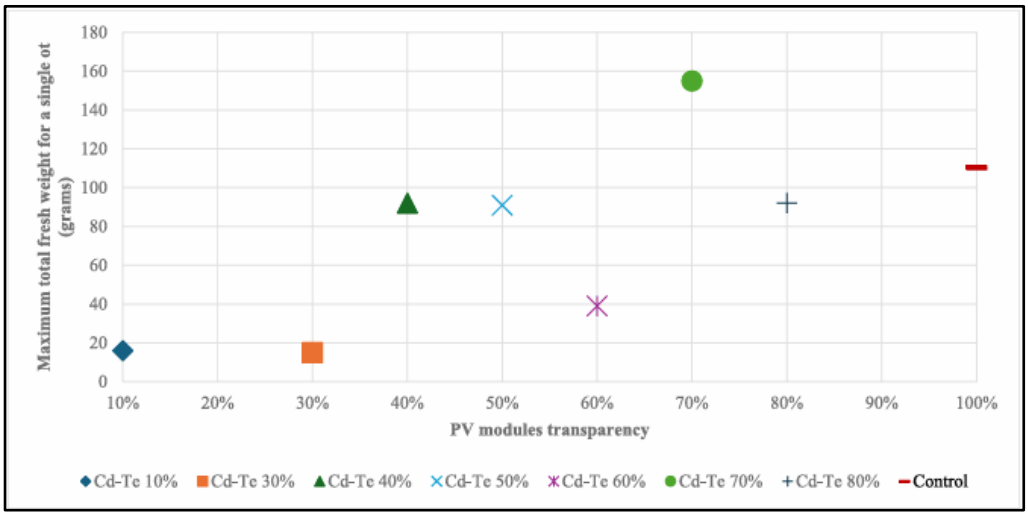

Figure 2.17: Maximum total fresh weight per pot versus the PV module transparency (Jamil & Pearce, 2025)

However, different crops would react differently according to the same shading effect. For example, based on the research by Yasoda *et al.* (2018), an experiment has been carried out at different shade levels on the growth and yielding performance of the cauliflower. The shading parameters

would be open field (25 %), single net house (50 %) and double net house (75 %). Firstly, in terms of light intensity, it decreases 47.6 % when the shading effect increases by 25 %. In addition, at the highest shading effect, the light intensity becomes the lowest, which is around 20 Klux. As for the growth condition of the cauliflower, the highest number of leaves was during 50 % and the lowest during 75 % shading level. In addition, the crop would also have maximum crop diameter and weight during 50 % shading level. This is due to when under 50 % shade level, it meets favourable environmental conditions such as relative humidity, temperature and light intensity.

In a nutshell, the shading effect would prevent the intensive high temperature and retain the moisture of the soil condition. However, the higher the shading effect, the lower the yield production, as the surrounding environment condition cannot fulfil the needs of the plants. From the literature review, it is found out that a 30 to 40 % shading level would be the favourable condition for crops.

2.3.4 Crop Simulation Software

Nowadays, to address the food scarcity and assess crop production as affected by environment and management, several numbers of crop simulation models have been developed. This simulation software usually requires many parameters that are not easy to get for researchers as the input variables. Furthermore, non-transparency parameters from NGOs, farmer associations and governmental departments also remain as a constraint for carrying out crop simulation modelling. To achieve the effectiveness of doing crop simulations, the United Nations' Food and Agriculture Organisation (FAO) has been developing AquaCrop software to seek balance among robustness, simplicity and accuracy. AquaCrop offers a straightforward operation, as it requires few input parameters that are based on intuition and little research. Besides, this simulation software is also based on fundamental biophysics to simulate the results.

A study done by Umesh *et al*. (2022) has evaluated the effect of climate change on maize yields in the southern India region by using AquaCrop. The study project is under RCP4.5 and RCP8.5 scenarios. The RCP stands for "Representative Concentration Pathway"; with the highest

RCP of 8.5, it has been indicating the effort to curb greenhouse gas emissions is the lowest. Therefore, the region needs higher costs to change and adapt to sustainable energy production. The higher the RCP level, the more the maize yield might drop, at most 18%. However, when simulated with different irrigation conditions, the percentage increase in grain yield ranges from 34.88 % with supplemental irrigation of 20 mm under MNF. The results simulation also found out that 50 mm of supplemental irrigation would have an expected increment of more than 30% in RCP8.5 from the near century to the end of the century. Lastly, the validation of the AquaCrop model was performed with 91 % model efficiency of grain yield and 73 % for water productivity.

Other than that, another study has been conducted by Alvar-Beltrán e*t al*. (2023) in Burkina Faso, which is an area with scarcity of water and extreme weather conditions. The simulated crops are using tomato, maize and quinoa for growing from year 2020 to 2021. On the other hand, the study group also carried out real-life experiments to compare the result with AquaCrop. It has been found out the simulated yields are highly matched with the real yielding value. For example, the simulated yield value of tomatoes is 2007.5 kg/ha, while the observed yield is 1989 kg/ha, with a 0.93% difference. In addition, Figure 2.18 also shows the comparison in terms of canopy cover. It shows that the simulation had a Pearson ratio of 0.99, which indicates excellent correlation. Thus, it supports AquaCrop as a robust simulation tool for crop yield.

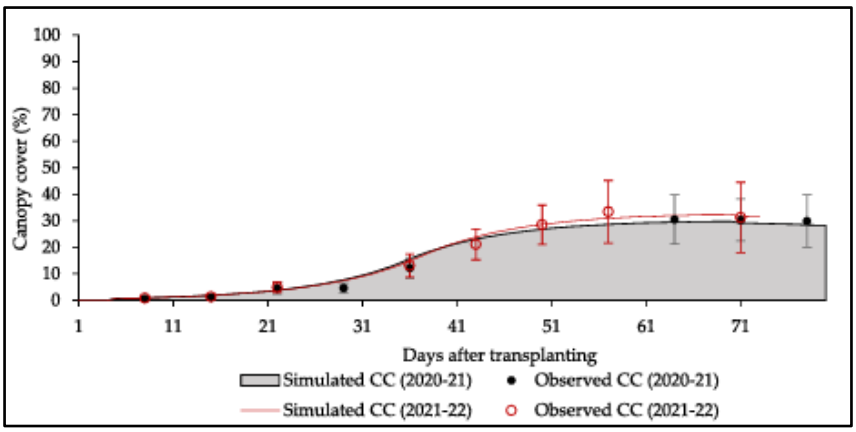

Figure 2. 18: Comparison of simulated and observe canopy over of tomatoes (Alvar-Beltrán *et al*., 2023). Reprinted with permission from Copyright 2023 Elsevier.

2.3.5 Multiple Criteria Growing Performance

In terms of measuring the growing performance of the crops, Technique for Order Preference by Similarity to Ideal Solution (TOPSIS) has been implemented to identify the growth performance of crops from different parameters such as plant height, number of new leaves, fruit diameter, number of fruits etc. Its core idea is that the best alternative is that which is closet to the ideal solution which means maximum benefit criteria and farthest from the anti-ideal (worst) solution.

Accoring to Biswas *et al*., (2024), their research has been focus on evaluating alternative conservation agriculture practice such as different tillage, fertilizer regimes asn residue in rice-wheat. The criteria included such as energy use, economics, agronomy and plant protection. By using the TOPSIS analysis, the best performing alternative was “Zero1” which consists o% residue and 100% NPK. This research similar structure to the current project as consisting multiple treatments and showing how conflicting criteria can be balanced.

Besides, from the research by Azadi *et al.* (2023), they evaluating land suitability for rice cultivation by comparing different evaluation methods. The results found out that TOPSIS were effective as allowed for motr criteria and promote suitability ranking matched known yields. Agrivoltaics often depends on land aspect, slope, solar irradiation, microclimate. Therefore, land suitability assessments by using TOPSIS analogous.

2.3.6 Photosynthetically Active Radiation

Photosynthetically Active Radiation (PAR) is the component of solar radiation in the 400-700nm band usable by plants for photosynthesis which reflect the critical determinant of plant growth under agrivoltaics system. Shading from photovoltaics panels will reduces incident PAR as alters the direct and diffuse light fraction and create spatial heterogeneity in light distribution. The implementation of PAR sensors in the agrivoltaics system used to determine the shading level caused by the photovoltaics panels.

Relatively few prior studies in agrivoltaics use PAR as an explicit criterion to determine the shading level. For examples, by the research by Campana *et al.* (2021), the row spacing and orientation of bifacial panels

significantly altered PAR distribution, leading to yield reduction up to 50% under tighter spacing due to lower PAR. On the other hand, another astudy on intercropping which is apple and coybean has demonstrated that decreased accumulated PAR under tree canopies and increased spartial heterogeneity of light severely reduced soybean yield components. (Peng *et al.,*2025).

The weighting of the PAR-related criteria should reflect their actual limiting potential in local conditions. Besides, with the reference of PAR value, it can modify the orientation of the crops to increase the productivity.

2.4 Agrivoltanic

In this subchapter, it would reveal the potential of agrivoltaics in Malaysia in terms of adequate land use and the policy support by the Malaysian government. Other than that, it is also needed to evaluate the efficiency of the agrivoltaics system by using the land equivalent ratio (LER). Next, several designs have also been studied which focus more on the support foundation of photovoltaic systems, such as concrete and helical piles. Lastly, this agrivoltaics also fulfils the Sustainable Development Goals (SDG), and the SWOT of agrivoltaics has been analysed.

2.4.1 Potential of Agrivoltaics in Malaysia

In recent years, many research organisations have explored the multifaceted potential of the agrivoltaic systems beyond their initial conceptual appeal. Engineers have dedicated themselves to examining the method to optimise the system in different climates, crop types and technologies. This section reviews key studies and findings that reveal the potential of agrivoltaic systems across various dimensions, including environmental impacts and socio-economic implications.

In the ASEAN countries, Johnson, B.A., *et al.* (2024) have analysed the potential of agrivoltaics while also considering the simultaneous goal of expanding agroforestry. The member countries of ASEAN include Brunei, Indonesia, Malaysia, Laos, Myanmar, etc. According to the ASEAN Centre of Energy, the whole of ASEAN’s electricity consumption is expected to triple from 2020 to 2050 until it reaches the value of 3388 TWh/year. Therefore, there is a high demand for expanding resources for ASEAN’s countries.

During the research, some areas in ASEAN countries are not considered for launching agrivoltaic systems, which are extremely steep slopes (more than 15°), poor soil structure, and Environmental Sensitive Areas (protected areas, key biodiversity, and wetlands). After excluding ESA, the geographical potential of agrivoltaics on herbaceous croplands in ASEAN is calculated as 369841 km², which is 68% of the total ASEAN land area. In terms of Malaysia, the geographic potential is more than 70% to construct the agrivoltaic system. The ESA constraint doesn't have too much effect on Malaysia, despite there being many croplands in Malaysia that have slopes that are more than 15°, which is due to croplands being located within multiple overlapping ESAs. In conclusion, agrivoltaics has the potential to meet the significant electrical power generation need of ASEAN's countries by only just utilising 10% of geographic potential, which would theoretically fulfil ASEAN's renewable energy ambitions.

In Malaysia, photovoltaic systems are highly encouraged to be installed for commercial and residential purposes. For example, the Malaysian government has introduced a specific incentive programme to encourage the installation of Solar PV systems for consumers, which is known as the Solar for Rakyat Incentive Scheme (SolaRIS), which offers a one-time cash rebate of RM1000 per kilowatt of installed capacity and is capped at RM4000. (Seda, 2024). In addition, Malaysia's SEDA also introduced the Net Energy Metering Scheme (NEM) with a quota allocation of 500 MW to encourage Malaysia's renewable energy development. The NEM mentions excess electrical energy generated would be exported to TNB at the prevailing displaced cost. According to PETRA. The NEM programme would also be open to agricultural electricity users and would offer benefits from the installation of PV panels. (Malay Mail, 2024) Existing NEM applied has increased the solar system capacity and transition to the latest NEM terms. These policies reflect Malaysia's commitment to promoting renewable energy and putting effort into creating a more sustainable energy landscape.

2.4.2 Efficiency of agrivoltaics system

Agrivoltaic systems combine the usage of solar energy production with agricultural activities on the same piece of land, offering a dual-use solution

that improves land productivity. It is important to measure the efficiency to understand how successful the implementation of agrivoltaic systems is. Efficiency in agrivoltaics is not just about yielding electricity but also about how well the crop grows underneath. The land equivalent ratio (LER) is the most common method introduced to assess the performance of the agrivoltaics system, which determines whether the combined value of agricultural production and solar energy generation is equivalent to or greater than the value when land is used alone. LER is computed using the equation (2.4) below. When the LER value is equal to one, it has indicated the system efficiency is the same as separate farming and solar farms. However, when the LER is less than 1, the system is not making profit. Most importantly, the LER should be more than 1, which proves that the agrivoltaics efficiency is higher than that of an agriculture farm or photovoltaic farm alone.

$$LER = \frac{Y_{Crop-APV}}{Y_{Crop}} + \frac{Y_{PV-APV}}{Y_{PV}} \tag{2.4}$$

where

LER = Land Equivalent Ratio

$Y_{Crop\text{-}APV}$ = Yield of crops under agrivoltaics system (kg/m^2)

Y_{Crop} = Yield of crops under agriculture farm alone (kg/m^2)

$Y_{PV\text{-}APV}$ = Yield of electricity power under agrivoltaics system (Wh/m^2)

Y_{PV} = Yield of electricity power under photovoltaic farm alone (Wh/m^2)

In addition, Ground Coverage Ratio (GCR) is also an important parameter to identify the density of PV panels in the agrivoltaics farm. As higher the GCR values, the panels are more tightly packed and there is less sunlight for crops. On the other hand, when the GCR value lowers, the panels are less dense and more solar radiance absorb by the crops. The GCR equation is shown as below:

$$GCR = \frac{Area\ Covered\ by\ PV\ Panels}{Total\ farm\ Area} \tag{2.5}$$

Based on the study done by Mazzeo *et al.* (2025), there are different crops, such as lettuce, maize and turnip, that have been experimented on under

various GCR values to identify the LER values. Higher LER, which is close to 2.0, occurs when the agrivoltaic system has a clearance height of 2.5 m and a lower GCR value in the range of 0.2 to 0.3. The highest LER value (2.05) is obtained when the crops are shade-tolerant crops, lettuce. In addition, maize would have a low LER value, as it is shade-sensitive when the GCR is set high (0.6) and has a low clearance height. However, the lowest value of LER is more than 1 (1.04), which also shows the efficiency of agrivoltaics is higher. In conclusion, the journal shows that a well-designed solar panel layout can be optimised with double land productivity when compared to separate agriculture and solar setups.

In conclusion, based on the LER ratio, the yield of agrivoltaics should be larger than yield of crops only or PV yielding. Therefore, optimization of agrivoltaics design is important to achieve higher LER values.

2.4.3 Design of agrivoltaics system

Several commercial and research agrivoltaics have been focusing on the design of the layout of the agrivoltaics system. The design of an agrivoltaics system reveals critical considerations such as the height, structural design, fixed or tracked PV panel, etc. Additionally, environmental factors such as local climate and soil condition should also be considered during the system design to ensure the rigidity of the rack. Existing models of agrivoltaic systems have occurred widely across different regions around the world. While some designs employ fixed tilt and angle, others use a tracker design in which the solar panels would be moving along the direction of the sun. In addition, some designs are using semi-transparent modules with adjustable shading mechanisms in the system. There are two exciting agrivoltaics system has been design and utilize in South Korea by Lee *et al.* (2023). The crops for the first and second models are rice paddy and cabbage fields as shown in the Figure 2.19. Firstly, for the foundation of the structure is using screw pile-type instead of concrete foundation. This is because concrete foundation is more difficult to construct and affects crops by decreasing the utilizable area. The screw pile also referred to a helical pile which below having welded helical plates that help to improve the tension capacity. (Appendix A) Screw pile is also easy to be installed on soft ground such as soil area. In addition, screw

piles also many highlights such as quick installation and removability. (Jeans, 2024) For the design of structural support of these 2 different has shown in Table 2.3 and Figure 2.20 below. For model 1, there is more power generation capacity can be obtained and more safety structure due to the PV module is installed in the landscape orientation without gaps. In addition, for design of model 2, there is gap between the portrait orientation of solar panels which allow more solar radiance absorb by the crops. However, additional structure reinforcements would be needed.

Figure 2. 19: The agrivoltaics design in South Korea (Lee *et al.*, 2023)

Table 2.3: Dimension of land and panel information

Land Area	**Model A**	**Model B**
Length	4.5m	5.1m
Width	5.1m	4.5m
Height	3.8m	3.8m
PV Infomation		
Power Rating	450W	580W
Length	2115mm	2416mm
Width	1052mm	1134mm
Thickness	40mm	35mm

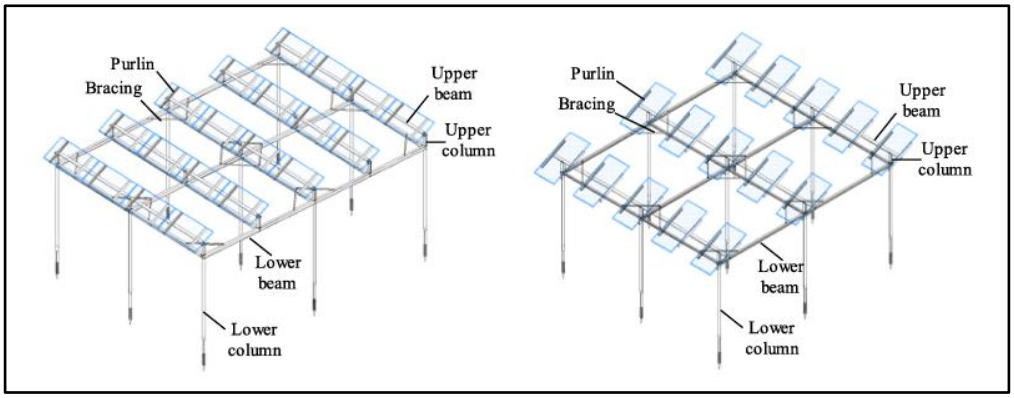

Figure 2. 20: Schematic view of type 1 and type 2 (Lee *et al.,*2023)

Other than that, there is also 2 agrivoltaics design in Tanzania and Kenya. According to Randle-Boggis *et al* (2025), for the Tanzania's case study as shown as Figure 2.21 below, it is an off-grid system which can achieve total capacity of 36.6kWp. The system is designed to meet the electrical demands in the rural area that previously the area is relying on diesel generators. The system consists of 36 PV panels with each rating at 345W. The arrangement would be 34 x 13-meter area total in 442m^2. The panels are grouped into arrays by 4 modules along the width sides of total area. There arrays were mounting on galvanized steel support structures which are mounted into concrete foundations. The tilt angle also set into 10^o facing north which is also easy for rainwater runoff and shade optimization. The height of the panel has been adjusted to 3m as it allows for farming activities. In addition, the panel density is around 50% which is providing higher shading effect that suitable for crops such as Swiss chard and sweet peppers. Lastly, another highlight is the rainwater harvesting system. The gutters run along the bottom edge of the panel's sides then channel into the 10000-liter tanks. The water storage from the rainwater use for irrigation needs contributes to 12.7% of total irrigation.

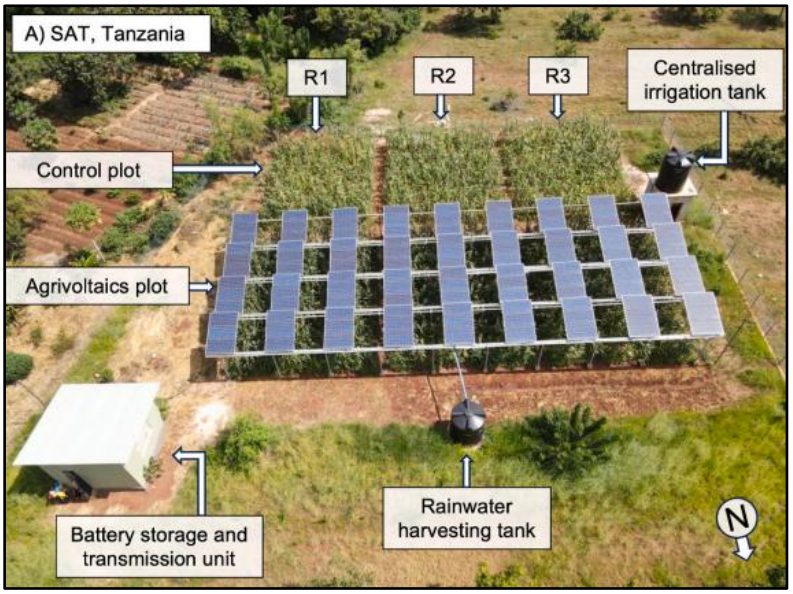

Figure 2. 21: Agrivoltaics design in Tanszania (Boggis *et al.*, 2025)

On the other hand, for the site in Kenya as shown in Figure 2.22 below, the design in a grid-tied which focus on reduce electrical operating cost and improve sustainability. The system reaches a peak capacity of 62.1kWp by using 60 PV modules with 345 Wp each installed in an 800m^2 area. The tile angle is also set at 10^o and mounted on a concrete foundation. Besides, the panels also raised 3m which is for farming activation. The same rainwater harvesting system as in Tanzania has also been applied in Kenya for water storage purpose. For overall, the system has saved electrical energy costing about 5727 USD/year and improved land productivity. The land equivalent ratio (LER) has achieved 1.77 which proves that the agrivoltaics system is having advantages than single land-use purpose.

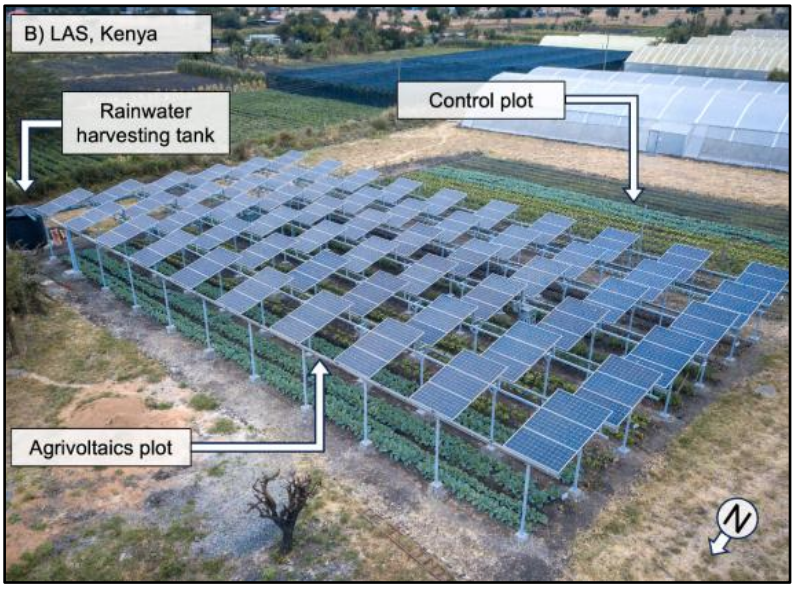

Figure 2. 22: Agrivoltaics design in Kenya (Boggis *et al.*, 2025)

In addition, based on comprehensive research by Toledo & Scognamiglio (2021), there are also different designs of agrivoltaics system around the world which are summarized in the Table 2.4 below.

Table 2.4: Various Agrivoltaics design from different countries

Location	Description	Image
France	Mono-crystalline PV modules at height of 4m. PV panels has been split into "Full Density" and "Half Density". The incident radiation difference is 20% for both densities. Few rows single axis tracking PV systems added to the original system (Inrae, 2024)	

Table 2.4: Continued

Fraunhofer, Germany	Having a size of 0.3 ha and a capacity of 194kWp power generation. The solar modules were mounted 5m above ground. (Energiebau, 2020)	
Babberich, Netherlands	The field has a capacity of 2.7 M Watts peak with semi-transparent PV modules without frames are mounted on the beam with semi-enclosed single-row system. Besides, it also provides better ventilation and reduces pesticides usage. (Baywa-re, 2019)	
La Reunion, French	There are 2 modulus stripes that are deliberately spaced to allow growth of lemongrass. In order to create a more harmonious scene, the ground has not been graded to match the natural terrain. (Ballandras, 2019)	

2.4.4 Sustainable Development Goals (SDGs) and SWOT

Sustainable Development Goals (SDG) are a global initiative which is carried out by the United Nations that have 17 goals to create a sustainable future for every people, balancing economic growth and environmental protection. SDG covers a wide range of important areas in human circumstances which include terminating poverty and hunger, providing quality education, ensuring health and well-being, promoting sustainable energy resources, providing clean water and sanitation, protecting and preserving mother nature, reducing inequalities, building resilient infrastructure, making cities sustainable, and fostering economic growth and decent work. Each SDG's goals are related which means progress in one goal would also support the development of another goal. For example, improving education quality can also reduce the inequalities and promote economic growth. The success of SDG requires cooperation among all walks of life as everyone plays an important role in pushing the goals. (United Nation, 2020)

Agrivoltaics system has strongly support the development of SDG by providing food security and sustainable energy source. Firstly, the main yielding from agrivoltaics which is crop has boosted the development of 2nd goals of SDG which is "Zero Hunger". As agrivoltaics can increase crops yielding by reducing the microclimate effect such as stress heat and maintain soil moisture. This supports food security in rural livelihoods. In addition, the electricity generated by solar power also supports affordable and clean energy resources. It makes the residents reduce reliability on the electricity which is generated from burning fossil fuels and eventually reduce carbon emissions. By generating renewable solar energy alongside farming activities, agrivoltaics have improved in affordable and sustainable in terms of modern energy. Lastly, agrivoltaics also help is economic growth in rural areas as set up a new agrivoltaics areas required jobs related personnel such as PV installation and maintenance. The excess electrical yield can also sell to third parties and act as an extra income for the farmers. Through the integration of clean technology with agriculture, agrivoltaics systems have been proven as an industry that are fulfilling SDG goals by promoting environmental sustainability and social development.

According to the study by Cuppari *et al*. (2024) revealed a comprehensive evaluation of how agrivoltaics system can positively and negatively affect the SDG progress throughout different regions. By applying the SWOT (Strength, Weakness, Opportunities and Threats), this research identifies the direct and indirect effects towards SDG development. From the Figure 2.23 below, the SWOT analysis shows many strengths and opportunities while lesser weakness and strength. In terms of strength, agrivoltaics support zero hunger while also supplying clean energy. Agrivoltaics are dedicated to increasing land productivity by boosting the land equivalent ratio (LER). Besides, agrivoltaics have the potential of increasing waste generation such as worn-out batteries which impact sustainable consumption and production patterns (Goal 12). The implementation of agrivoltaics also required higher starting costs and capital, therefore it makes this system less affordable for smallholder farmers which eventually decreases economic growth. On the other hand, the electrification from farm to rural areas has been supported in implementation of quality education. This is because the development of agrivoltaics system required engineering knowledge to optimize the yielding of system. In this scenario, development of quality education in rural areas would be a potential opportunity to fulfill SDG's fourth goals. As more agrivoltaics system applied in every nation, it would also be having potential to combat climate change (SDG goal 13) as reduce the reliability on burning fossil fuels. Lastly, the threats of agrivoltaics are the gender equality which is due to agrivoltaics powered electrification might increase women's unpaid and paid work together. Based on the research, rural area's women having risk that the electrification increase their overall workload as they needed to continue unpaid domestic work and added new paid work such as working in agrivoltaics farm. However, the threats level is relatively small compared to opportunities and strength.

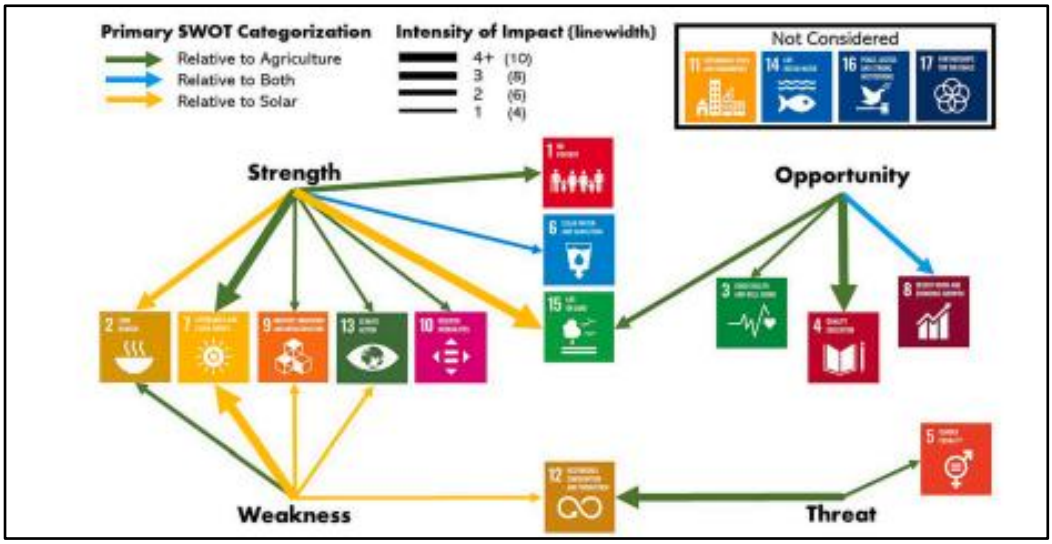

Figure 2. 23: SWOT analysis for agrivoltaics (Cuppari, 2024). Reprinted with permission from Copyright 2024 Elsevier.

2.5 Summary

After conduct the literature review, it is proven that agrivoltanics system is a sustainable method to increase both photovoltaics and agriculture output on the same piece of land in Malaysia. From the configuration of PV layout, it is conclude that 15° tilt angles and 180° (South) would be obtaining the highest photovoltanis output. In addition, in order to minimize the shading affect on the behind PV array, the pitch should be more than or equal to 4m. The pitch distance would also depends on the shading creating towards the crops. Therefore, simulation would be needed to conduct the shading test. Next, for the nominal Pnom ratio is fall between 1.25 to 1.3 to avoid overrated DC current generated by the PV. For the passion fruit, the crop should be growth around 29℃ and required 1500mm rainfall per year. For the passion fruit density, the suggested planted density is 625 plants/hectare. The implementation of agrivoltaics system avoid extensive sunlights and protect excessive heat from passion fruits. Lastly, there is high potential for Malaysia to launch agrivoltaics system as adequate land-use and subsidy from Malaysia government for installation of photovoltaic system. The land equivalent ratio (LER) would be use to evaluate the performance of agrivoltaics system .

CHAPTER 3

METHODOLOGY AND WORK PLAN

3.1 Introduction

This chapter discusses the methodology that was employed for the analysis of the performance and feasibility of the agrivoltaics system. The methodology is primarily simulation-based to investigate the balance between solar power generation and crop yielding on a share piece of land. System parameters such as shade effect, solar irradiance, crop yielding value, panel layout and panel configuration were simulated with proven software tools. This method is aimed at providing a realistic and data-driven analysis of the agrivoltaics system. Lastly, the simulation results obtained form the basis of land-use efficiency and overall system performance determination. The detailed workflow and Gantt Chart outlining the project schedule also included in the appendix B for reference.

3.2 Simulation

As mentioned in chapter 2, the simulation is used to evaluate the yielding of the photovoltaic power output and crop yielding conditions. Throughout the simulation, it provide reference and suggest improvements for optimize the output yielding. In this rearch, PV syst is chosen for simulate electrical power yielding. Besides, the methodology also reveals the calculation method of PVsyst to obtain the simulated values. On the other hand, the explanation of AquaCrop (simulation for crop yielding) calculation would also be provided in this subchapter.

3.2.1 PV Syst

PVsyst, a photovoltaic simulation software with current version 7.4 has been widely used in employs transposition models to convert global horizontal irradiance (GHI) data into plane-of-array (POA) irradiance. GHI is the key parameter that determines the energy output of PV systems and viability of solar energy projects. GHI would be essential for solar energy generation scheduling, grid integration and the management of energy storage systems.

(Imam et al, 2024). In definition, GHI is the amount of solar radiation reaching a horizontal surface (tilt angle = 0°) which combination of direct solar radiation and scattered solar radiation which is scattered by the atmosphere then reaches the surface of PV. Therefore, the higher the GHI, the higher the power output generated from the PV system. Accurately forecasting and modelling of GHI is important for designing and optimizing PV output values which using satellite data and optical flow techniques to predict the GHI. (Prada M.P. Garniwa *et al*, 2023). For the calculation equation below, it shown the calculation of GHI value.

$$GHI = DHI + DNI \times \cos(\theta_z) \quad (3.1)$$

According to Solar Anywhere (n.d.), the GHI value is presented in W/m2 and can be using direct normal irradiance (DNI) and diffuse horizontal irradiance (DHI) to form equation. Notice that due to diffuse horizontal irradiance, it would having different azimuth angle. Therefore, when azimuth angle is equal to 180°, the DNI value would be maximum.

In addition, the POA refer to solar irradiance incident on the surface of a PV module which accounting on specific tilt and azimuth angle. It is different from GHI as GHI only measure solar radiation on a horizontal plane. Therefore, POA is providing more accurate representation of solar energy available for conversion into electrical energy. Accurate estimation of POA also important for designing a reliable PV system that increases the performance. POA is consist of beam (direct) irradiance (E_b), Diffuse Irradiance (E_d) and Ground-Reflected Irradiance (E_g). In addition, PVsyst has been using transposition model, Hay Model to convert the GHI into POA which would be more accurate as it considers the angular dependence of the direct beam and anisotropy of diffuse radiation. Besides, the Hay-model also recognizes the sun's position causes more diffuse light from the direction near the sun. The model firstly has been developed during 1980 by Hay, J.E. & Davies, J.A. According to PVsyst (2025), the estimates sky diffuse irradiance on a tilt surface can be shown in below.

According to Sandia National Laboratories (n.d.) and PVsyst (2025), E_b, E_d and E_g can be calculated as below equations. Firstly, beam irradiance (E_b) can be calculated as below equation 3.2.

$$E_b = DNI \times \left[\frac{sin\ (Hsoli)}{sin\ (Hsol)}\right] \quad (3.2)$$

From the equation above, DNI refer to the Direct Normal Irradiance which measure in W/m^2. Besides, Hsoli and Hsol are sun height on the plane (90^o – incidence angle) and sun height on horizontal plane. After that, the diffuse irradiance (E_d) can be calculated as equation 3.3 below.

$$E_d = DHI \times \left[(1 - K_b) + \left(\frac{1+cos\beta}{2}\right) + K_b \left(\frac{sin\ (Hsoli)}{sin\ (Hsol)}\right)\right] \quad (3.3)$$

Whereas β is the tilt angle and K_b is the clearness index of beam which can be presented as DNI divided by $I_o\ sin(Hsol)$. Lastly, I_o is the solar constant in W/m^2 unit. Next, the Ground-Reflected Irradiance (E_g) is shown in equation 3.4 below.

$$E_g = GHI \times albedo \times \left(\frac{1-\cos(\theta_{T,surf})}{2}\right) \quad (3.4)$$

$\theta_{T,surf}$ is the tilt angle of the surface and Albedo being refer to the fraction of GHI reflected. When dark surface, albedo = 0; when bright surface, albedo = 1. Albedo can be also calculated as:

$$Albedro = \rho \cdot GlobalHor \cdot \frac{(1-cos\beta)}{2} \quad (3.5)$$

where

ρ = Albedo coefficient usually is 0.2

After determing all the POA's parameters, the POA irradiance finally can be calculated by using the above parameters which are represented as equation 3.6 below.

$$POA = E_b + E_g + E_d \quad (3.6)$$

In addition, PVsyst also utilizes the single-diode equivalent circuit model to simulate PV system performance. The single-diode equivalent circuit model is derived from the P-N junction theory which constitutes the core of a solar cell. Based on the basic understanding from P-N junction, the electron-hole pairs would form when sunlight excites the kinetic energy of the electron and resulting in photocurrent. The single-diode model transforms this scenario into the electrical equivalent circuit as shown in Figure 3.1.

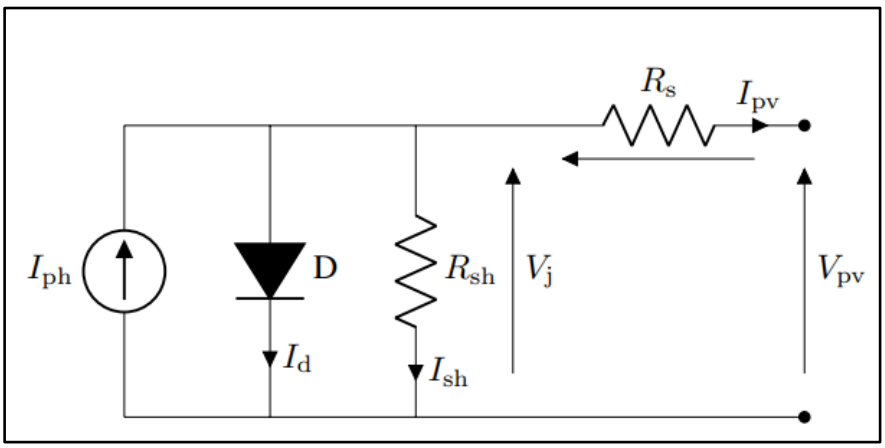

Figure 3. 1: Electrical diagram of single-diode model (Suman *et al.*, 2021). Reprinted with permission from copyright 2021 Elsevier.

According to Cardenas-Bravo et al (2024), the circuit consisting of 5 core parameters. Firstly, the photogenerated current (I_{ph}) is the current generated by light absorption. The ideal diode (D) is a model that recombination losses and series resistance (R_s) represent the resistive loss in the semiconductor and metal contacts. Next, shunt resistance (R_{sh}) accounts for leakage current due to defects of the mechanical parts. Lastly, diode ideality factor (n) means the difference factor with the ideal diode. The photocurrent formula can be calculated as the equation 3.7 below.

$$I_{ph} = I_o \left[exp\left(\frac{V_j}{A}\right) - 1 \right] + G_{sh}V_j + I_{pv} \quad (3.7)$$

From the equation above, I_o represents the saturation current of the diode. In addition, I_{pv} = Photovoltaic current. Besides, V_j is the junction voltage across the diode which can be calculated by $V_j = V_{pv} + R_S I_{pv}$. Next, the equivalent factor of the diode is represented by A. Lastly, G_{sh} is accounting for shunt conductance from the calculation $G_{sh} = \frac{1}{R_{sh}}$.

After determining the photocurrent, the output current (I) would be the focus to identify the output current from the whole system. According to Villalva, M. G et al (2009), the output current can be calculated as:

$$I = I_{pv} - I_o \left[exp\left(\frac{V + R_S I}{V_t n}\right) - 1 \right] - \frac{V + R_S I}{R_{sh}} \quad (3.8)$$

Whereas I_{pv} and I_o are PV current and saturation current. Next, V_t is the thermal voltage of the array with number of cells (N_s) connected in series which can be represent as $V_t = \frac{Ns \cdot k \cdot T}{q}$ as k is the Boltzmann's constant, T is absolute temperature in Kelvin and q is the elementary change.

Other than that, PVsyst (2025), the system evaluates the shading effect by considering three irradiance components. Firstly, for direct irradiance, the shading factor would be dependent on the sun's position of different locations. Next, the diffuse component would be defining an integral overall sky direction which is independent of sun position. After that, the shading factor for albedo which calculated based on geometry and reflection from the ground is also independently of sun position. These shading factors would be combined and become total global shading loss also label as ShdLoss. In addition, electrical shading losses also take into consideration when shaded and unshaded modules are connected in series. PV syst is using unlimited sheds orientation, module strings, and detail 3D module layout to compute the electrical shading losses. These losses would affect direct irradiance (beam component), but diffuse irradiance does not contribute to mismatch. In addition, shading factor table is also considered as a reference during the simulation and Iso-shading diagram illustrates shading conditions across the sun path. Lastly, 3D shading animations also provide a vivid presentation to showcase the shading patterns for better understanding.

From the explanation of theory behind, it is proven that PVsyst is a reliable simulation software to determine the simulated power output from the PV system. In this research, the performance of agrivoltaics systems in terms of PV systems vary under various tilt angles, azimuth orientations and shading conditions. The first step is creating a simulation environment based on corresponds to a region in Ipoh, Malaysia where the solar irradiance is adequate. In addition, Meteorological data such as GHI is imported from the weather database of PVsyst. After that, the grid-connected PV system was selected to fulfill the requirements of the company. Next, the PV modules and inverters models provided by the solar installation company have been used as simulation modules. After that, the first simulation is conducted for various tilt and azimuth angles. This parameter can be modified under the "Orientation" category. Simulations were performed for different tilt angles ranging from 0° to 30° with the increment of 5°. This range reflects practical agrivoltaics designs that optimize the power output and crosscheck the results obtained from the literature review. In Chapter 2 under configuration of solar panel sub-chapter, when the tilt angle reaches approach 0°, the solar power generation would be the highest. However, this software doesn't consider too much in thermal stress analysis, therefore the result simulated would be ideal. In addition, different azimuth angles also need to analyze the effects of east and west-facing orientation. Simulation is planned to conduct different azimuth angles which are 0°, 90°, 180° and 270° representing north, east, south and west. Each combination of tilt and azimuth angles were needed to observe how the deviation from optimal orientation affected the total energy yield per year, losses and performance ratio. PVsyst's simulations process to run the output with different PV configurations and recorded for comparative analysis to identify the optimal tilt-azimuth setup. Other than that, shading analysis is also important in agrivoltaics system due to need for different pitch and row arrangements that allow sufficient irradiance to reach the crops below. There is a 3D scene can be simulating the real life agrivoltaics layout and PV modules can be modeled with required spacing based on typical agricultural needs. Besides, obstacles such as trees and other buildings can be also included in the 3D scene to simulate the real-world shading environment. The simulation animation would reveal the shading movement throughout the whole day.

Therefore, it can observe the shading position and helped determine critical periods when having most energy losses. After completing the system configurations and shading setup, key parameters such as annual energy yield (kWh/kWp), percentage ratio (%), system losses and shading losses are important for comparison and suggestion for further improvement. Lastly, the final step involved interpreting the data and deciding an optimal system design. The best-performing tilt and azimuth angles were determined based on the highest power output. In addition, the shading analysis also provides suggestions about maintaining appropriate spacing and elevation to avoid too much shading and provide adequate sunlight for the crops. Finally, these findings improve the design of agrivoltaics systems that are both increase yielding of agricultural and power output.

3.2.2 Aquacrop

According to Wale *et al* (2022), AquaCrop simulates the yield response to water that irrigates to the crops as the key factor in crop yielding. Other than that, Aqua Crop also needed input parameters including meteorological data, crop characteristic, soil profile, irrigation system and initial soil water condition. For the result simulated, AquaCrop provides the crop water balancing, crop yield formation and total dry matter obtained at the harvest stage. Firstly, AquaCrop does not simulate the leaf area index, while it is calculated the green canopy cover (CC) which is the fraction of the soil surface covered by the green part of the crop also known as the leaves. As the reason for using CC is because it better relates to evapotranspiration and light interception that focuses on how much sunlight is blocked from reaching the soil. Theoretically, the CC indicates the crop conditions over the period. The planted density and crop type would also be the factors of CC values. On the other hand, AquaCrop controls the development of CC daily using stress coefficients which are based on soil water content, salinity and temperature stress.

The first phase of the determining the green canopy cover phase is initial canopy cover (CC_o). It focuses on the time that there is only a small area of soil covered by the young seedings. It also can be calculated by using canopy size per seeding and plant density. It also means the growth of the crop

has just started. Next, the initial canopy cover phase would turn into Canopy Expansion Phase. The CC values would increase over time as the plant grows. This phase is governed by the Canopy Growth Coefficient (CGC) as it defines the rate of expansion per unit of growing degree days (GDD). After that, the crop would expect to reach Maximum Canopy Cover (CCx). The crop has reached its optimal state which is often close to 100%. The peak coverage of green canopy cover has been reached. The value is also influenced by plant density and crop type. Lastly, the last step is senescence. After the maturity of the crop, the green canopy cover gradually decreases. It needs to be concerned about the canopy decline coefficient (CDC) which measure rate of crops senescence.

After that, AquaCrop would calculate the crop transpiration as the next steps of simulation. Crop transpiration refers to vaporization of liquid water contained in plant tissues that release to the atmosphere. (FAO, n.d.). Crop transpiration is important to determine as it is directly linked to biomass production. The Eto needs to determine as it means the standard evapotranspiration which indicates the rate at which water evaporation from soil and transpiration from plants under ideal conditions. The ETo is calculated based on solar irradiance, surrounding temperature, wind speed, humidity and atmospheric pressure. From the equation 3.9 below, the crop transpiration coefficient Kc_{Tr} is proportional to the CC and its caries between 1 to 1.2 for different crops. The term CC^* refers to the adjusted canopy cover and Ks is the stress coefficient.

$$T_r = Ks\ (Kc_{Tr}\ CC^*)ETo \tag{3.9}$$

Based on research by Vanuytecht *et al* (2014), AquaCrop accumulates the daily biomass production to the end of the simulation form daily Tr with the corresponding Eto. The biomass means the mass of plant material but excluding the roots. Simulated biomass production only considers above ground crop production because there are few quantitative data for calculating root biomass. Next, the WP^* is a special factor that indicates how efficiently the plant is converting water into biomass. WP^* is affected by Eto and CO_2 level. As higher the Eto, the hotter the weather. Besides, the higher

the CO_2, it would improve plant growth and water-use efficiency. In addition, the stress factor K_{Sb} is also used to calculate the biomass production which ranges from 0 to 1. The equation to calculate biomass (B) is shown below.

$$B = K_{Sb} \times WP^* \times \sum(\frac{Tr}{ETo}) \quad (3.10)$$

Lastly, the crop yield (Y) would be based on the value of final biomass and a harvest index as calculated using the equation below. The harvest index indicated by adjustment from the reference harvest index (HIo). The reference harvest index is the fraction of biomass that become harvestable yield under non-stress conditions and each crop would have different reference harvest index. In addition, the HIo would also be modified by f_{HI} based on environmental stresses such as water or temperature.

$$Y = f_{HI} \times HIo \times B \quad (3.11)$$

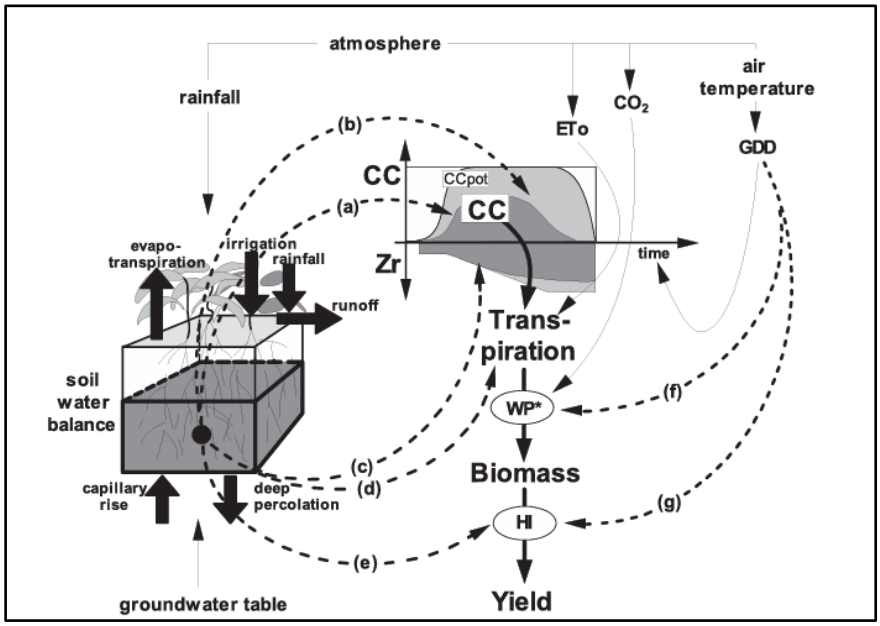

Figure 3. 2: Calculation scheme for AquaCrop (Houma *et al.*, 2021). Reprinted with permission from Copyright 2021 Elsevier

This study is using AquaCrop model which was developed by Food and Agriculture Organization (FAO) to simulate the impact of different shading conditions on crop yield in agrivoltaics system. By reducing the

sunlight and microclimate conditions, AquaCrop can simulate crop productivity based on water availability and climate factors. Since AquaCrop does not include passion fruit for simulation models, tomato would be replaced with simulation crops as it has similar vine structure. Before the simulation starts, detail local climate data would be needed for AquaCrop software as the input parameters. The climate data such as monthly min and max temperature (℃), rainfall (mm), solar radiation (MJ/m^2) and sunlight hours would be obtained from the Malaysia Meteorology Department (MetMalaysia). After that, reference evapotranspiration (Eto) is also needed as the input parameter for AquaCrop. Eto rate is required to ensure adequate water to meet crop demands and measure the water lost through evapotranspiration from a hypothetical, short, actively growing grass surface and well-watered. (Marinwater, n.d.) According to Raes e& Munoz (2009) as cited in Scherrer et al (2022), Eto is based on the Penman-Monteith approach which is more consistent and accurate in both arid and humid climates. The Penman-Monteith approach also has been used in ASCE and European studies widely. A few parameters should be determined before calculating the Eto.

Firstly, the psychrometric constant would be calculated as below equation 3.12. From the equation 3.12, γ is the psychrometric constant (kPa $℃^{-1}$) and P is atmospheric pressure in kPa. Other than that, λ is latent heat vaporization with the constant of 2.45 MJ/kg and C_p is specific heat at constant pressure with the constant of $1.013x10^{-3} kg^{-1}℃^{-1}$. Lastly, ε is ratio molecular weight of water vapour or dry air in the value of 0.622.

$$\gamma = \frac{C_p P}{\varepsilon \lambda} = 0.664742 \times 10^{-3} P \quad (3.12)$$

Next, the saturation vapour pressure at the air temperature, $e^o(T)$ can be calculated as below equation 3.13.

$$e^o(T) = 0.6108 \, exp\left[\frac{17.27T}{T+237.3}\right] \quad (3.13)$$

After that, the below equation shows the saturation vapour pressure (e_s) in kPa Based on the terms, e^o (T_{max}) is the saturation vapour pressure at

the mean daily maximum air temperature (kPa) while e^o (T_{min}) shows saturation vapour pressure at the mean daily minimum air temperature (kPa).

$$e_s = \frac{e°(T_{max}) + e°(T_{min})}{2} \quad (3.14)$$

Other than that, actual vapour pressure e_a in kPa would also be considered as an important parameter to be determined while T_{dew} is the dew point temperature ℃.

$$e_a = 0.6108\, exp\left[\frac{17.27T_{dew}}{T_{dew} + 273.3}\right] \quad (3.15)$$

Next, the slope of saturation vapour pressure curve at air temperature (Δ) in kPa $℃^{-1}$ would be determined and using the equation 3.15 below.

$$\Delta = \frac{4098\left[0.6108exp\left(\frac{17.27T}{T+237.3}\right)\right]}{(T+237.3)^2} \quad (3.16)$$

Other than that, the wind speed U_2 in m/s can also be calculated which is shown in equation 3.16. The U_z is wind speed that measures at z m above the ground surface and z is the height of measure which measures above ground surface.

$$u_2 = u_z \frac{4.87}{ln(67.8z-5.42)} \quad (3.17)$$

Afther determine all the parameters, the reference evapotranspiration (Eto) is the unit of mm/day can be calculated as equation 3.17. The R_n refers to the net radiation at the crop surface in MJ m^{-2} day^{-1}.

$$ETo = \frac{0.408\Delta(R_n-G)+\gamma\frac{900}{T+273}u_2(e_s-e_a)}{\Delta+\gamma(1+0.34u_2)} \quad (3.18)$$

After entering the climatic data, the simulation scenarios were designed to reveal different shading conditions. The shading conditions are to be tested in 20%, 30%, 40% and 50% with different panel density conditions.

The higher the shading conditions, the lower the solar irradiance, surround temperature and humidity. Next, the shading level would adjust the fraction of solar radiation (FRS) and affect the crop canopy in Aqua Crop's field. In addition, tomato crop model was selected and modified to reflect yielding condition in Malaysia. Besides, the irrigation schedule and other parameters have been set as default parameters. In addition, in order to broaden the scope of the simulation and evaluate agrivoltaics sustainability for different crops, additional crops such as sunflower and sugar crane were also selected for simulation models alongside with tomato crops. Each of the plants would have different characteristics, tomato is prior to being chosen as substitute for passion fruits due to similar vine-growing patterns. Next, sunflower is a tall and heliotropic crop with singular harvest cycle. As the growth of the sunflower is strongly reliable on amount of sunlight as drastically decreased of light intensity would reduce the leaf-area of sunflowers. (Samidjo, 2019). Lastly, sugarcane is a high-biomass and long duration crop with heavy dense green canopy. It is also used to compare with the yielding of tomato and sunflower. By incorporating the three different crop models, the simulation function as evaluates the different agrivoltaics layout that affect short-terms versus long-terms crops and light-intensive versus moderately shade-tolerant crops. In a nutshell, multi-crop approach aims to identify feasibility of integrating a wider variety of crops under agrivoltaics in Malaysia.

3.3 Site

The agrivoltaics system is specially designed for passion fruit farm, Hami Ecofarms which located in Ipoh, Malaysia. The exact coordinate of the location is 4.4986, 101.0447. In addition, the altitude of the location is 33 meters with 108.27 feet. Before the planning of implementation of agrivoltaics system, Hami Ecofarms had already planted passion fruits as minority crop production in the farm. Based on the planning of the owner of the farm, the rough sketch of layout of the agrivoltaics system is shown as below figure 3.3.

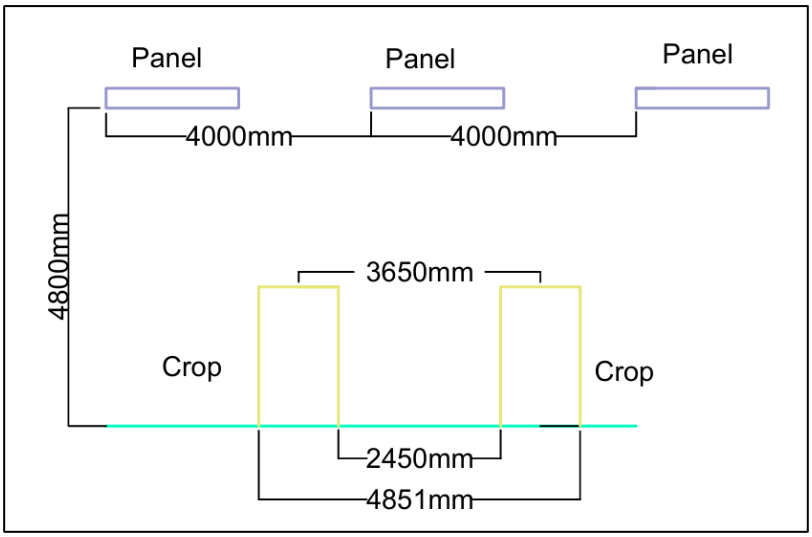

Figure 3. 3: Rough sketch layout of agrivoltaics system

From the planning, the passion fruit estimated height is 2.1m and the distance of the crops is 2.4m. Based on these estimation, the configuration of the PV layout can be determined as follow description. Firstly, the PV height is set to 4.8m because the farms also need transportation to pass through the farms which are purpose in cultivation. In addition, the PVs are designed to face towards south direction and tilt angle with 15° based on the results from literature reviews to obtain optimal electrical power yielding. Lastly, the pitch of the PV panels would be adjusted to 4m to 5m. The actual pitch meters would be confirmed once having site visit and conduct shading simulation.

On the other hand, the area of the farms also important parameters to determine the overall yielding of the agrivoltaics system. The result can be obtained from Google Satellite and using scaling method to measure the dimensions of the farm. The map and direction are shown below the figure 3.4. The length and width of the farm are 43.66m and 90.97m which corresponds to 3971.75m^2. Besides, from the satellite picture, it can be shown there are 25 rows of passion fruit crops.

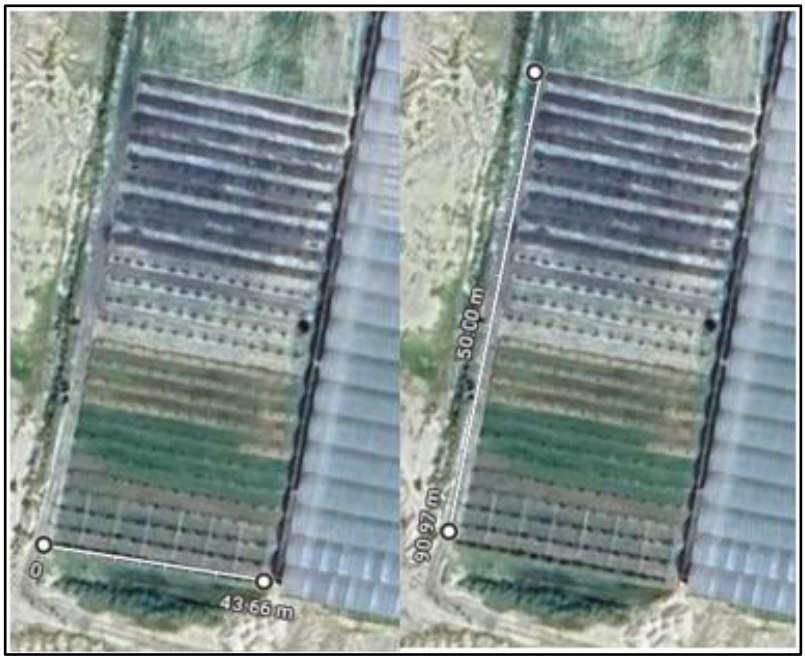

Figure 3. 4: Dimension of Hami EcoFarm

Lastly, from the direction of Google Maps, the front part of the farm is facing south direction with an azimuth angle of 191°. Therefore, it is having optimal azimuth angle.

Figure 3. 5: Azimuth angle

3.4 Agrivoltaics Design

The design of agrivoltaics would direct affect the power output of photovoltaics and crop yield. Therefore, this section would introduce the PV model and inverter model that would be use in photovoltaics area. Besides, the designs are plan as full-density and medium-density PV array to identify the shading effect and compare overall output. Other than that, structural simulation of PV rack would also plan to conducted for enhancing during different load conditions. Lastly, land equipvalent ratio would be needed for evaluate the performance of agrivoltaics system.

3.4.1 Photovoltaics panels and inverter

The specification of the PV module is provided by a solar company which is named JA Solar. The exact model is JAM66D45 620W which has maximum power (P_{max}) of 620W. Further information on this PV modules would be obtained from the official JA Solar website. The parameters are tested under Standard Test Conditions (STC) which have 1000 W/m^2 irradiance and 25℃ of cell temperature. By using STC, manufacturers can specify the performance of panels and consumers can compare them among other brands based on their STC rating. (Seaward, 2025) However, in actual real-world, the panels' performance would be different for STC performance ratings as affected by weather, shading and dust conditions. The information of panels and inverter can be summarise in Table 3.1, Table 3.2 and Table 3.3.

Table 3.1: Electrical parameters of JAM66D45 620W under STC testing

Rated Maximum Power (P_{max}) [W]	620
Open Circuit Voltage (V_{oc}) M	48.50
Maximum Power Voltage (V_{mp}) [V]	40.21
Short Circuit Current (I_{sc}) [A]	16.13
Maximum Power Current (I_{mp}) [A]	15.42
Module Efficiency (%)	23%
Power Tolerance	0 to 3%

Table 3.2: Mechanical Properties of JAM66D45 620W

Cell	Mono
Weight	33.1kg
Dimension	2382±2mm x 1134±2mm x 30±1mm
No. of cells	132 (6x22)

In addition, an inverter would also be needed during the installation of the PV system. In the solar panel system, the inverter functions as converting the direct current (DC) into alternating current (AC) which is used for homes's applications. Solar inverters would have Maximum Power Point Tracking (MPPT) function which optimizes the power output from the panels by filtering the ideal voltage and current for maximizing the energy extraction. Without the MPPT, the inverter might overdraw or draw too little current from the panel which leads to reduced efficiency. During cloudy conditions, MPPT help to boost the power output by 10-30%. The inverter used is from Solis company which models S5-GR3P 20K.

As part of the simulation methodology, PVsyst would use the electrical parameters of the selected PV panel and inverter. Inputting these data into the PVsyst would help in accurate modeling of the system performance and energy yield estimation. In addition, the dimensions of the PV module are needed for space estimation and arrangement of PV layout. Lastly, the weight of the PV module would be able to do static load analysis which tests the supportive structure analysis.

Table 3. 1: Electrical Parameter of S5-GR3P 20K

Input DC	
Recommended max. PV power	30 kW
Max. input voltage	1100 V
Start-up voltage	180 V
Rated voltage	600 V
Max. input current	32 A
MPPT voltage range	160 - 1000 V
Max. short circuit current	40 A / 40 A
MPPT number / Max. input strings number	2 / 4
Output AC	
Rated output power	20 kW
Max. apparent output power	22 kVA
Max. output power	22 kW
Max. output current	31.8 A
Power factor	> 0.99 (0.8 leading - 0.8 lagging)

3.4.2 Layout Design

From the dimension obtained from Google satellite, it can be planned to simulate 2 design of PV layout which are full solar density scenario and medium soalr density scenario with fixing tilt angle to 15° and facing south 11°. For full density scenario, PV modules are arranging closely and lower pitch across the full yield. The design would maximize energy generation but allows limited sunlight to absorb by the crops. From the dimension obtained of the PV modules, one piece of PV panel would be occupied 0.068% of the total field area. Firstly, for the full solar density layout, the pitch distance is adjusting as 4m based on the results from the literature review. For each row, it is estimated that there are at most 38 PV panels that can be arranged in a row. With the constraint of 4m pitch distance, the farm can place 23 row of PV panels. On the other hand, when applying half solar density scenario, the pitch distance is increased to 6m. The PV number in a row remains at most 38 PV

panels, however the total number would be reduced to 15 rows. This is because the half solar density scenario means an alternate row of PV modules has been removed in facts increase the space when compared to full solar density layout. The reduction of density would increase the solar irradiance penetrate to the crops. Therefore, this layout would aim to balance crop growth with moderate electrical energy production. The electrical power output would be simulated in PVsyst and compare the percentage drop when applying medium-density layout.

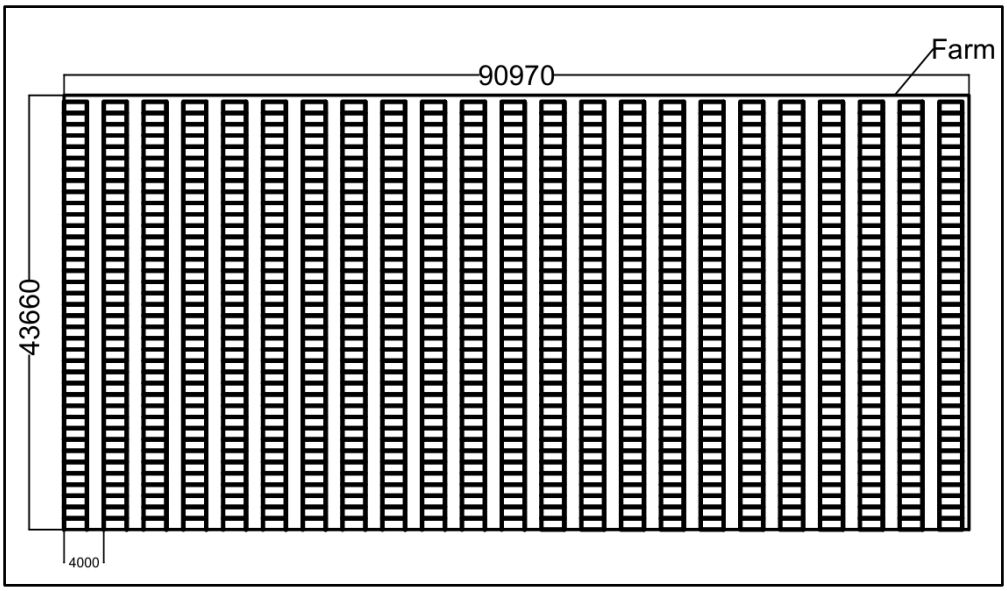

Figure 3. 6: Full solar density scenario

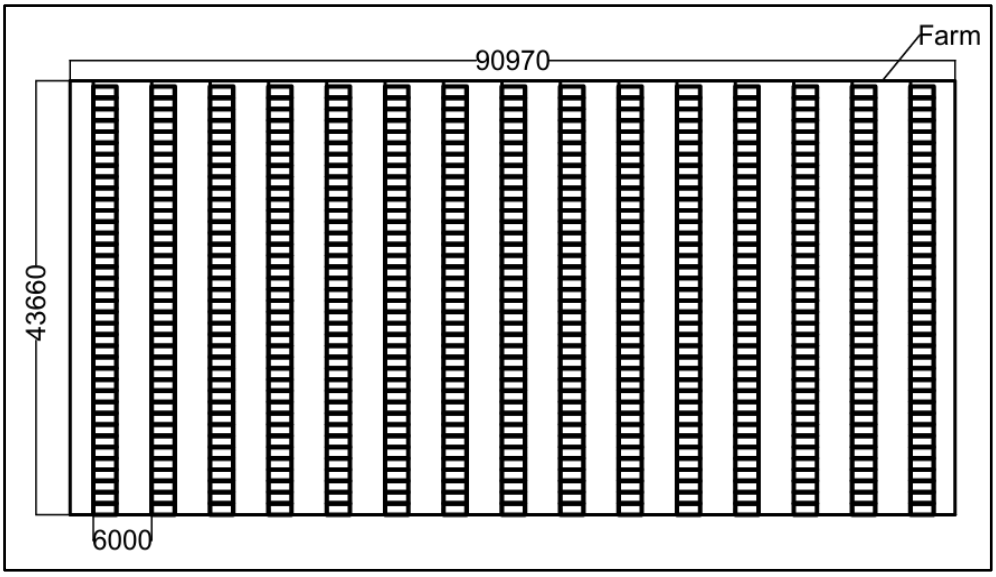

Figure 3. 7: Half solar density scenario

3.4.3 Structural support and mounting rack

The mounting of the PV panels would be mainly based on strength and rigidity. Therefore, a solid foundation is required as a fundamental support of the PV system. Firstly, the choice of the foundation is among helical piles or ballasted foundation (concrete block). Before building the foundation, it is required to do soil analysis such as soil texture classification and penetration test which is needed for actual site visit. Generally, helical piles are considered more rigid than ballasted foundation due to anchored deep into the ground. However, helical piers usually cost more than concrete support. On the other hand, once the optimal amount of PV modules has been confirmed, the design of rack is required. The mounting rack is usually used beam for horizontal support and column for vertical structural support. The number of column and beam are based on the number of PV panels. In addition, the mounting point of the PV panels as shown in the appendix c below. The strength of the supportive structure would be simulated in SolidWorks by applying static load test and wind-load test. Lastly, the density of the PV panels would affect the amount of structural support needed and eventually related to installation fees. Therefore, optimal design of agrivoltaics system is needed to reduce unnecessary costs.

3.4.4 Agrivoltaics System Evaluation

The main purpose of this research would be evaluating the effectiveness of increase economic and save cost in agrivoltaics system after implementation of agrivoltaics system. Therefore, the Land Equivalent Ratio (LER) equation, which has been extensively discussed and justified during literature review is used to assess the land-use efficiency. However, the LER value cannot be determined during the design phase. It must instead estimate through simulation based on input parameters such as crop yield value, solar irradiance, system layout and shading analysis. These factors prove a theoretical benchmark that improve system optimization before physical implementation of agrivoltaics system. Besides, the actual LER value can only be calculated after the agrivoltaics system has been deployed and both crop and energy yields have been measured over a period. Therefore, simulations and small scale experiment are important in planning and decision-making process

which validate through real-world performance data. The LER ratio obtained at the end of the research is consider as expected LER ratio.

3.5 Experiment Setup

Due to fund and land area constraints, it would be the limitation of constructing the experiment to verify the output of electrical and crop yielding. Therefore, the actual experiment carried out would be in small scale which fulfilling the cost factors and easy for research students to construct.

The actual experiment would be studying the crop yielding which cause by the shading effect from the soalr panels. To getting abundant sunlight, the experiment would be conducted at UTAR Sg Long KB 12th floor which is the rooftop from week 4 (14/7/2025) to week 12 (12/9/2025) for 2 months duration. In this experiment, it would needed for collect growth data from the crop by measuring the average fruit size, crop height, number of new leaf and existing fruits. Besides, PAR (Photosynthetically Active Radiation) would be also measured for different condition of the shading towards the crop. The condition tested would be open condition (no shading), partially shaded condition and heavy shaded condition.

3.5.1 Photovoltaic Rack Setup

The aluminium rack as shown in Figure 3.8 would be use as the experiment apparatus and simulating the real-site conditions. There is 2 sturucture would be use in the experiment and they are borrow from Dr Lim Boon Han.

Figure 3. 8: Photovoltaic Rack

In addition, to create shading effect, the hollow corrugated plastic PP board would be use instead of using actual photovoltaic (PV) panel. This is because the board would not use to provide shading purpose as the same function as PV panel. The plastic PP board would be cutted into the desire site to fit into the slot of the PV structure as shown in Figure 3.9. On the other hand, for another structure, due to lack of aluminium rod that can create the slot, a large piece of plastic PP board would be use to act as shading effect and fixed by using nylon cable tie.

Figure 3. 9: Panel installation on the PV rack

Although there is structure provided which is convenient to be use, however the tilt angle cannot be adjusted which is fix at 35°. The tilt angle would be slight different from the desired tilt angle (15°) and causes more sunlight can pass through the structure. Therefore, in the actual conditions, it can be expected that the yielding would be slightly lower. On the other hand, the azimuth angle has been corrected to 191° from North which is exactly identical to the site's azimuth.

3.5.2 Experiment Crop

During this simulating experiment, the passion fruit would not be used as experiment crop model. This is due to lack of agricultural knowledge to take care of passion fruit as it required more effort. Instead, calamansi plant would be use as experiment crop model. This is due to calamansi plant generally would below 1.2m and tolerate a wide range of soil types. Besides, it also having fewer pest issues and is less prone to fungal diseases compared to

passion fruit. On the other hand, passion fruit required a higher PV structure (4m above) to conduct the experiment as the average passion fruit is more than 2m. Besides, it also needs regular pruning, training, and fertilization to maintain a healthy growth. Besides, due to time limitations for the experiment to conduct, the growing period for calamansi plant would be faster than passion fruit therefore easy can observe the experiment results.

3.5.3 Experiment Variable

To conduct this experiment, it would having 3 different conditions. As refer to Figure 3.10, there is 3 location that the plants would be placed.

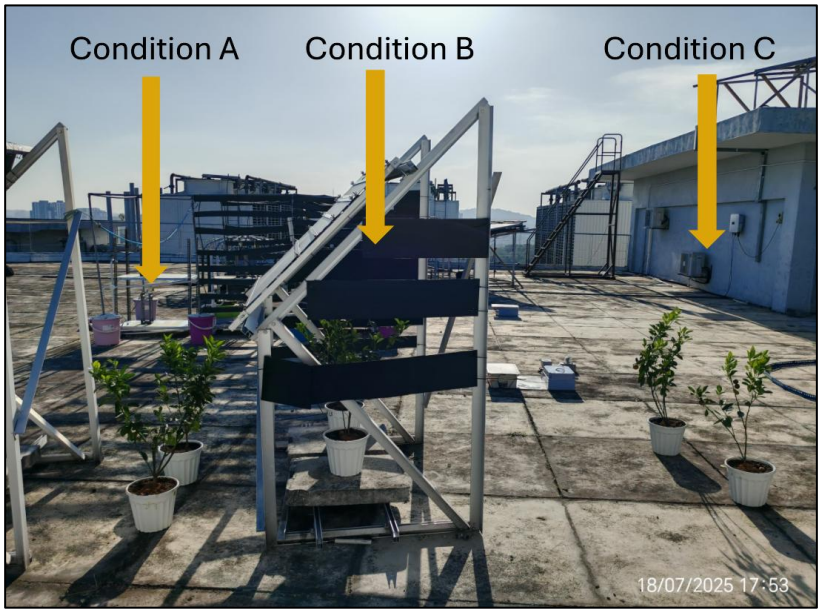

Figure 3. 10: Crop location for 3 different conditions

For the condition A, it is simulating the site conditions for full solar density solar panels. When compared to Figure 3.6, it can be observed that the plant is placed between 2 soalr panel rack structures. It also can be considered as partially shaded conditions as at the noon and afternoon time, the sunlight can be pass through the crops. Next, for conditions B, it can refer as heavy shaded conditions as the sides of the structure has also been covered by the plastic PP board to block additional sunlights. Lastly, condition C can be categorise as open condition as the crop can receive the most sunlight as doest

has the structure near to it. Therefore, it would place further away from the condition A and condition B.

In addition, to observe the characteristic of the plant, each crop would be having different number to be represented as show in Figure 3.11.

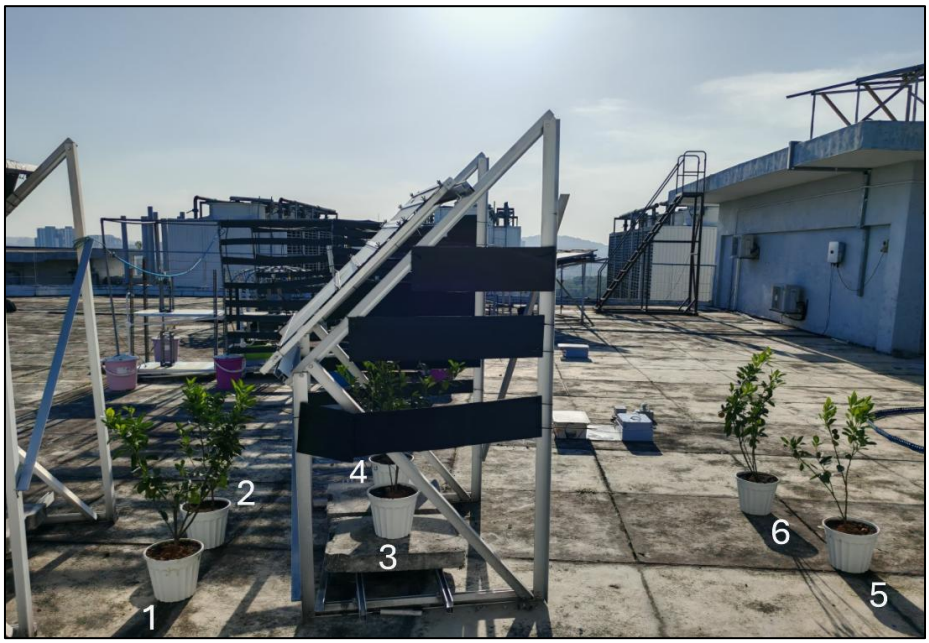

Figure 3. 11: Labeling for each crop

3.5.4 Photosynthetically Active Radiation

Photosynthetically Active Radiation (PAR) would be refer to the portion of sunlight that plant can be use for photosynthesis. As plants only use light in the 400nm to 700nm range of the spectrum, the range is considered as photosynthetically active radiation because it convert the carbon dioxide and water into sugars which also called as photosynthesis.

In addition PAR is usually measured the light intensity over an area and the unit using is μmol photons per square meter per second (μmol/m^2/s). The higher the unit, it indicates high amount of light particles would be useful for photosynthesis hit one square meter for every second. Therefore, more PAR means more energy for photosynthesis which lead to better growth.

In this simulating experiment, the PAR value indicates the actual amount shading conditions towards the crop and supported data for plant's growth conditions.

3.5.5 Photosynthetically Active Radiation sensors setup

For measuring the Photosynthetically Active Radiation (PAR) values, there are 3 PAR sensor has been installed near the crops. PAR sensors are using RS485 communication standard which allows ling-distance, noise-resistant data transmission with using 2 signal wires, VCC 24V and GND wires. Therefore, all the sensor data would be logged through the RS485 converter and into the data logger.

Figure 3. 12: RS485 Converter

For the data logger, Raspberry Pi model 4B would be use for record the PAR value. Insides the Raspberry Pi model 4B, the programe used in Python language has been command the PAR sensors to record data since 7am to 7pm everyday for different conditions. After that, all the PAR values would be save in the Txt file for future results reference. Firstly, to set up the Raspberry Pi, the Pi 4 operating system would has to be burn into the 32gb SD card and plug into the Raspberry Pi. After that, code would be written in Thonny application and setup the minimalmodbus connection by activate the virtual environment. Lastly, once the code has been debug, the Raspberry Pi would become the data logger for this experiment. The Python code can be founded in the appendix D.

On the other hand, since there is 3 PAR sensors, 1 RS485 converter and 1 DC power supply jack, Daisy chain would be use to connect and powered up all the sensor. Dasiy chain is the wiring method commonly used in connection of RS485 sensor which connected multiple devices one after another in parallel along the same communication line and power line. When refer to the Figure 3.13, it showing the connection circuit for overall system. As RS485 is a differential bus, it would need 2 120Ω to place at the start of the bus and end of the bus to prevent signal reflection. The benefit of using Dasiy chain connection instead of different connection method such as Star thopology is due to it can handling long distance and stable data transfer.

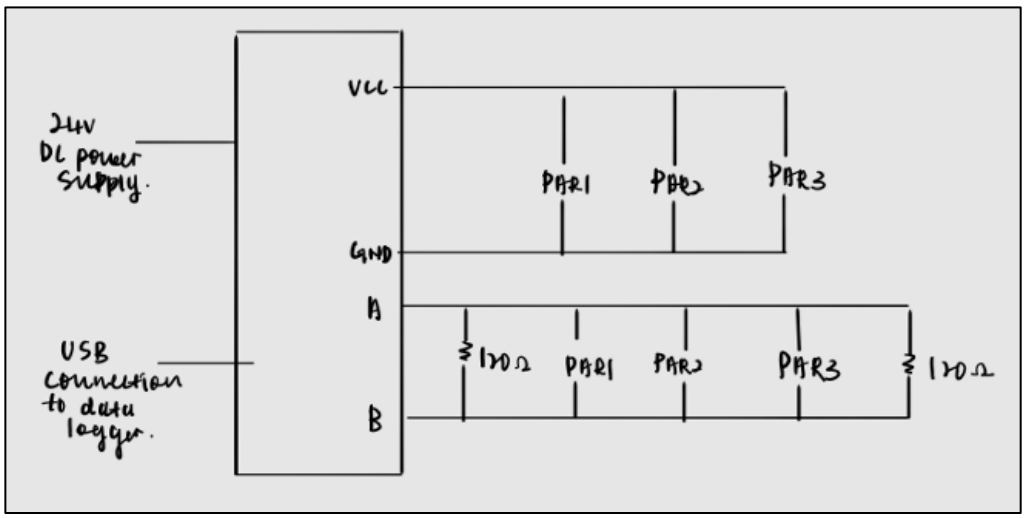

Figure 3. 13: Connection of sensors using Dasiy Chain

Besides, the sensors are planned to put at 1.2m height from the ground as it would make sure it would always higher than the plant height. Therefore, 3 customized sensor support stand has been fabricated at the UTAR mechanical workshop. The materials used to fabricate the sensor stand is from waste scrap which also fulfill the circular economy ideology. Figure 3.14 showing the exact sensor support which all are the material is mild steel. To prevent rusting issues, spray paint has been painted at the surface of the stand. Other than that, 2 concrete waster which obtained from UTAR civil lab would also placed at the bottom of the sensor stand as more stable foundation.

Figure 3. 14: Sensor Stand

Lastly, all the wire connection from the sensor would be directed to the waterproof box and place below the PV structure as shown in Figure 3.15. Inside the waterproof box, there are 2 gang socket plug, Raspberry Pi model 4B and a RS485 converter. In addition, the waterproof box would also placed inside the polystyrene box for extra waterproof guarantee.

Figure 3. 15: Location of the waterproof box

3.5.6 Result measurement

To achieve the ideal result, each plants has been treated equally. Firstly, the watering period is around 10am to 1030am everyday at UTAR KB rooftop. The water amount would be 350ml for each plants and fertilize once a week. The reason of watering plant during morning is avoid heat stress that might be create a sudden temperature shock to hot soil and roots. Besides, the croplets on leaves under strong sunlight may also act like tiny lenses which increase the chance of getting leaf burn.

For the measurement to indicates the growth conditions. Firstly, the plant height would be measured. The height is measure from the top of the leaf edge to the bottom of the pot by using tape ruler. Next, the fruits size would also be measured in diameter (mm) by using vernier caliper and number of new leaf & fruits would be counted. Lastly, the PAR values would be recorded everyday from 7am to 7pm then record into the txt. file. The physical collect crops' measurement would be taken for every Friday at noon.

3.5.7 Plants Evaluation Method

From the experiment, the plants has been measured its height, number of new leaf, number of fruits and average frutis's diameter to evaluate the growth performance of the plants in different conditions. Therefore, each plants has 4 parameters to evaluate the performance of the plants which has been considered as Multi-Criteria Decision Analysis (MDCA). MDCA is a structured method to decision-making that helps user to evaluated and prioritize options based on multiple, often conflicting criteria. (Dean, 2020).

Based on MDCA, Techniques for Order of Preference by Similarity to Ideal Solution (TOPSIS) is one of the MDCA's approach which helps in ranking and selecting the best alternative from various option based on multiple criteria. Therefore, in case od this experiment, TOPSIS would be needed to calculate which categorise of plant having the highest rank (best growing condition), therefore the highest value representing the best alternative. The advantage of applying TOPSIS is simple to implement and mostly important that it can handles multiple criteria.

There are few steps for TOPSIS approaches to be carry out. Based on Chakraborty (2022), the first step is form the performance rating for each alternative against each attributes can be displayed in the form of a decision matrix. From the matrix, the row in the matrix represent different parameters values while the column values are the recorded specific parameters value for various alternatives.

$$X = \begin{bmatrix} x_{11} & \cdots & x_{1j} \\ \vdots & \ddots & \vdots \\ x_{I1} & \cdots & x_{IJ} \end{bmatrix} \tag{3.19}$$

Next, each performance rating x_{ij} in X is divided by its norm which the normalized matrix (y_{ij}) can be calculated as below equation. The porpose of normalized is to provide a fair comparison among other factors. If without the normalized process, the larger values would dominate the analysis which lead to the result skewing to one of the sites. For example, the factor A recorded in ton unit while factor B recorded in micro unit, the factor A would

be dominating. Therefore, normalized process converts all the metrics into common scales (0 to 1).

$$y_{ij} = \frac{x_{ij}}{\sqrt{\sum_{i=1}^{I} x_{ij}^2}} \tag{3.20}$$

Whereas

$i = 1,2, \ldots., I$

$j = 1,2, \ldots., J$

$$Y = \begin{bmatrix} y_{11} & y_{12} & \cdots & y_{1J} \\ y_{21} & y_{22} & \cdots & y_{2J} \\ \cdots & \cdots & \cdots & \cdots \\ y_{I1} & y_{I2} & \cdots & y_{IJ} \end{bmatrix} \tag{3.21}$$

After that, weighted and normalized performance matrix would be calculated by multiplying weight factor with the normalized rating. The weight factor is based on user preference to decide which parameters are more important than others. The weight factor is between 0 to 1 which applying 1 to one of the factor would make other factor loss its measurement value.

$$v_{ij} = Weight\ factor * y_{ij} \tag{3.22}$$

Whereas

$i = 1,2, \ldots., I$

$j = 1,2, \ldots., J$

$$V = \begin{bmatrix} v_{11} & v_{12} & \cdots & v_{1j} \\ v_{21} & v_{22} & \cdots & v_{2j} \\ \cdots & \cdots & \cdots & \cdots \\ v_{I1} & v_{I2} & \cdots & v_{IJ} \end{bmatrix} \tag{3.23}$$

Next, the positive and negative ideal solutions would be determined based on the highest and lowest value from each factor. For example, if in term of benefit, the maximum would be positive ideal solutions. On the other hand, the if in term of cost, the minimum values would consider as positive ideal solution. It depends on how many factor in the system, if there is 5 factor,

there would be 5 positive and negative ideal values from each representing factors.

$$A^* \ (positive\ ideal\ solution) = \left[v_1^*, v_2^*, \ldots., v_J^*\right] \quad (3.24)$$

$$A^- \ (negative\ ideal\ solution) = \left[v_1^-, v_2^-, \ldots., v_J^-\right] \quad (3.25)$$

Lastly, the separation measure which consider as the distance of each alternative rating from both the positive and negative ideal solutions also needed to be calculated. The separation measures would be the input calculation for the overall TOPSIS score. Finally, the overall TOPSIS socre for each alternative would be determined.

$$S_i^* = \sqrt{\sum_{j=1}^{J}\left(v_{ij} - v_j^*\right)^2} \ ; \ S_i^- = \sqrt{\sum_{j=1}^{J}\left(v_{ij} - v_j^-\right)^2} \quad (3.26)$$

$$V_i \ (TOPSIS\ Score) = \frac{S_i^-}{S_i^- + S_i^*} \quad (3.27)$$

3.6 Simulation Setup

From this research, PVsyst would be using as the simulation software to get the yielding of the solar energy in different scenarios. On the other hand, the crop simulation would be using AquaCrop to compare the actual yielding between the theroritical and actual yielding.

3.6.1 Simulation – PVsyst Setup

Before starting the simulation, the panel and inverter specifications need to be insert to the software as an input. This is due to the panel and inverter are new to the market therefore PVsyst database doesn't having the information to run the simulation.

Firstly, the spec of the panel is provided by the solar company which is name as JA Solar JAM66D45. The information of panel would be added to the database and follow the spec (table 3.1). From the Figure 3.16, the information would be fill up and save in the PVsyst data base.

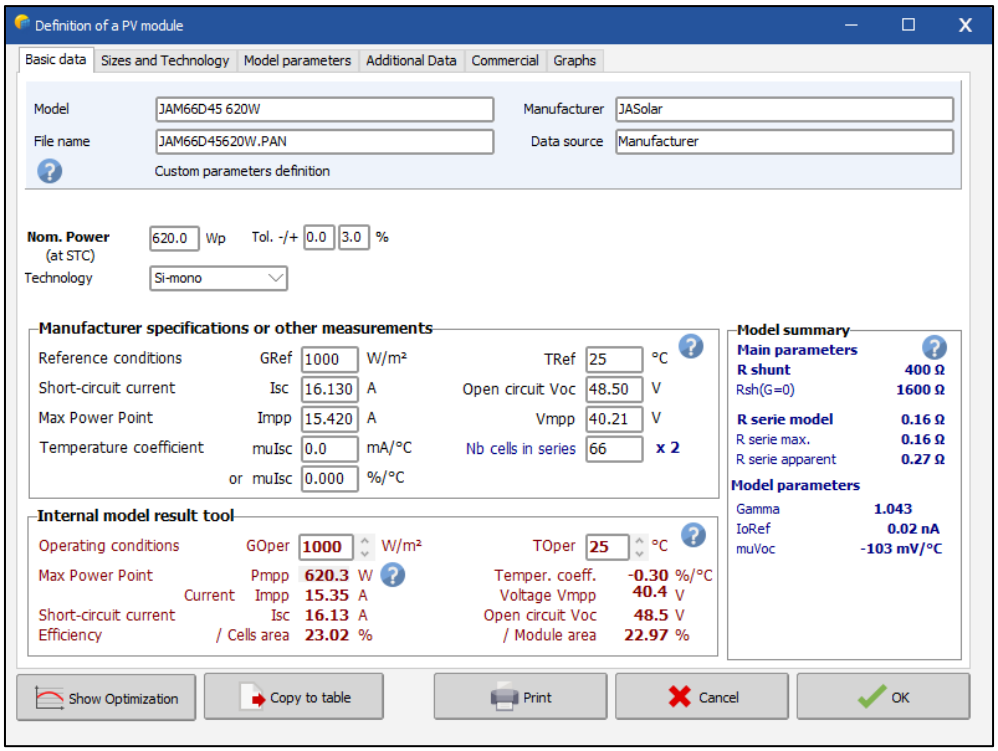

Figure 3. 16: Specification for Solar JAM66D45 insert in PVsyst

On the other hand, the inverter, Solis S5-GR3P(3-20)K's specification also provided the solar installation company. Figure 3.17 indicates the electrical information for the inverter.

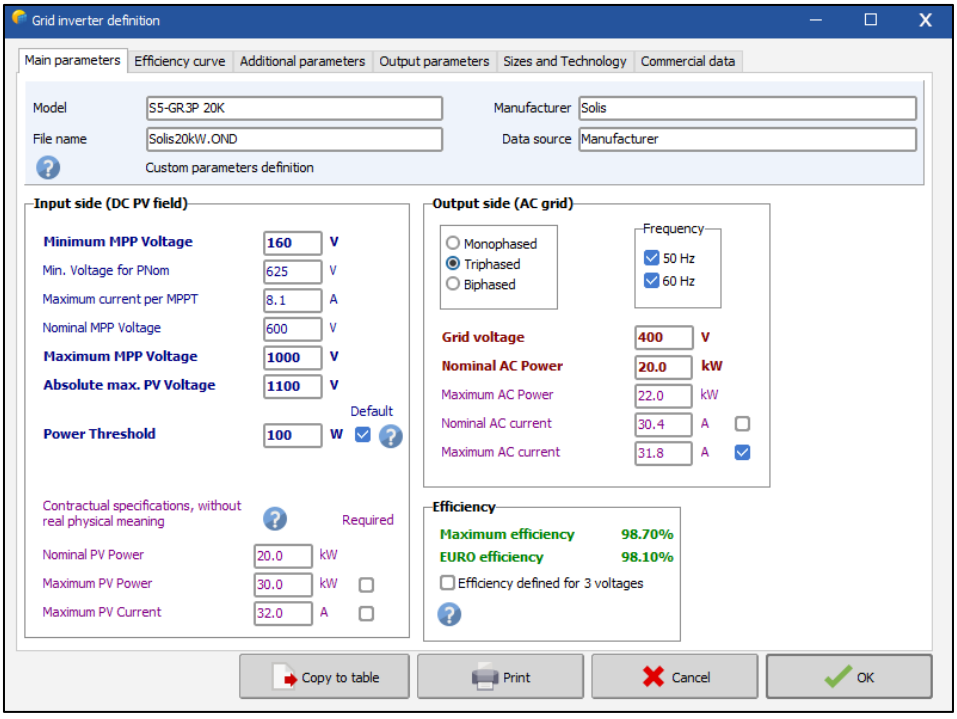

Figure 3. 17: Specification for Solis S5-GR 3P 20K insert in PVsyst

Other than that, the geographical sites also would be need to set as the PVsyst does not has the actual location for Hami Eco Farm. Firstly, the location coordinates can be determined from the Google Maps and insert the coordiantes to the PVsyst to pin point the location as shown in Figure 3.18. On the other hand, the whether data would be obtained from the Meteonorm 8.1. After choosing the right location and whether data, the sun path can be simulated as shown in Figure 3.19.

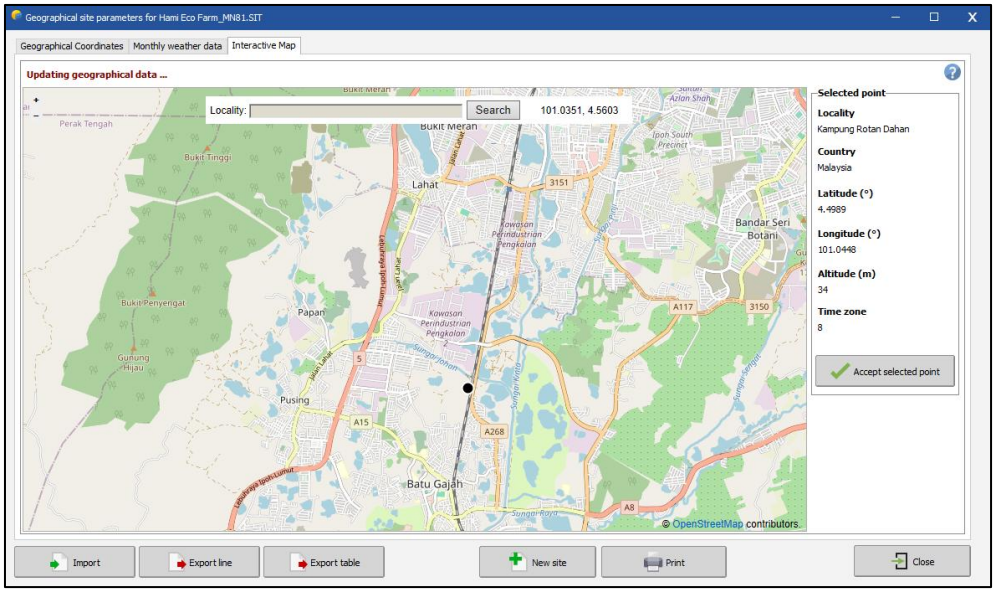

Figure 3. 18: Pin Point location for Hami EcoFarm

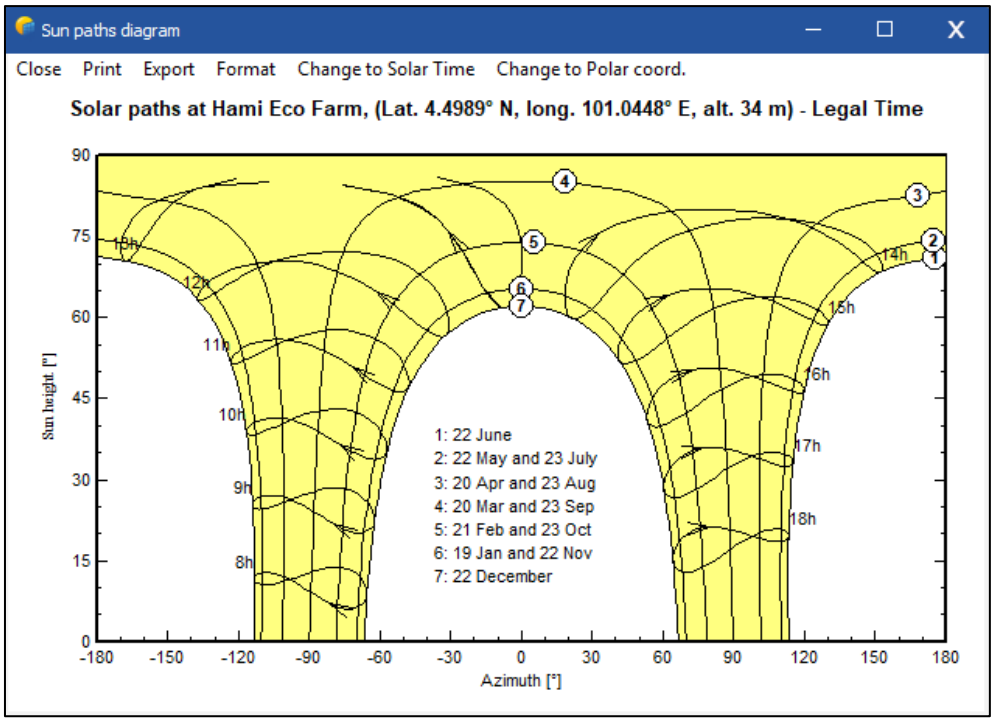

Figure 3. 19: Sun Path at Hami EcoFarm

Lastly, for the simulation settings, the project design and simulation would be choosing grid connected as the additional electrical power generated from the PV panel would be offset towards the electrical bills instead of saving power in the battery.

3.6.2 Simulation – AquaCrop

The important input parameters for the simulation setup would be the whether data for Malaysia. All the whether data of Malaysia can be downloaded at Malaysia Meteorological Department. Although the site location near Ipoh, the whether data is taken for whole Semenanjung Malaysia due to the whether difference is not significant. Due to there is differences in growth conditions, the whether data for each conditions would also be different by shading percentage differences.

Firstly, the whether data for open conditions can be refer exactly from the monthly's Malaysia data as there is no shading causes. The input parameters needed for the operation of simulation process would be the monthly rainfall data, reference evapotranspiration (Eto) and temperature.

After inserting the value, the whether data can be shown as Figure 3.20, 3.21 and 3.22.

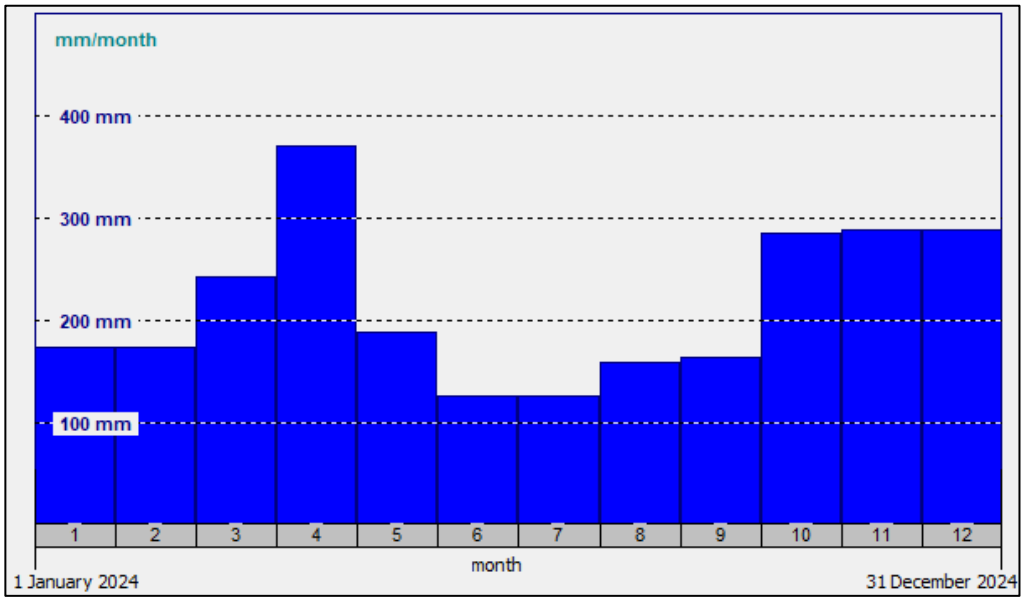

Figure 3. 20: Rainfall data for open conditions

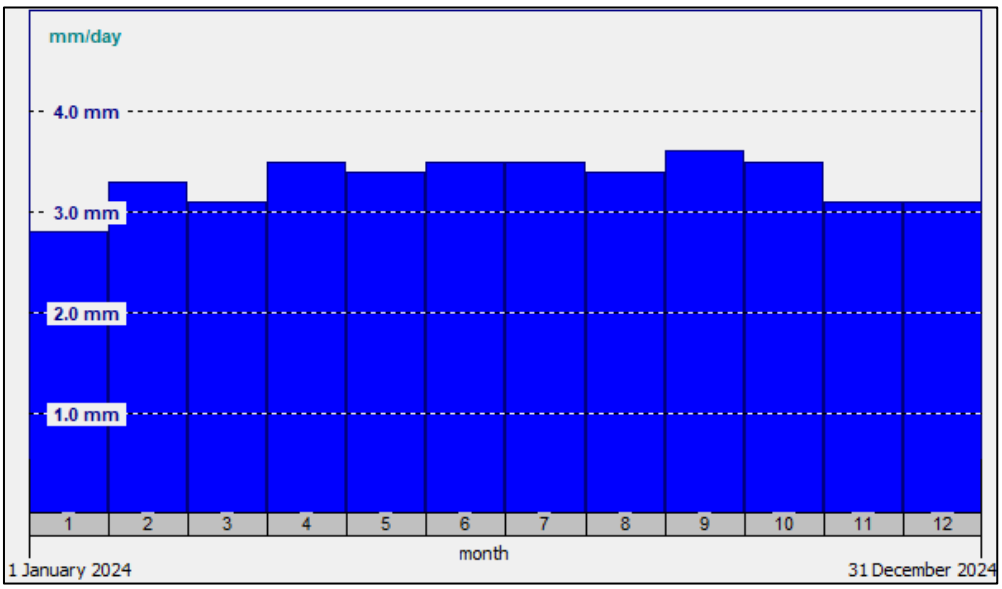

Figure 3. 21: Eto data for open condition

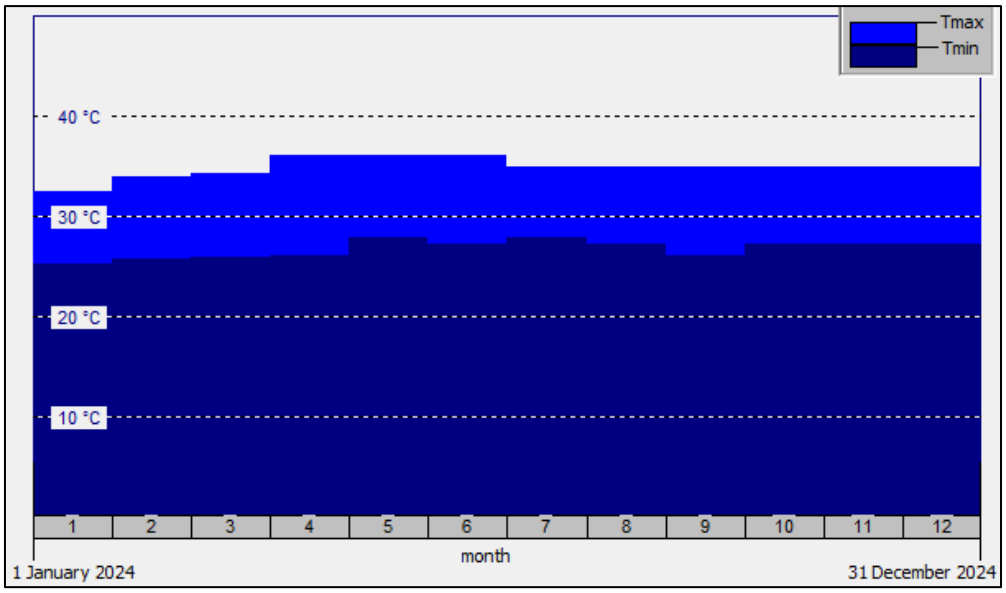

Figure 3. 22: Max and min temperature for open condition

On the other hand, for the whether data for partially shaded condition and heavy shaded condition, it would needed to determine the shaded percentage for these 2 conditions. The shaded percentage would be affect the rainfall, ETo and temperature due to the crops are under the roof. Therefore, the rainfall, ETo and temperature would be expected to be lower than the open conditions. After determine the PAR values for each conditions, then it can only be modifying the whether data for partially shaded and heavy shaded conditions.

Besides, calamansi was the target crop for this study. However, the AquaCrop software does not include calamansi in the database. To solve with this issues, there are few replacement crops can be use as modeling crops. Based on the selection, the suitable replacement crop is tomato as widely grown in tropical regions. Besides, the irrigations and soil profile would be using the default setting which suitable for tropical plants.

Lastly, the purpose of this modeling was not to obtain exactly yield of calamansi but to provide a comparative reference between the actual yield and the simulated yield. It can be believe that the simulating tools would reveal the percentage drop after applying shading condition and compare with the percentage drop in actual experiment. This substitution allows assessment of yield trend and relative differences rather than precise yielding of Calamansi plant

3.7 Summary

To conclude, the methodology of this study would be extensive use of simulation tools and small scale experiment to evaluate the performance of the agrivoltaics system. Through the integration of AquaCrop and PVsyst, the overall analysis of both photovoltaic energy and crop yielding under same land-use conditions were conducted. The simulation method provides a framework for investigating different designs and the resulting impact which allow for detailed comparison before actual implementation. After the simulation, it provides guidelines for future empirical validation. In a nutshell, simulation not only provides reference for decision-making but also reveals the practicality of agrivoltaics as a sustainable solution for optimizing land-use. On the other hand, the actual experiment reflect the actual situation that would face by the crop which can improve the actual site's layout after referring the crops growth conditions. TOPSIS multi criteria analysis method would also been used to determine the best growth conditions of plants among all the growth conditions.

CHAPTER 4

RESULTS AND DISCUSSION

4.1 Photovoltaics panel simulation of different tilt angles

A series of simulations of tilt angles of the PV panels were conducted to evaluate the impact of tilt angles to the performance of the agrivoltaics system. The tilt angles varied from 0° to 30° with the increment of 5°. With the increase of tilt angles, the solar irradiance receive by the surface of the PV panel and thermal stress would decrease. Ideally, when the tilt angle is 0°, the power output would be highest without considering the thermal stress. Besides, the thermals stress is not considerate in this simulation as the PVsyst ignore the heat dissipated within the panels. During the simulation, the setup of the PV arrays is using high-density layout which is the system having lower pitch distance (4m).

The comparative result would be in terms of produced energy per year (kWh/year) and specific production (kWh/kWp/year). The energy produced per year is the total amount of energy generated by a solar photovoltaic (PV) system over a year which is considered as an absolute value. On the other hand, the specific production refers to the normalized energy output per installed capacity (kWp). This comparison is regardless of the land size which is used for performance benchmarking across different tilt angles. The comparative results of different tilt angles would be shown in the Figure 4.1 and 4.2. In addition, detailed losses and output are listed in the appendix E. Lastly, based on the dimension of the panels, the required panels number, area required and performance ratio of the system can be estimated through PVsyst modeling as shown in Table 4.1.

Table 4.1: Performance Ratio and Panel Required Area

PV module	JA Solar JAM66D45 620W
Inverter	Solis S5-GR3P 20K
Pitch	4m
Total Panel	532 modules
Area Required	1437m
Total Panel Pnom	312 kWp
Total Inverters Pnom	260kWac
Pnom Ratio	1.20
Azimuth	180° (Facing South)

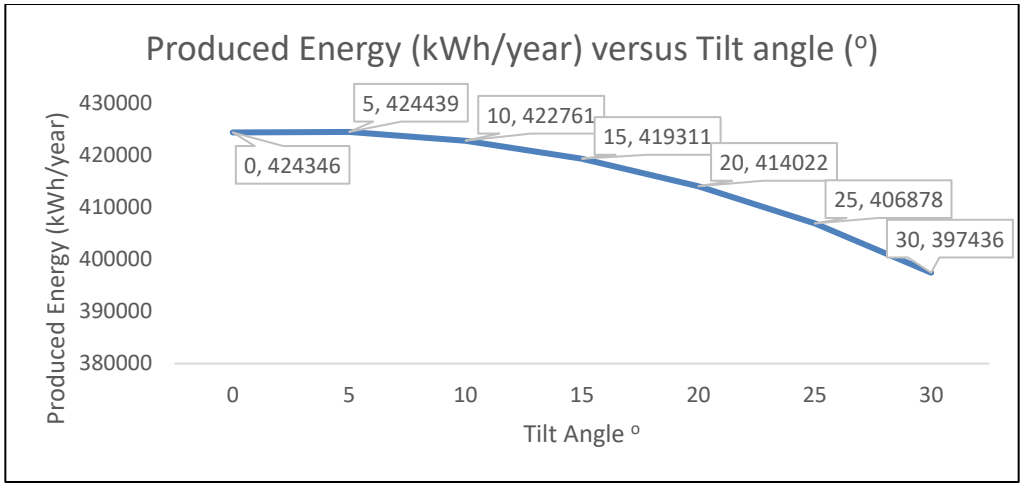

Figure 4. 1: Graph of Produced Energy (kWh/year) versus Tilt angle (°)

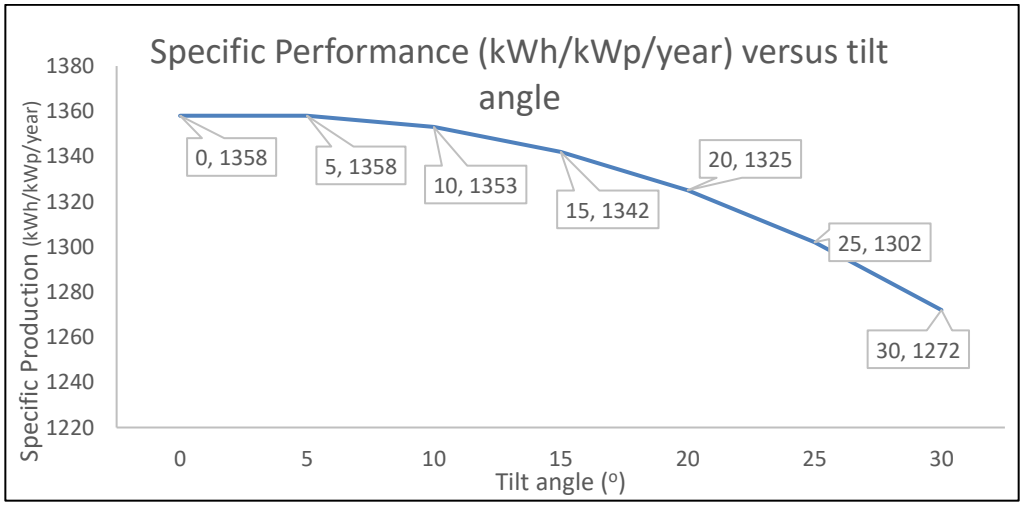

Figure 4. 2: Specific Performance (kWh/kWp/year) versus tilt angle (°)

From the Figure 4.1 and Figure 4.2, the produced energy when 5° tilt angle is slightly higher than 0°. This is due to when 0° tilt angle, the rainwater and dust doesn't easily run off which decrease slightly the efficiency. At 5° tilt angle, it has enough incline to create gravitational acceleration for naturally cleaning the dust and rainwater. However, the energy produced in percentage difference of 0° and 5° is only 0.02%. Besides, when referring to specific performance, they are producing identical values which is 1358kWh/kWp/year. In a nutshell, there is an average 1.27% drop of produced energy and 1.06% drop of specific performance with 5° tilt angle increment. In addition, based on Poobalen *et al.* (2020)'s result, they also proving that when tilt angle increases, the power output would be reduces. However, the power output value would be different which is due to the different PV configuration. Therefore, without considering the thermal stress and thermal dissipates factor, the lower the tilt angles, the higher the energy output.

4.2 Photovoltaic Panels output simulation according to different density

Based on the site situation, there are 2 scenarios of PV layout that can be installed due to the geometric constraint and existing farm layout. Firstly, it would be the full solar density scenario. Full solar density scenario indicates that above the farm are fully crowded by the PV panels. From figure 4.3 below, which shows the actual site condition, full density means the panel is not only installed on the walk way also would be installed above the crops with a pitch distance of 4 m. Therefore, there is very little sunlight that can penetrate through it and be received by the plants. In this configuration, it would provide the highest electrical yield but heavily affect the yield of the crops, as less sunlight can be absorbed for photosynthesis.

Figure 4. 3: Actual layout of the Hami EcoFarm

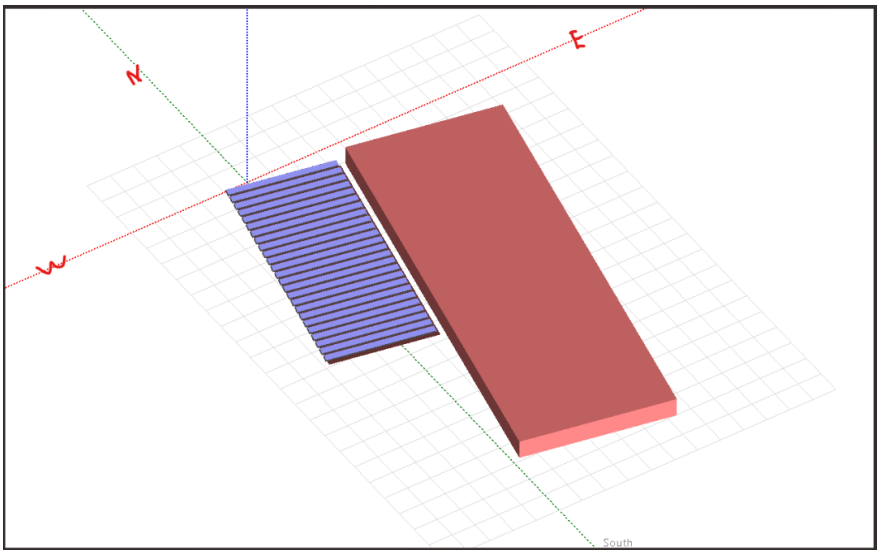

Figure 4. 4: Full solar density of the PV panels arrangement

On the other hand, there is also a half solar density scenario, which means that the PV panels would be placed only above the walkway instead of covering the full area. This scenario would be more friendly for plant growth, as it can allow more sunlight to penetrate to the crops.

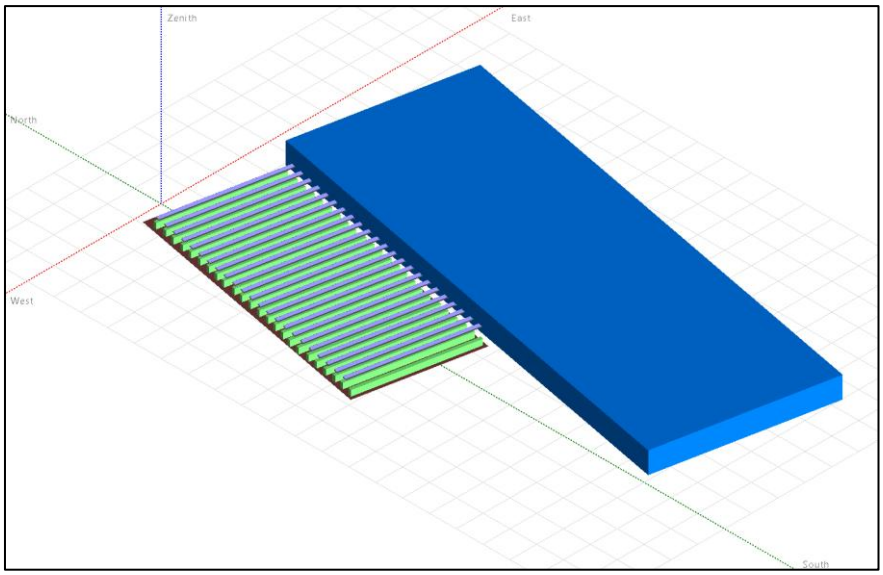

Figure 4. 5: Half solar density of the PVpanels arrangement

The simulation results from PVsyst indicate the performance differences between full solar density and half solar density across various dimensions. Firstly, the half solar density scenario has a higher Performance Ratio of 75.33% compared to the full solar density scenario, which has a Performance Ratio of 73.45%. The performance ratio indicates how efficiently the PV system converts the available solar irradiance energy into usable electrical energy, which is independent of the system size. This is due to the half solar density scenario having lower shading losses of nearly 0% when compared to the full solar density scenario, which has 3.20% near shading loss. In the full solar density scenario, the panels are highly densely packed, having a slight overlap from neighboring rows, which decreases the energy capture efficiency even if the total module count is higher. Besides, at the half solar density scenario, the panels are less densely packed, which allows better cooling airflow. Based on the research by Al-Quraan *et al.*, (2022), the research also highlights that many PV installation use too small inter-row spacing because of high land cost but would causing energy losses due to mutual shading which lead to decrease in performance ratio. Cooler panels operate closer to their optimal voltage, which also avoids voltage drop and increases the output.

In terms of energy yield, the full solar density scenario generates more power than the half solar density scenario. Firstly, the full density has 536

kWp installed capacity (kWp), while the half density only has 246 kWp. Therefore, it led to the full density having 372528 kWh more energy produced per year than the half density, which only had 330402 kWh. The full solar density scenario setup generates more because of the higher panel amount. Other than that, the building beside the agrivoltaic farm, which is shown above the figure, is the greenhouse. The greenhouse actually exists in the real situation, which is expected to cause some shaded effect to the agrivoltaic system. In addition, the simulated electric yielding outputs are also considering this shading factor.

Table 4.2: Summary yielding for full solar density scenario and half solar density scenario

	Full Solar Density	Half Solar Density
Performance Ratio	73.45%	75.33%
Maximum power output	536kWp	246kWp
Actual energy produced	702930kWh	372528kWh

4.3 Growth Condition

Based on the experiment, which has been carried out for 7 weeks on the UTAR KB rooftop, it can be concluded that the results of different growth conditions of the calamansi plants can be evaluated by using multiple criteria evaluation, which is TOPSIS. By identifying the final evaluation values, it can be determined in which conditions the plant would have the highest index performance, which reflects the most ideal growth conditions for the plants. In addition, the Photosynthetically Active Radiation (PAR) sensors have also been installed in each growth condition to identify the actual shaded amount of different conditions.

4.3.1 Multiple Criteria Growing Performance

The results of the observation include various criteria used to evaluate the growing conditions of the plants. The criteria are plant height, number of new leaves, number of fruits, and average fruit diameter. Each criterion would be

measured once a week for every 6 plants, with 2 plants in each specific shaded condition.

On the other hand, in terms of average fruit diameter, there are 5 marked fruits from each plant that would be locked for recording diameter purposes. As time goes on, the average fruit diameter would be increased, although there are few fruits for either plant. Therefore, average fruit diameter would not be affected by the number of fruits; instead, the average fruit diameter is needed to predict the growth trend in terms of fruit yield. As the trend grows, the yield of the fruits is predicted to be higher.

Figure 3.11 shows a total of six plants, categorized into three different conditions**.** It can be categorized as plants 1 and 2 are in partially shaded conditions, plants 3 and 4 are in heavily shaded conditions, and plants 5 and 6 are in open conditions. Therefore, each condition would be the average of the two plants' performances in the four performance criteria. Firstly, Figure 4.6 shows the average plant height for three conditions. According to the graph, the plants in open condition would have the highest average height, however the open conditions would also have the lowest average height during the performance evaluation in Week 9. The height is measured from the highest position of the leaf to the bottom of the plant's pot. In addition, the height are flucturating instead of increment due to the leaves are dropping. It leads to measurements would not having linear going up trend.

The heavily shaded plants have a higher average height because they stretch upward to reach more light, indicating that they are experiencing low light stress. Based on this scenario, the research by Roig-Villanova and Martínez-García, (2016) highlight that this phenomenon called the Shade Avoidance Syndrome or in extreme-low light, etiolation. Additionally, the heavily shaded conditions reduce rainfall stress on the plants, allowing for further growth. In contrast, the plants in the open area would have a lower height because they receive sufficient sunlight. However, plant height indicates the growing conditions; thus, analyzing the growth trend can help identify these conditions. The scenario illustrates that the rainfall pressure has a decreasing trend on open-condition plants. Therefore, in terms of plant growth, the open condition shows a higher decreasing rate than the other conditions' plants, which is due to sufficient sunlight.

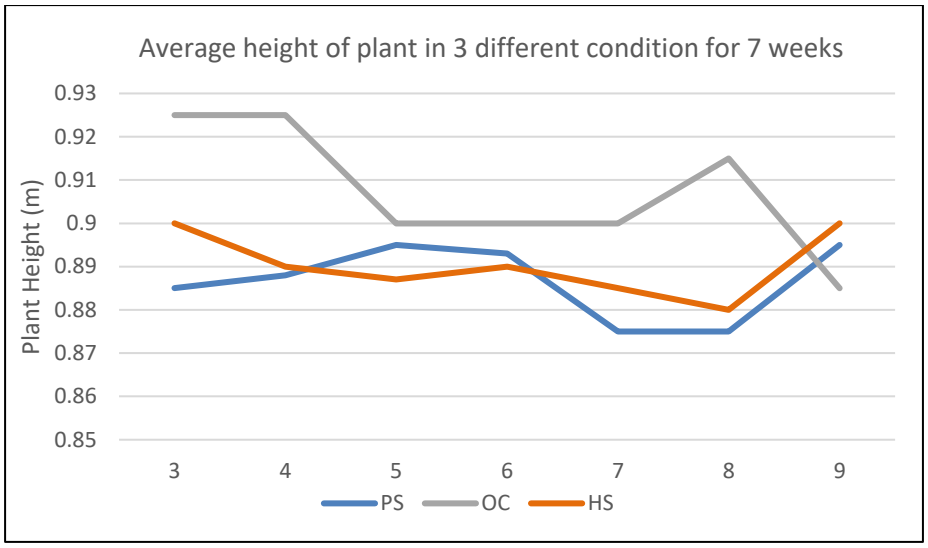

Figure 4. 6: Average plant height of different condition

In addition, when discussing the number of new leaves, a higher increment of new leaves for calamansi indicates there is active vegetative growth. Firstly, it shows that the plants are having adequate sunlight, water and sufficient nutrients for the plants. It means that the plant is in an active growing phase, developing more photosynthetic surface area for energy production. On the other hand, excess new leaf growth is also caused by excess nitrogen fertilization, which promotes leaf growth over flowers and fruits. (Perchlik and Tegeder, 2018). By observing the Figure 4.7, each condition is also showing a decreasing trend of new leaf production, which is due to the fact that the cycle of leaf production has ended. From the partially shaded condition, the number of new leaves started high in week 3 but decreased until week 5 and then increased again and reaching another peak in week 7 before it slightly declined. On the other hand, the open conditions generally remain lower new leaves production with slightly variations and a small increase towards week 9. Lastly, heavy shaded condition increased number of new leaves sharply at week 4, dropped drastically to the lowest point at week 6 and then recovered slightly before declining again at week 9. However, when referring to the average number, partially shaded conditions overall had the highest number of new leaves when compared to open shaded conditions. Although it is partially shaded,the shaded conditions are less than 10%, which does not have a significant effect. On the other hand, the slightly shaded conditions also reduce heat stress and rainfall pressure towards the

plants; therefore, they would have higher new leaf growth. Lastly, the heavily shaded area has the lowest number of new leaves due to the dense shade and insufficient light conditions.

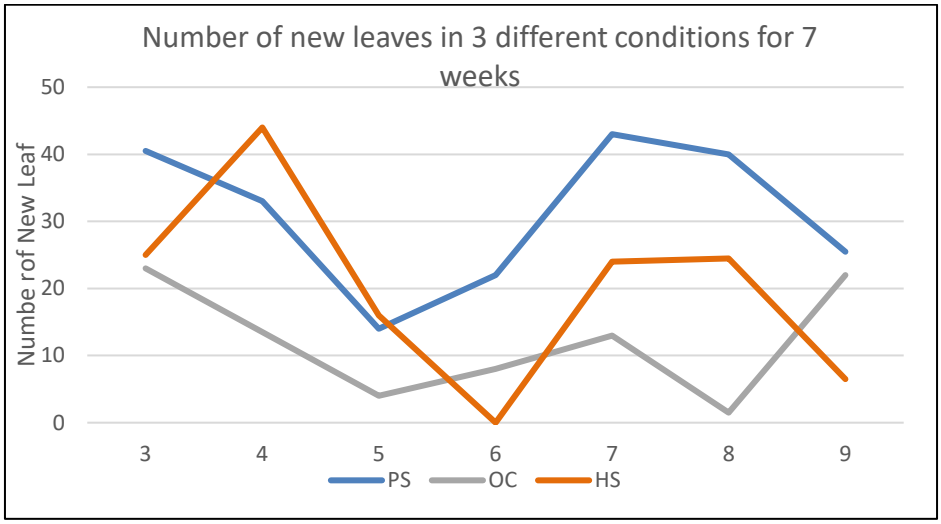

Figure 4. 7: Number of new leaf in 3 differnet conditions for 7 weeks

Other than that, the number of fruits has been directly reflecting the yielding condition of the plants. Partially shaded conditions always maintain the higher number of fruits when compared to other conditions. On the other hand, the number of fruits for heavy shaded conditions shows decreasing due to fruits ripped and lower growing rate. For the open conditions, the number of fruits shows an increasing trend; for future reference, the number of fruits would be identical to or slightly higher than in partially shaded conditions.

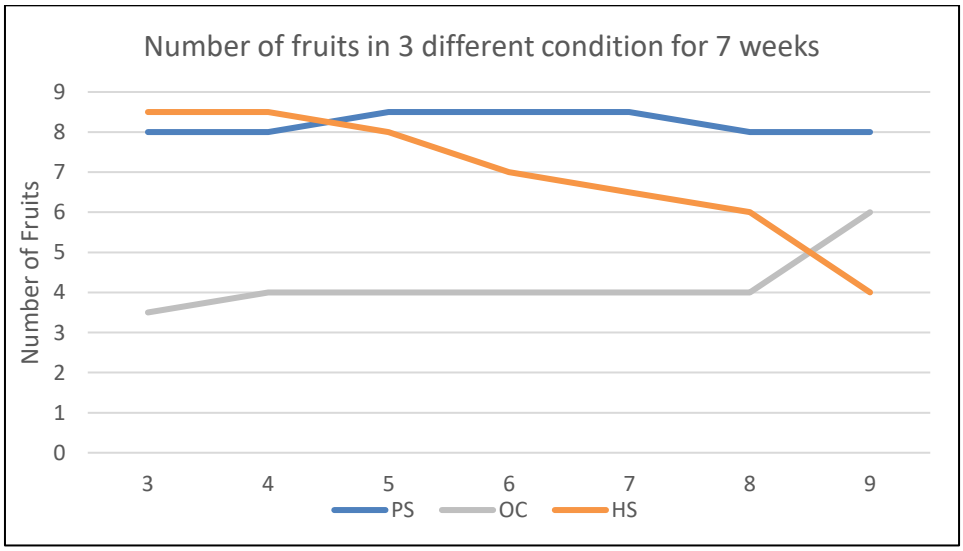

Figure 4. 8: Number of fruits in 3 different condition for 7 weeks

Lastly, Figure 4.9 shows the average fruit diameter for different conditions. In week 9, the data shows that the fruit diameter is slightly higher under heavy shaded conditions. This is due to there being a lesser number of fruits in heavily shaded plants; therefore, all the nutrients are distributed to fewer fruits, which causes more nutrients to be absorbed by particular fruits. When compared to other conditions, there are more fruits, which indicates fewer nutrients can be absorbed by particular fruits. However, when analyzing the growing trend, the partially shaded conditions would have higher gradients, which would have an average diameter for future reference.

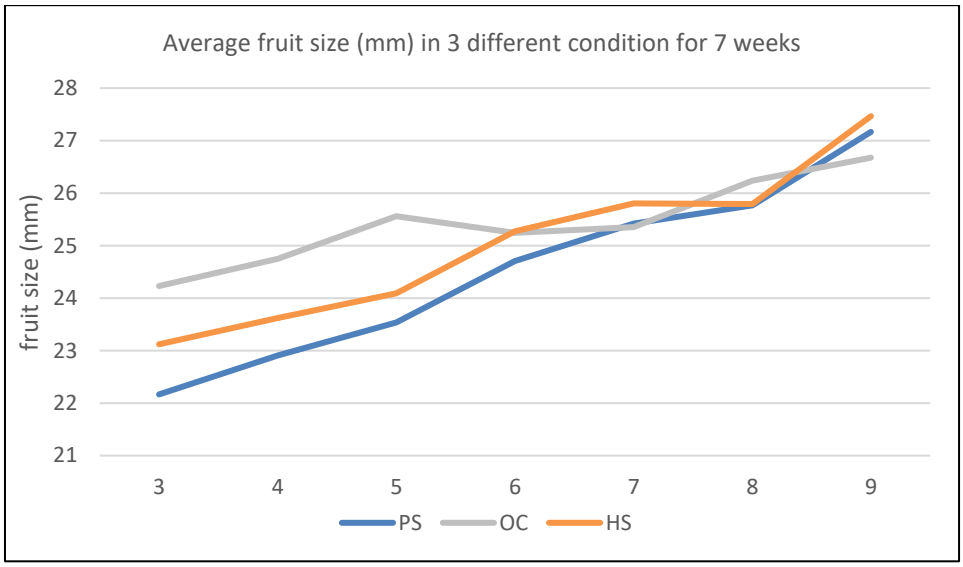

Figure 4. 9: Average fruit size (mm) in 3 different condition for 7 weeks

4.3.2 TOPSIS Value for each performance

Due to there being multiple criteria (height, number of new leaves, average diameter of fruits, and number of fruits), multi-criteria decision analysis (MCDA) would be used and Technique for order of preference by similarity to ideal solution (TOPSIS) would be used as a method to categorize the growth index under different conditions.

Although there are only 3 growth conditions (partially shaded, heavily shaded, and open condition), there are 6 plants, with 2 plants belonging to each condition. Therefore, each plant's TOPSIS value would be calculated. Next, the average TOPSIS value for 2 plants would be determined, and the overall TOPSIS value would be determined.

Firstly, Area Under Curve (AUC) would be used to determine and quantify the cumulative change in plant parameters over time, including over different weeks. Instead of considering the start and end values, AUC takes all intermediate measurements, capturing growth trends and fluctuations. By using the equation below, it can be determined each parameter's AUC for different plants.

$$AUC = \sum_{i=1}^{n-1} \frac{y_i + y_{i+1}}{2} \times (t_{i+1} - t_i) \quad (4.1)$$

From the equation above, y_i shows the plant parameter at time t_i while $(t_{i+1} - t_i)$ shows the time step. In this experiment, the time step is considered as 1 week as the data is recorded every week. By referring to the sample calculation for plant 1 in Table 4.3, it can be concluded the AUC value for each parameter for a plant. Besides, other plants's parameters AUC value can be found in the appendix G' s Table G.1 to Table G.6.

Table 4.3: AUC of 4 parameters for plant 1

Plant 1				
Week	AOC Height	AOC Leaf (unit)	AOC Fruit (unit)	AOC Fruit Diameter (mm)
3	0	0	0	0
4	0.925	36	12	19.71
5	0.94	27.5	12.5	20.04
6	0.9475	25	13	20.74
7	0.9325	18.5	13	21.916
8	0.92	14.5	13	22.764
9	0.93	7	13	23.688
	5.595	128.5	76.5	128.858

Next, after the AUC calculation, it can be concluded as in Table 4.4 below. When referring to the result, it can be noticed that the unit for each parameter is different. For example, the fruit's diameter is taken in units of mm per week, while the number of leaves is in units per week. Therefore, the value has to be normalized.

Table 4.4: AUC Table of each parameter for plant 1 to plant 6

Plant	Height (m)	Leaf (unit)	Fruit (unit)	Diameter (mm)
1	5.595	128.5	76.5	128.858
2	5.035	241.5	22.5	165.035
3	5.495	73	35.5	146.31
4	5.153	36.5	12	159.675
5	4.875	190.5	32	165.19
6	6.03	98.5	54.5	133.76

The purpose of normalization is to provide a fair comparison. Without the normalized step, larger values would dominate the analysis, skewing the result to either site. For example, the AUC of a leaf has a larger value when compared in Table 4.4; it would hide the plant's height contribution, as the plant's height has the smallest value. Normalized data would convert all the data to common scales (0 to 1). Table 4.5 shows the parameter norm and norm factor value for each parameter. Additionally, sample calculations for the height norm and the norm factor of plant 1 would be presented at appendix G.

Table 4.5: Norm for each parameter and norm factor value

Height :	13.173087			
Leaves:	357.05497			
Fruits:	108.4297			
Diameter:	368.67754			
Plant	Height (m)	Leaf (unit)	Fruit (unit)	Diameter (mm)
1	0.4247296	0.3598886	0.705526249	0.349514101
2	0.3822187	0.6763664	0.20750772	0.447640501
3	0.4171384	0.2044503	0.32740107	0.39685086
4	0.3911764	0.1022252	0.110670784	0.433102051
5	0.3700727	0.5335313	0.295122091	0.448060922
6	0.4577515	0.2758679	0.502629811	0.362810273

After normalizing the matrix, each parameter needs to be assigned a weightage. To ensure fairness in evaluating the performance of the plants, each factor would be assigned a weight of 25%, contributing to a total distribution of 100% as shown in Table 4.6. On the other hand, since the plants have been pre-purchased instead of growing from seeds, the plants were not tracked from seed. Baseline data is needed to identify which early growth

traits are missing and how they most influence the final yield. Therefore, giving equal weight would also avoid bias towards traits. Besides, height and leaf developments would also still affect fruiting potential. Equal weightage also ensures these vegetative parameters would not be undervalued. Lastly, if giving too much weightage to the number of fruits and average fruit diameter, it would have the risk of overlooking whether the plants have the structural capacity to sustain the future yield, especially if the plants are still in the ongoing fruiting stage. Therefore, after finalizing, the weightage norm matrix can be shown, and the highest & lowest value of each parameter has been determined for further steps in calculations.

Table 4.6: Weightage apply to the norm matrix

Plant	Height (m)	Leaf (unit)	Fruit (unit)	Diameter (mm)			
1	0.1062	0.0900	0.1764	0.0874			
2	0.0956	0.1691	0.0519	0.1119			Highest Value
3	0.1043	0.0511	0.0819	0.0992			Lowest Value
4	0.0978	0.0256	0.0277	0.1083			
5	0.0925	0.1334	0.0738	0.1120			
6	0.1144	0.0690	0.1257	0.0907			

Next, the highest and lowest values from each parameters back to weightage calculation above would be needed to calculate the overall TOPSIS value. The highest and lowest value would also determined as positive ideal solution (A^*) and negative ideal solution (A^-). The ideal solution showing in the appendix G below.

After that, the S_i^* and S_i^- needed can be determined. These values would be the value input to calculate the TOPSIS values for each growth conditions. By using the calculation method mention in methodology part, S_i^* and S_i^- for each plants can be determined as Table 4.7. Besides, sample calculation for plants 1 wil also be shown in appendix G below.

Table 4.7: S_i^* and S_i^- values for each plant

Plant	S^*_i	S^-_i
1	0.083277	0.16264
2	0.125929	0.147647
3	0.15206	0.062188
4	0.207387	0.021553
5	0.110827	0.119833
6	0.114246	0.109444

Lastly, the TOPSIS of each plant can be calculated and shown in Table 4.8. Since plant 1 and plant 2 are in partially shaded conditions, plant 3 and plant 4 are in heavily shaded conditions, and plant 5 and plant 6 are in open areas, the TOPSIS value for each condition would be the average of those 2 plants's TOPSIS value. Example calculation of TOPSIS plant 1 and the partially shaded condition would also be shown in appendix G below.

Table 4.8: TOPSIS values for each plants

Plant	C
1	0.661363
2	0.539693
3	0.290263
4	0.094142
5	0.519523
6	0.489267

Table 4.9: Summary of TOPSIS value for each growth condition

Growth Condition	Average TOPSIS
Partially Shaded	0.600528
Heavy Shaded	0.192202
Open Condition	0.504395

Table 4.9 result indicates that partially shaded conditions have the highest TOPSIS values, with open conditions following closely behind. Besides, the heavy shaded conditions show the lowest TOPSIS values. Even if open conditions offer greater sunlight intensity for photosynthesis growth of

the plants, the TOPSIS method combines all the evaluation parameters, as few typical scenarios explain the results. Firstly, the fruiting would dominate the score because shaded plants produced more fruits and a higher number of new leaves, which showed better growth conditions when compared to open areas. These 2 parameters have contributed 50% of the weight, which can outweigh any advantage the open condition had in height and average fruit diameter. Therefore, these high normalized parameters have pulled the partial-shade condition closer to a more positive ideal. In addition, the open condition may also cause suffocating heat stress that reduces the fruit sets. In full sun conditions, crops would experience higher heat stress and evapotranspiration. Therefore, it would lead to flower drop and evaporation of water, which leads to lesser water absorption by the crops. This would result in lower fruit-yielding conditions, and the weighted normalized vector for the open condition would be further away from the positive ideal. Lastly, the heavily shaded crops show the lowest TOPSIS values, mainly due to low sunlight irradiance. Lower sunlight has been indicated to lower photosynthesis, which directly affects lower growth and reproduction. This is because heavy shade reduces biomass, such as leaf production, average fruit diameter, and fruit number. Therefore, when reviewing the normalized values for each parameter, it would have the lowest weighted values and produce lower yields. On the other hand, Jamil and Pearce (2025) highlight that the shading level of 30% having the highest yield while the yielding is the lowest during 80% shading. This research shows slightly different in terms of maximum yielding due to different crops has been experimented. In the research, strawberries are used for experiment model therefore required lesser sunlight which optimal at 30% shading level. On the other hand, the growth conditions would also slightly different as the experiment is carried out in in door conditions therefore temperature and air flow would be different. However, both research and experiment also highlights that having partially shading effects would be more advantageous for crop productivity than open growth conditions as reduce heat stress. In addition, the heavy shaded condition's growth performance showing identical results in both experiment and research's result. Therefore, for this research, the partially shaded conditions is optimal growth conditions for the crops.

4.3.3 Photosynthetically Active Radiation (PAR) value for each conditions

Photosynthetically active radiation (PAR) for each condition has been set up and recorded for one month (August). The data would be recorded daily from 7 am to 7 pm (12 hours). PAR value refers to the specific range of light that plants can use for photosynthesis to produce energy. PAR sensors have been optimized for lighting in greenhouses or assessing light conditions in fields, and the amount of PAR a plant receives directly impacts its ability to produce carbohydrates, which are essential for its survival and yield. Therefore, identifying the PAR values for each growth condition would reflect the shaded conditions of each growth condition.

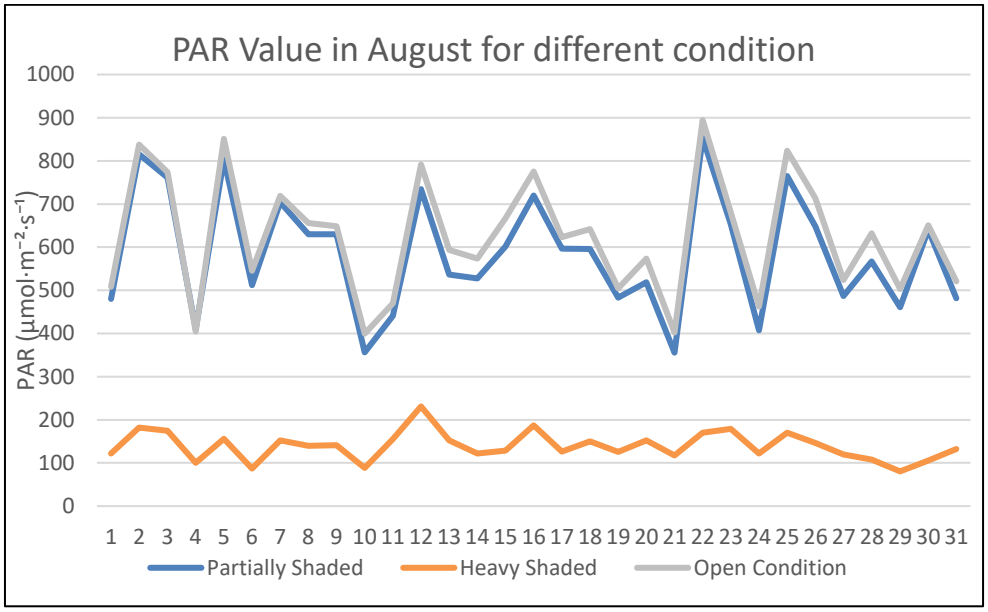

Figure 4. 10: PAR value in August for different condition

When referring to the Figure 4.10, it can be shown that the heavy shaded values have the lowest PAR values, while open conditions' PAR values would be slightly higher than partially shaded conditions. The average PAR for each condition is summarized in the Figure 4.11.

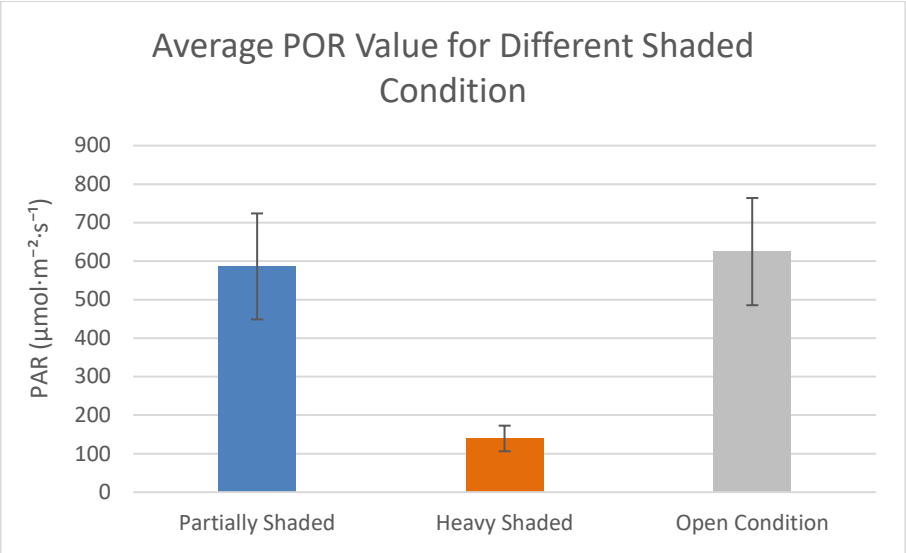

Figure 4. 11: Average POR value for different shaded condition

From the result computed at Figure 4.11, it can identify the shading conditions for each growth condition. From the result above, it shows that at open condition, the average PAR value is the highest among these 3 conditions. On the other hand, heavy shade shows the lowest PAR value. Therefore, the open condition can be used as a reference to determine the actual shading percentages for both heavily shaded and partially shaded areas, since the shading conditions of the open condition are expected to be 0%. Therefore, partially shading indicates 6.15% and heavy shaded represent 77.68% of shading level. The calculation for shaded level of each shaded condition would be shown in appendix H below.

In addition, the setup of PAR sensors can also determine the at which time period the area would have shade. For example, on 20th August, the PAR data of this day can be used for reference, as there is no rain. From the figure 4.12 below, the PAR values follow a daily solar pattern, which is starts at near 0 (morning period), peaks at midday (afternoon) and end at near 0 (dusk period). The highest PAR values occur in open areas, followed by partially shaded areas, while the lowest values are found in heavily shaded areas. For the open condition, the PAR peaks at around 1800μmol/m^2/s which indicates the full sun exposure. Next, the partially shaded peak is around 1500 μmol/m^2/s and the heavily shaded condition shows the lowest PAR value, which are about 350 μmol/m^2/s. The lower the PAR values meaning strong

shading reduces available light for photosynthesis. In addition, significant spikes and dips happened in the afternoon (1pm to 3pm) for open conditions and partially shaded conditions, which are due to cloud cover or intermittent shading. On the other hand, heavy shading remains relatively stable with fluctuations, indicating consistent shading. For many crops, the optimum PAR is around 1000 μmol/m^2/s for better photosynthesis. (Liu & Van Lersel, 2021). Rapid dips reduce photosynthetic activity momentarily, but most of the plants can tolerate short interruptions without significant effect on yield. If fluctuations are frequent but short, crops prove that it can adapt. Besides, heavy shaded conditions trades off lower total energy for higher electricity yield which can delay growth and overall yield. In addition, both situations show lower PAR values before 1pm. This is due to being a building beside the experiment venue. The building can act as the greenhouse besides the agrivoltaic farm which reflects the actual site conditions. Therefore, the PAR is relatively lower than the period after 1pm, which is due to shading caused by the building. (Figure 4.13). In conclusion, open condition exceeds the optimal PAR values for the plants during the plants' lives meaning some light is wasted and the surrounded area has higher temperatures. Next, partially shaded conditions stay closer to the optimum range, which shows potentially improved yielding for the crops during the TOPSIS analysis. Lastly, heavy shaded condition is below optimum most of the day and causes limiting growth and yielding.

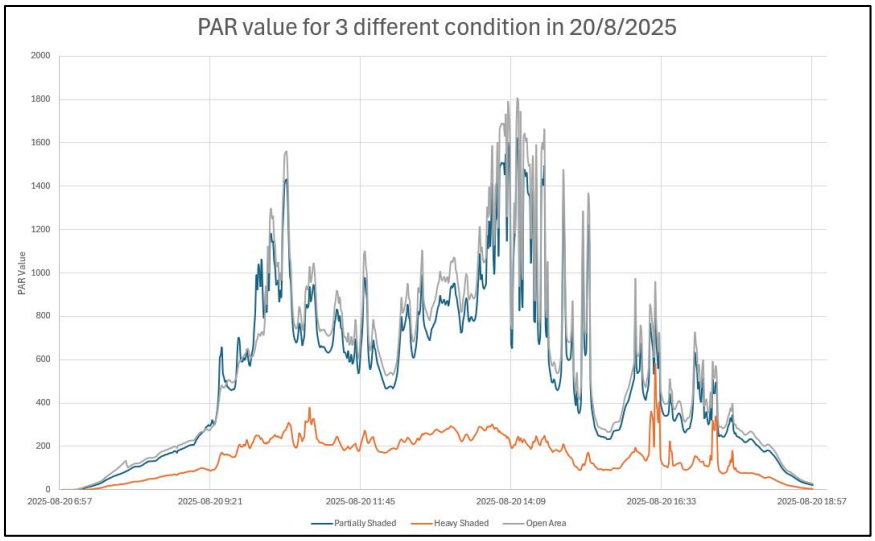

Figure 4. 12: PAR value for 3 conditions in 20th August

Figure 4. 13: Building besides the experiment area

4.3.4 Crop output simulation according to different shaded conditions

From the shading values of each condition, it can be modifying the weather data based on the different shaded conditions.

Firstly, the partially shaded condition is having shading of 6.15%. For the design factor, the shading percentage would be increased to 7%. Therefore, the rainfall in the area, reference evapotranspiration (Eto), and temperature are expected to drop around 7%. The Figure 4.14, 4.15 and 4.16 shown the weather data after modifying based on the open conditions weather data.

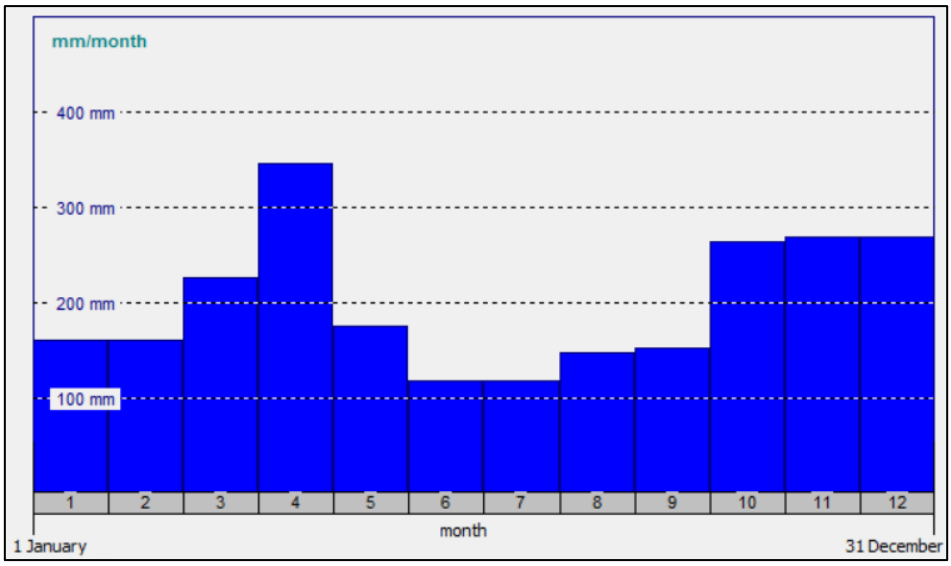

Figure 4. 14: Rainfall data for Partially Shaded condition

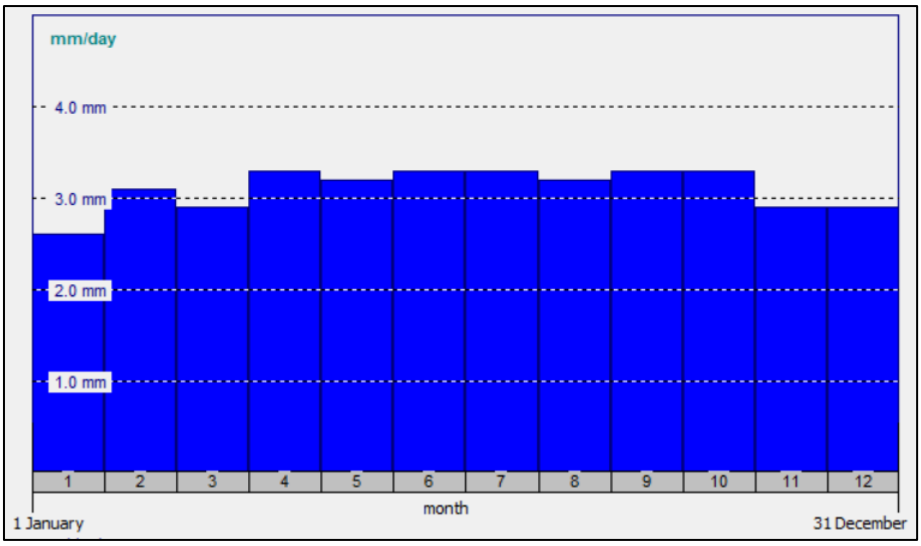

Figure 4. 15: Eto data for Partially Shaded Condition

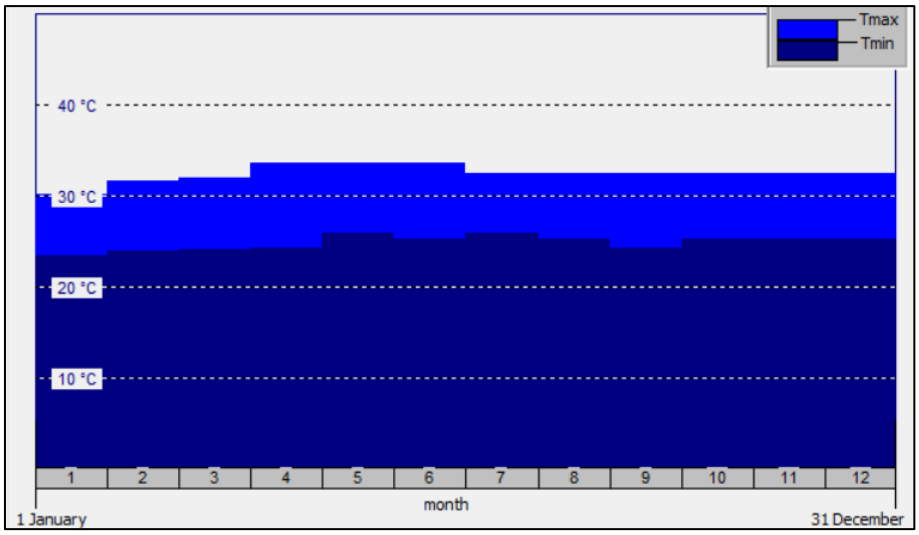

Figure 4. 16: Temperature data for Partially Shaded Condition

Next, the heavy shaded condition is having shading of 77.68%. For the design factor, the shading percentage would directly take 80%. The rainfall and Eto would be reduced by 80%. However, the temperature difference would not be reduced by 80%, as the deduced results would not be suitable for Malaysian weather. In this shading scenario, the temperature does not decrease proportionally under heavy shading. Therefore, the temperature reduction is assumed to follow the 8% shading case instead. The whether parameter for heavy shaded condition can be shown at Figure 4.17, 4.18 and 4.19.

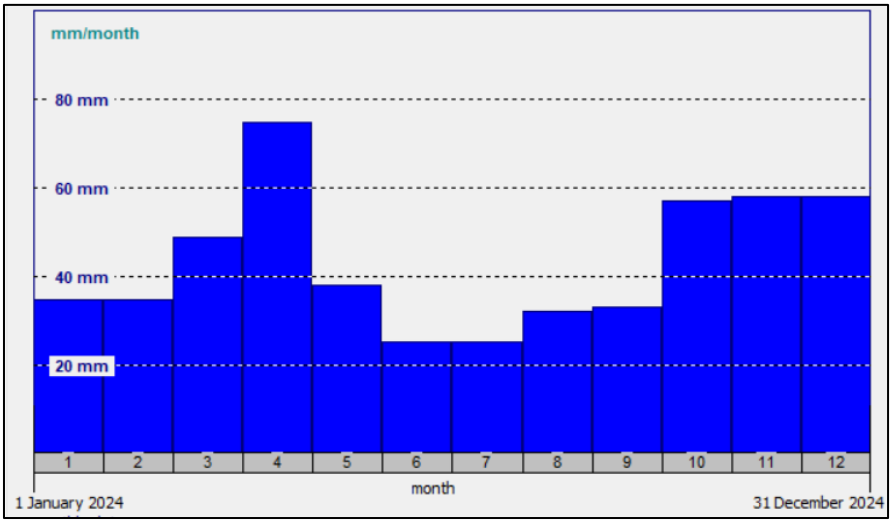

Figure 4. 17: Rainfall data for Heavy Shaded Condition

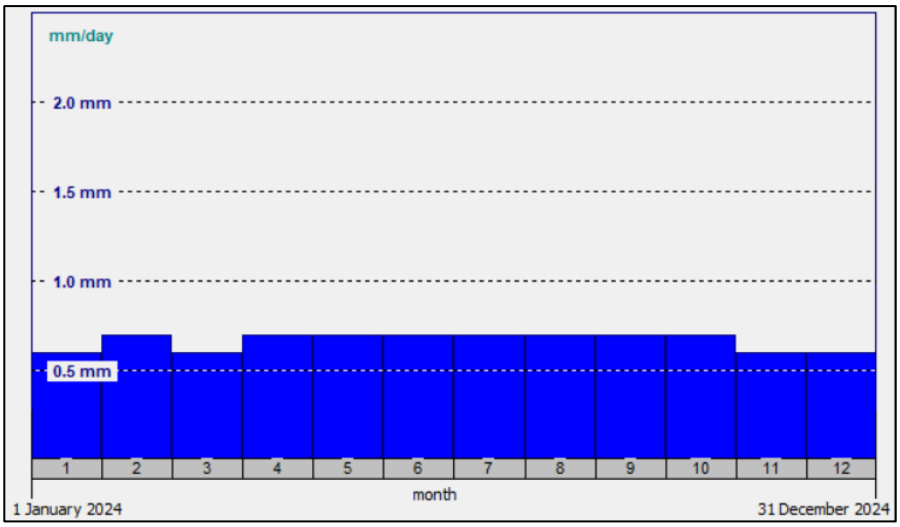

Figure 4. 18: Eto data for Heavy Shaded Condition

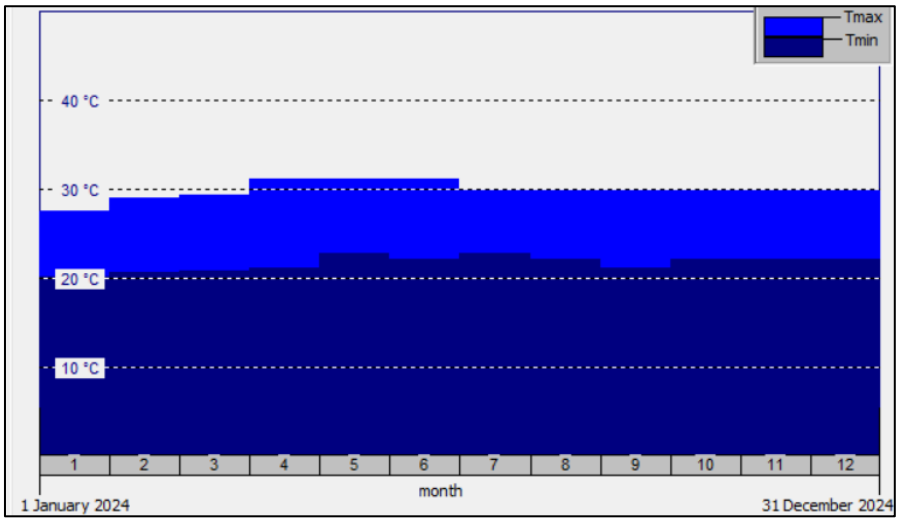

Figure 4. 19: Temperature data for Heavy Shaded Condition

After inputting the weather parameters, the expected output results showing are the yields (ton/ha). From the result, the open conditions's crop yield was 7.533 tons of crops per hectare in a 3-month period. On the other hand, the partially shaded conditions had 7.089 tons of tomato yield per hectare in a 3-month period with a percentage drop of 5% in crop output. Lastly, the heavy shaded condition shows the least crop output with only 6.184 with a percentage drop of 18%. Besides, detailed results would be shown in the appendix I.

When compared to the actual experiment, the percentage drop between partially shaded and open conditions is 20%, while the simulation

results' percentage drop is only 5%. On the other hand, heavy shaded conditions show the highest percentage drop, which is 62%, while the simulation results' percentage drop is only 18%. Therefore, the yielding drop of the actual experiment is higher than the simulation results due to considering the actual heat stress environment. The purpose of doing simulations is to prove that heavy shading would affect the most the yielding, causing a heavy drop of crop yield.

From the simulation results above, it shows that open conditions have the highest yield. However, when compared to the actual growth performance (TOPSIS), the partially shaded conditions yield higher than the open conditions. Besides, the heavy shaded condition remains the lowest yielding in both simulation and actual experiment. Firstly, the main reason is the difference in crop physiology. Calamansi is a tropical crop that is sensitive to heat stress and excessive sunlight. Partially shaded would reduce the heat stress and reduce radiation that causes water loss and leaf scorch. On the other hand, tomato is considered by Aquacop to be a high-light-demand plant where yielding is affected mostly by maximum solar irradiance. In addition, due to Aquacrop limitations, calamansi is not included in the database of Aquacrop, so it cannot account for crop-specific adaptations for partial shade. Aquacrop would also be putting more weight on the importance of radiation. Therefore, there is a direct relationship between higher radiation causing higher photosynthesis and producing higher yield. This would put the heat stress effect not very significantly. Therefore, shading reduces photosynthesis energy, which directly lowers the yielding in simulation results. In a nutshell, in terms of the experiment field, calamansi in partially shaded conditions is beneficial because it balances light and reduces heat stress. Besides, open conditions reflect more positive results, as the simulation process assumes more light would equal more yielding.

Table 4.10: Summary simulated and actual experiment result

Simulation result	
Condition	Yielding (ton/ha)
Partially Shaded	7.089
Heavy Shaded	6.184
Open Condition	7.533
Experiment Result	
Condition	Growth Performance Index
Partially Shaded	0.600528
Heavy Shaded	0.192202
Open Condition	0.504395

4.4 Land Equivalent Ratio (LER) calculation

Land Equivalent Ratio (LER) can be calculated once the electrical yielding for full solar density & half solar density PV layout and growth performance for open condition, partially shaded condition & heavily shaded conditions are determined. From the table 4.10 below, the total yielding has been summarized.

Table 4.11: Yielding for solar energy and growth performance of crops

Yielding for solar energy	
Conditions	Yielding
Full Solar Density	702.930MWh/year
Half Solar Density	330.402MWh/year
Growth Performance of Calamansi from TOPSIS score	
Conditions	Growth Performance
Partially Shaded	0.600528
Heavy Shaded	0.192202
Open Conditions	0.504395

Based on the equation of calculation of LER values, the yielding of crops and solar energy would be the input parameters of the equation. However, since there is no actual yielding of calamansi from the experiment. This is because all the experimental calamansi are implemented after they

have borne fruit, and the experiment period is a short period, which only consists of 7 weeks. Instead, the growth performance index (TOPSIS) would be used as the parameters. Growth performance can also represent the yielding condition, as the higher the growth performance index, the higher the possible yield for the crops. The computed results indicate two scenarios for the agrivoltaics design. Firstly, there is half solar density and partial sunlight for the crops; the solar panels are installed on half of the land capacity, while the crops' conditions are undergoing partially shaded conditions. Next, the other scenario is full solar density and heavy shading for crop, the solar panels cover all the area of the farm, and the crops are experiencing 77.68% shading. Below appendix J are the LER value calculations of each scenario.

The LER values indicate the presence of conditions. In the half-solar density scenario, the LER value (1.64) means the owner needs only 61% of the land to attain the same combined outputs as two separate individuals. For a more detailed explanation, consider that the owner has one unit of land. If the owner wishes to conduct monoculture, 1 unit of land would generate 702.930 MWh/year, while 0.38 unit of land can also obtain the crop's performance index of 0.192202. However, the total of this monoculture would require 1.38 pieces of land. Instead of using 1.38 separate pieces of land, the owner can choose to combine them into a single piece of land, which introduces the concept of agrivoltaics. Therefore, if using a half-solar density scenario, the solar output might drop to 330.402 MWh/year, which is 47% of the full-density solar farm. Besides, the crop growth performance index does even better than open conditions, as the TOPSIS performance shows a 19% improvement. Therefore, these values have contributed to LER values of 1.64. For a better understanding of the 1.64 meaning, it just indicates that with just 1 unit piece of agrivoltaic land, the owner can produce as much as he would have with 1.64 hectares if implementing monoculture. On the other hand, in the full solar density scenario, the solar can reach 100% of the full farm yield, which is 702.930 MWh/year. However, the crops suffer with a growth performance index of only 0.192, which is only 38% of the performance from open conditions. In this scenario, the LER of 1.38 means with 1 unit of land, the owner would get the same output as he would need 1.38 pieces of land for if he were implementing monoculture.

If the owners are doing monoculture, which indicates the LER of PV farm is 1 and the agriculture farm is also 1. So each single-use scenario has an LER with one definition. On the other hand, when compare research done by Amaducci *et al.*, (2018), the research also highlight calculation of LER in 4 different conditions with multiple variation such as existence of sun track and ratio of panels surface to crop surface. The LER ratio calculated is within range of 2.05 to 1.31. On their research, the higher the panels surface ratio, the LER ratio obatained would be higher. However, this result having conflict with current LER ratio because in Hami EcoFarm case, the higher panels surface ratio is getting lower LER. This is mainly due to the yielding of the crops conditions as the result done by Amaducci *et al.* is using different crop models for simulation, therefore the crop yielding would be different. Thus, the LER value calculated would be different. By comparison with other research, the LER value also depends on the crop type while each crop would be having different yielding at different yielding conditions. If the crop are having higher yielding in shaded conditions, the LER values would also be higher.

When LERs are above 1, it proves that the agrivoltaic layout shows the advantage. In a nutshell, the half-solar density scenario is more advantageous than the full-solar density scenario, as the land saved would be more. Additionally, both scenarios save land when compared to monoculture farming.

Table 4.12: Summary LER value

Scenario	LER
Half Solar Density	1.64
Full Solar Density	1.38

4.5 Discussion

The findings from subtopic 4.1 to subtopic 4.4 in chapter 4 have provided a comprehensive view of the performance of the agrivoltaic systems, which combine both the yielding of crops and solar energy. Based on the results, the outcomes highlight a few important aspects that can proceed for further discussion.

4.5.1 Economic Value

Firstly, the Land Equivalent Ratio (LER) of the half-solar scenario has proven to be higher than the full-solar-density scenario. The results have indicated that the half-solar scenario provides higher economic value compared to the full-solar-density scenario, as more combined output can be obtained per unit of land. This reflects that the owner can generate greater overall returns by producing crops and energy power simultaneously rather than implementing monoculture. However, it should be taken into account that the LER the economic profitability, depends not only on LER values of each scenario but also on the market price of the crops and the electricity tariff. Based on the actual market prices, it can predict the monetary revenue of different conditions after implementing the agrivoltaics system. For the yielding of solar panels, the sites area (Hami Eco Farm) used is a total of 1437 m² of available area. From the simulation results, the full-density solar scenario has 702.930 MWh/year, while the half-density solar scenario generates only 330.402 MWh/year. In Malaysia, the electricity price is RM0.45/kWh. (Refer to appendix K for calculation).

On the other hand, in terms of the yield of plants, from the overall plantation area of 3600 m², approximately 0.36 hectares. Based on the literature review, it has been found out the marketplace for passion fruits is RM2300 per ton, which might have a yield of RM41300 per hectare. Therefore, for the available land that exists in Hami EcoFarm, the highest yield of passion fruits would be RM14868 per year. Based on the topsis growth performance index, we can roughly estimate the yielding of passion fruits. Although the TOPSIS analysis is using calamansi plants as an analyzing model, their characteristics can be roughly similar due to both of the crops belonging to tropical fruits. Thus, the growth performance index can be assumed to be similar to passion fruits. The revenue can be expected to be multiple with the growth performance index, as it shows an estimate of how many yields can be grown under the particular conditions. Below calculation shows the estimated yield of passion fruits.

After the calculations of the yield of both PV and crop (appendix K), it can determine the overall revenue for each scenario. For the first scenario,

which is the full-density solar scenario, the overall yield would be RM354,322.66 per year. On the other hand, in the second scenario, which is the half-density solar scenario, the overall yield is RM174,130.42 per year. The equation below shows how to calculate the revenue for both scenarios.

Based on the calculation results in Appendix K, the overall revenue for the full solar density scenario is higher than the half solar density scenario. However, the Land Equivalent Ratio (LER) of full solar density is lower than the half solar density scenario. This is due to LER being a dimensionless measurement to identify that adds two relative terms, which are crop factor and PV factor, but the LER doesn't consider the monetary magnitude of each term. If one of the scenarios produces much more electricity while the other produces more crop output, the scenario with lower LER but with much PV income can overtake the revenue of the higher LER scenario. When discussing monetary revenue, the LER would act as an index to determine the area efficiency. But if one of the yields, such as electricity, is worth RM1000 per unit and the crop is only worth RM10 per unit, the revenue would follow the high-value products no matter the level of LER. Therefore, a half-density scenario using the half-density PV which means a higher crop fraction but lower PV income, would result in lower revenue even though LER was higher. On the other hand, a heavy-shaded layout likely used full-density PV which means higher PV income, and a small crop fraction would produce higher revenue but lower LER values. In a nutshell, the half-density scenario focuses more on larger crop contribution but smaller PV output, which gives a total revenue of RM174,130.42. In contrast, full solar density increases the larger PV output but decreases crop production, resulting in higher revenue of approximately RM354,322.66.

4.5.2 Energy-Crop Trade-off

From the system simulation, the results reveal that PV performance is maximized during low tilt angles, and from the literature review, the optimal tilt angle is 15 which also considers low angles. However, the crop yield is more sensitive to the degree of shading.

Full density scenario focuses more on electricity generation but reduces the crop yield. On the other hand, half-density scenarios provide more

balanced yielding by supplying adequate PV energy and reduce the shading effect, which increases the yielding of the crops. The trade-off highlights the importance of selecting a design that optimizes both yields rather than focusing only on monoculture. Therefore, in the Hami EcoFarm case, if the owner desires more revenue, full solar density is more suitable. However, when the owner has established a mutual production and marketing line for his product, passion fruits, then the half-solar scenario would be suitable for him.

4.5.3 System Efficiency and Land Use Optimization

The overall efficiency of both scenarios has proven that the LER values are greater than 1, which confirms the advantageousness of dual use on the same piece of land rather than monoculture on a piece of land. In Malaysia, the land is gradually becoming limited; the agrivoltaic approaches can empower food security but also provide sustainable energy targets.

From a sustainability perspective, the results support Malaysia's renewable energy and agricultural studies, which contribute to fulfilling the Sustainable Development Goals (SDGs). Firstly, it is related to food security, as it supplies crops as food in the industry. Additionally, the clean energy generated from PV panels demonstrates that Hami EcoFarm operates in a more sustainable manner. The positive results reflect that agrivoltaic systems might benefit from national incentives such as Net Energy Metering (NEM) and agricultural subsidies. These policies have provided financial support and helped increase the number of Agrivoltaic implementations in Malaysia.

4.6 Summary

Based on the finding, the half solar density having yielding of 702.930MWh/year while full solar density having yielding of 330.402MWh/year. On the other hand, partially shaded crops achieving highest growth performance index which is 0.6 follow by open conditions (0.50) and heavy shaded (0.19). Besides, the crops experienced 6.15% and 77.68% of shading level in partially shaded and heavy shaded areas. Lastly, land equivalent for half-solar scenario is 1.64 which is higher than full solar density (1.38). In a nutshell, half-solar density is suitable for Hami EcoFarm as it more focus on crop yielding which fulfil the needs of the farm.

CHAPTER 5

CONCLUSIONS AND RECOMMENDATIONS

5.1 Conclusions

This study intends to evaluate the technical and economic performance of an agrivoltaic system by implementing both photovoltaic energy and agricultural production on the same piece of land but varying shading and panel configurations. The comparison between full solar density and half solar density revealed a trade-off between electricity revenue and crop yield. Based on current farm layout, the half solar density photovoltaic panels layout would be suggested to Hami EcoFarm. With the yielding of 330.402MWh/year, the crop's performance index can be achieve higher value (0.60) when compare to full solar density panels layout. In addition, the partially shaded conditions provide the highest crop's growth performance index which is 0.60. While the open condition and heavy shaded condition's crop performance index is 0.50 and 0.19. Lastly, best configuration for Hami EcoFarm is half solar density scenario as it maximise Land Equivalent Ratio (1.64) and provide highest crop yielding which fulfill the needs of the farm. Based on the Hami EcoFarm case, the PV configuration is half solar configuration, although it is not optimal solar energy yielding, but it can balance the productivity of both yields and consider solar power generation as a side income. Lastly, the best configuration for Hami Eco Farm would be half-solar density along with partially shaded conditions for crops, as it achieves the highest LER value and is more optimized for crop productivity, which fulfills the needs of Hami EcoFarm.

5.2 Recommendations for future work

Research on agrivoltaic systems shows that some aspects can be changed to improve comparison results. Therefore, there are few recommendations for future studies in this research.

Firstly, the crop growth analysis should be done by observing the crops from seeds. In this research, the crops (Calamansi) were pre-growth

plants that already had fruit. Due to time constraints, if the results are from plants that are grown from seed, it might not be possible to present the results, as the growing period is longer. Therefore, running experiments from germination until harvest rather than starting with established plants will effectively capture early-stage mortality until final yield. In this scenario, the actual final yield of each plant for 3 shaded conditions can be used as the input parameter to the Land Equivalent Ratio (LER) rather than using the growth performance index.

Other than that, it also suggested running the experiment on a larger scale. This is because there are only 2 crops in each shading condition, which limits the statistical strength and makes it difficult to capture natural variability in crop yielding. For example, if each condition has 20 plants, it establishes a large database allowing more reliable comparison between each shaded condition. In addition, a larger sample size will also be capable of using statistical tools such as ANOVA to identify the differences between each shaded condition with greater confidence. Besides, expanding the crop-yielding experiments will minimize the effects of outliers, which are exceptionally strong plants skewing the results. Larger-scale experiments will improve the accuracy of conclusions and results and provide more convincing evidence of the effects of partial shading on crop performance.

Besides, it must be highlighted that this research did not implement actual solar panels to measure the crop yield under realistic conditions. Instead, the solar energy generation is yielding simulation values, which are useful for preliminary results but not capable of reflecting actual real-world yielding. Some important factors are not taken into account, which are reflected radiation, heat accumulation below the modules, and airflow change. These factors will also affect the yielding. For future studies, it is suggested to conduct experiments with actual solar panel installations. However, this step required more capital to be invested in the installation and maintenance of the solar panels. Real panels will also allow the reflection of the microchange and effects caused on plant physiology. This will strengthen the results of the shading caused by the solar panels, which affects crop growth.

Another important future recommendation is to quantify the microclimates mechanisms that explain how partial shading reduces crop heat stress and evaporation losses. In this experiment, the Photosynthetically Active Radiation (PAR) sensors were already installed but only recorded the sun intensity of each shading condition and light distribution. To strengthen the findings, future experiments should install more environmental sensors, such as air temperature sensors, infrared thermometers, relative humidity, soil moisture, and soil temperature sensors, for continuously monitoring the microclimates under each shading condition. By referring to the data from all these sensors and crop physiological responses, future research could provide a more persuasive mechanism that, with partial shading, enhances plant performance in agricultural systems.

REFERENCES

'Des panneaux ? Oui mais pas trop !' |INRAE (2024) *Inrae.fr*. Available at: https://www.inrae.fr/dossiers/agriculture-forets-sources-denergie/panneaux-oui-pas-trop (Accessed: 10 May 2025)

Al-Quraan, A., Al-Mahmodi, M., Alzaareer, K., El-Bayeh, C. and Eicker, U. (2022). Minimizing the Utilized Area of PV Systems by Generating the Optimal Inter-Row Spacing Factor. *Sustainability*, 14(10), p.6077. doi:https://doi.org/10.3390/su14106077.

Alvar-Beltrán, J., Coulibaly Saturnin, Baki Grégoire, Jose Luís Camacho, Dao, A., Jean Baptiste Migraine and Anna Dalla Marta (2023). Using AquaCrop as a decision-support tool for improved irrigation management in the Sahel region. *Agricultural water management*, 287, pp.108430–108430. doi:https://doi.org/10.1016/j.agwat.2023.108430

Amaducci, S., Yin, X. and Colauzzi, M. (2018). Agrivoltaic Systems to Optimise Land Use for Electric Energy Production. *Applied Energy*, 220, pp.545–561. doi:https://doi.org/10.1016/j.apenergy.2018.03.081.

Azadi, A., Jalali, A.S. and Navidi, M.N. (2023). Land evaluation approaches comparing TOPSIS and SAW with parametric methods for rice cultivation. *Environmental Monitoring and Assessment*, [online] 195(11), p.1296. doi:https://doi.org/10.1007/s10661-023-11849-8.

Azimuth Angle | PVEducation (2019) *Pveducation.org*. Available at: https://www.pveducation.org/pvcdrom/properties-of-sunlight/azimuth-angle (Accessed: 10 May 2025)

Ballandras, J. (2019) *ENERGY INNOVATION National Renewables in Agriculture Conference*. Available at: https://assets.cleanenergycouncil.org.au/documents/events/Renewable-Agg-Conf/Jean-Ballandras_Floating-Solar.pdf (Accessed: 10 May 2025)

Baqir, M. and Channi, H.K. (2021) 'Analysis and design of solar PV system using Pvsyst software', *Materials Today: Proceedings*, 48(5), pp. 1332-1338. Available at: https://doi.org/10.1016/j.matpr.2021.09.029

Biswas, T., Majumder, A., Dey, S., Mandal, A., Ray, S., Kapoor, P., Emam, W., Sahely Kanthal, Alessio ISHIZAKA and Adelajda Matuka (2024). Evaluation of management practices in rice–wheat cropping system using multicriteria decision-making methods in conservation agriculture. *Scientific Reports*, 14(1). doi:https://doi.org/10.1038/s41598-024-58022-w.

Campana, P.E., Bengt Stridh, Stefano Amaducci and Colauzzi, M. (2021). Optimization of vertically mounted agrivoltaic systems. *arXiv (Cornell University)*. doi:https://doi.org/10.48550/arxiv.2104.02124.

Cárdenas-Bravo, C., Lespinats, S. and Dutykh, D. (2024) 'A Practical Example of the Impact of Uncertainty on the One-Dimensional Single-Diode Model', *2024 IEEE International Symposium on Systems Engineering (ISSE)*, pp. 1–5. Available at: https://doi.org/10.1109/isse63315.2024.10741111

Chakraborty, S. (2022). TOPSIS and Modified TOPSIS: A comparative analysis. *Decision Analytics Journal*, 2, p.100021. doi:https://doi.org/10.1016/j.dajour.2021.100021

Climate Change Knowledge Portal (2021) *World Bank Climate Change Knowledge Portal*, *climateknowledgeportal.worldbank.org*. Available at: https://climateknowledgeportal.worldbank.org/country/malaysia/climate-data-historical (Accessed: 10 May 2025)

De Rooij, D. (2024). *Solar Panel Angle: how to calculate solar panel tilt angle?* Available at: https://sinovoltaics.com/learning-center/system-design/solar-panel-angle-tilt-calculation/ (Accessed: 10 May 2025).

Dean, M. (2020). *Chapter Six - Multi-criteria analysis*. [online] ScienceDirect. Available at: https://www.sciencedirect.com/science/article/abs/pii/S2543000920300147

Definitions of GHI and POA (no date) *SolarAnywhere*. Available at: https://www.solaranywhere.com/support/data-fields/definitions/ (Accessed: 10 May 2025)

Dhilipan, J. *et al.* (2022) 'Performance and efficiency of different types of solar cell material – A review', *Materials Today: Proceedings*, 66, pp. 1295–1302. Available at: https://doi.org/10.1016/j.matpr.2022.05.132

Evapotranspiration (ET) Explained (no date). Available at: https://www.marinwater.org/sites/default/files/2020-10/Evapotranspiration%20%28ET%29%20Explained.pdf (Accessed: 10 May 2025)

Ghada, B. *et al.* (2020) 'Recovery of Anthocyanins from Passion Fruit Epicarp for Food Colorants: Extraction Process Optimization and Evaluation of Bioactive Properties', *Molecules*, 25(14), p. 3203. Available at: https://doi.org/10.3390/molecules25143203

Government introduced Solar For Rakyat Incentive Scheme (SolaRIS) and Offers Additional Quota for NEM Rakyat – SEDA Malaysia, (2025) *Seda.gov.my*. Available at: https://www.seda.gov.my/government-introduced-solar-for-rakyat-incentive-scheme-solaris-and-offers-additional-quota-for-nem-rakyat/?utm (Accessed: 10 May 2025).

Gross, M. (2023). *What is PVsyst? Comprehensive Guide 2023*. [online] Partner Engineering and Science, Inc. Available at: https://www.partneresi.com/resources/articles/what-is-pvsyst-comprehensive-guide-2023/.

He, J. (2018) 'The development and utilization of microgrid technologies in China', *Energy Sources, Part A: Recovery, Utilization, and Environmental Effects*, 41(13), pp. 1535–1556. Available at: https://doi.org/10.1080/15567036.2018.1549131

Hernández, V. *et al.* (2015) 'Impact of Shading on Tomato Yield and Quality Cultivated with Different N Doses Under High Temperature Climate', *Procedia Environmental Sciences*, 29, pp. 197–198. Available at: https://doi.org/10.1016/j.proenv.2015.07.259

Houma, A.A. *et al.* (2021) 'Climate change impacts on rice yield of a large-scale irrigation scheme in Malaysia', *Agricultural Water Management*, 252, p. 106908. Available at: https://doi.org/10.1016/j.agwat.2021.106908

Imam, A.A. *et al.* (2024) 'Accurate Forecasting of Global Horizontal Irradiance in Saudi Arabia: A Comparative Study of Machine Learning Predictive Models and Feature Selection Techniques', *Mathematics*, 12(16), pp. 2600–2600. Available at: https://doi.org/10.3390/math12162600

Introduction to evapotranspiration (no date) *FAO*. Available at: https://www.fao.org/4/X0490E/x0490e04.htm. (Accessed: 10 May 2025)

Jeans, S. and Jeans, S. (2024) *Understanding Screw Pile,* The Ground Screw Centre. Available at: https://www.groundscrewcentre.co.uk/under-standing-ground-screw-piles. (Accessed: 10 May 2025)

Koons, E. (2023) *Wind Energy in Malaysia - Protentional for Growth*, *Energy Tracker Asia*. Available at: https://energytracker.asia/wind-energy-in-malaysia/. (Accessed: 10 May 2025)

Koons, E. (2023) *Wind Energy in Malaysia - Protentional for Growth*, *Energy Tracker Asia*. Available at: https://energytracker.asia/wind-energy-in-malaysia/. (Accessed: 10 May 2025)

Kumar, R. *et al.* (2020) 'Design and simulation of standalone solar PV system using PVsyst Software: A case study', *Materials Today: Proceedings*, 46(11), pp.. 5322-5328. Available at: https://doi.org/10.1016/j.matpr.2020.08.785

Lee, S. *et al.* (2023) 'Agrivoltaic system designing for sustainability and smart farming: Agronomic aspects and design criteria with safety assessment', *Applied Energy*, 341, pp. 121130–121130. Available at: https://doi.org/10.1016/j.apenergy.2023.121130

Liu, J., Li, S., Luo, J. and Chen, Z. (2023). Experimental study on critical wind velocity of a 33-meter-span flexible photovoltaic support structure and its mitigation. *Journal of Wind Engineering and Industrial Aerodynamics*, 236, p.105355. doi:https://doi.org/10.1016/j.jweia.2023.105355

Liu, J. and van Iersel, M.W. (2021). Photosynthetic Physiology of Blue, Green, and Red Light: Light Intensity Effects and Underlying Mechanisms. *Frontiers in Plant Science*, [online] 12(12). doi:https://doi.org/10.3389/fpls.2021.619987.

Mah, C.-Y. *et al.* (2019) 'Investigating the Performance Improvement of a Photovoltaic System in a Tropical Climate using Water Cooling Method', *Energy Procedia*, 159, pp. 78–83. Available at: https://doi.org/10.1016/j.egypro.2018.12.022

Mail, M. (2024) *Solar panel rebate of up to RM4,000 extended to April 2025, NEM upgrades to promote renewable energy, says ministry*, *Malay Mail* . Malay Mail. Available at: https://www.malaymail.com/news/malaysia/2024/12/23/solar-panel-rebate-of-up-to-rm4000-extended-to-april-2025-nem-upgrades-to-promote-renewable-energy-says-ministry/160829 (Accessed: 10 May 2025).

Md Nor. S *et al*. (2022). 'Passion Fruit—A Potential Crop for Exploration in Malaysia: A Review', *Pertanika Journals*, 45(3), pp. 761-780. Available at: https://www.cabidigitallibrary.org/doi/pdf/10.5555/20220372096

Noor Fadzlinda Othman *et al.* (2023) 'Advancement in Agriculture Approaches with Agrivoltaics Natural Cooling in Large Scale Solar PV Farms', *Agriculture*, 13(4), pp. 854–854. Available at: https://doi.org/10.3390/agriculture13040854

Physical models used > Irradiation models > The Hay transposition model (2025) *Pvsyst.com*. Available at: https://www.pvsyst.com/help-pvsyst7/models_meteo_hay_model.htm (Accessed: 10 May 2025).

POA Beam (2021) *PV Performance Modeling Collaborative (PVPMC)*. Available at: https://pvpmc.sandia.gov/modeling-guide/1-weather-design-inputs/plane-of-array-poa-irradiance/calculating-poa-irradiance/poa-beam/ (Accessed: 10 May 2025)

Patil, M., Sidramappa, A., Shetty, S.K. and Hebbale, A.M. (2023). Experimental study of solar PV/T panel to increase the energy conversion efficiency by air cooling. *Materials Today: Proceedings*. [online] doi:https://doi.org/10.1016/j.matpr.2023.05.007

Peng, R., Xu, H., Bi, H. and Wang, N. (2025). Accumulated Photosynthetically Active Radiation and Its Heterogeneity Collectively Decrease Soybean Yield in Apple-Based Intercropping Systems. *Agronomy*, 15(3), p.581. doi:https://doi.org/10.3390/agronomy15030581.

Perchlik, M. and Tegeder, M. (2018). Leaf Amino Acid Supply Affects Photosynthetic and Plant Nitrogen Use Efficiency under Nitrogen Stress. *Plant Physiology*, 178(1), pp.174–188. doi:https://doi.org/10.1104/pp.18.00597.

Poobalan, B. *et al.* (2020) 'The study of photovoltaic systems performance using various azimuth angles and solar array tilt positions', *Journal of Physics: Conference Series*, 1432(1), p. 012050. Available at: https://doi.org/10.1088/1742-6596/1432/1/012050

Pranda M.P. Garniwa *et al.* (2023) 'Intraday forecast of global horizontal irradiance using optical flow method and long short-term memory model', *Solar Energy*, 252, pp. 234–251. Available at: https://doi.org/10.1016/j.solener.2023.01.037

Project design > Grid-connected system definition > Inverter / Array sizing (2025) *Pvsyst.com*. Available at: https://www.pvsyst.com/help-pvsyst7/inverter_array_sizing.htm? (Accessed: 10 May 2025).

Randle-Boggis, R.J. *et al.* (2024) 'Harvesting the sun twice: Energy, food and water benefits from agrivoltaics in East Africa', *Renewable and Sustainable Energy Reviews*, 208, p. 115066. Available at: https://doi.org/10.1016/j.rser.2024.115066

Rittick Maity, Sudhakar, K. and Razak, A.A. (2024) 'Agri-Solar Water Pumping design, energy, and environmental analysis: A comprehensive study in Tropical Humid climate', *Heliyon*, pp. e39604–e39604. Available at: https://doi.org/10.1016/j.heliyon.2024.e39604

Roig-Villanova, I. and Martínez-García, J.F. (2016). Plant Responses to Vegetation Proximity: A Whole Life Avoiding Shade. *Frontiers in Plant Science*, [online] 7. doi:https://doi.org/10.3389/fpls.2016.00236

Rosa Isabella Cuppari, Branscomb, A., Graham, M., Negash, F., Angelique Kidd Smith, Proctor, K., Rupp, D., Abiyou Tilahun Ayalew, Gizaw Getaneh Tilaye, Higgins, C.W. and Majdi Abou Najm (2024). Agrivoltaics: Synergies and trade-offs in achieving the sustainable development goals at the global and local scale. *Applied energy*, 362, pp.122970–122970. doi:https://doi.org/10.1016/j.apenergy.2024.122970

Savin, R. and Slafer, G.A. (1991) 'Shading effects on the yield of an Argentinian wheat cultivar', *The Journal of Agricultural Science*, 116(1), pp. 1–7. Available at: https://doi.org/10.1017/s0021859600076085

Scherrer, S.C. *et al.* (2022) 'Trends and drivers of recent summer drying in Switzerland', *Environmental Research Communications*, 4(2), p. 025004. Available at: https://doi.org/10.1088/2515-7620/ac4fb9

Selvaraj, J. (2021) 'Effect of tilt angle on the performance and electrical parameters of a PV module: Comparative indoor and outdoor experimental investigation', *Energy and Built Environment*, 3(3). pp. 278-290. Available at: https://doi.org/10.1016/j.enbenv.2021.02.001

Shen *et al.* (2024) 'Impact of dust and temperature on photovoltaic panel performance: A model-based approach to determine optimal cleaning frequency', *Heliyon*, 10(16), p.e35390. Available at: https://doi.org/10.1016/j.heliyon.2024.e35390

Solargis (2021) *Solar resource maps & GIS data for 200+ countries.* Available at: https://solargis.com/resources/free-maps-and-gis-data?locality=malaysia. (Accessed: 10 May 2025)

Starmühler, H. (2020) *Agro-Photovoltaik vereint Agrar- und Energiewende*, *Energie-bau.at*. Available at: https://www.energie-bau.at/meinung/3469-agro-photovoltaik-vereint-agrar-und-energiewende (Accessed: 10 May 2025).

Suman, Sharma, P. and Goyal, P. (2021) 'Analysing the effects of solar insolation and temperature on PV cell characteristics', *Materials Today: Proceedings*. 45(6), pp. 5539 - 5543Available at: https://doi.org/10.1016/j.matpr.2021.02.301
Supangkat Samidjo, G. (2021) 'Growth Pattern of Sunflower on Some Light Intensity in The Coastal Land', *IOP Conference Series: Earth and Environmental Science*, 752(1), p. 012019. Available at: https://doi.org/10.1088/1755-1315/752/1/012019

Taitano et al. (2023). *Calamansi*. Available at: https://projects.sare.org/media/pdf/2/0/2/2023-july-ceo-pub-calamansi.pdf (Accessed: 14 September 2025)

The ETo Calculator Evapotranspiration from a reference surface Reference Manual Dirk Raes Food and Agriculture Organization of the United Nations Land and Water Division (2009). Available at: https://www.caminoscastillayleon.es/wp-content/uploads/Documentacion%20Tecnica/Manual%20ETo%20Calculator%20(2009).pdf (Accessed: 10 May 2025).

Thokchom, R & Mandal, G. (2020). ' Production Preference and Importance of Passion Fruit (Passiflora Edulis): A Review', *Journal of Agricultural Engineering and Food Technology,* 4(1), pp. 27-30. Available at: https://www.researchgate.net/publication/342734984_Production_Preference_and_Importance_of_Passion_Fruit_Passiflora_Edulis_A_Review. (Accessed: 10 May 2025)

Types of solar cells explained | FMB (no date) *Federation of Master Builders*. Available at: https://www.fmb.org.uk/homepicks/solar-panels/types-of-solar-cells/. (Accessed: 10 May 2025).

U.S. Department of Energy (n.d.). *Agrivoltaics: Solar and Agriculture Co-Location*. [online] Energy.gov. Available at: https://www.energy.gov/eere/solar/agrivoltaics-solar-and-agriculture-co-location.

U.S. Energy Information Administration (2023) *Photovoltaics and Electricity*, *Eia.gov*. U.S. Energy Information Administration. Available at: https://www.eia.gov/energyexplained/solar/photovoltaics-and-electricity.php. (Accessed: 10 May 2025)

Umesh, B. *et al.* (2022) 'Assessment of climate change impact on maize (Zea mays L.) through aquacrop model in semi-arid alfisol of southern Telangana', *Agricultural Water Management*, 274, p. 107950. Available at: https://doi.org/10.1016/j.agwat.2022.107950

United Nations (2020) *Department of Economic and Social Affairs*, *sdgs.un.org*. Available at: https://sdgs.un.org/#goal_section. (Accessed: 10 May 2025)

Vanuytrecht, E. *et al.* (2014) 'AquaCrop: FAO's crop water productivity and yield response model', *Environmental Modelling & Software*, 62, pp. 351–360. Available at: https://doi.org/10.1016/j.envsoft.2014.08.005

Villalva, M.G., Gazoli, J.R. and Filho, E.R. (2009) 'Comprehensive Approach to Modeling and Simulation of Photovoltaic Arrays', *IEEE Transactions on Power Electronics*, 24(5), pp. 1198–1208. Available at: https://doi.org/10.1109/tpel.2009.2013862

Wale, A., Dessie, M. and Kendie, H. (2022) 'Evaluating the Performance of AquaCrop Model for Potato Production Under Deficit Irrigation', *Air, Soil and Water Research*, 15, p. 117862212211082. Available at: https://doi.org/10.1177/11786221221108216

What is STC and why is it significant? | Seaward (2025) *Seaward*. Available at: https://www.seaward.com/gb/support/solar/faqs/88663-what-is-stc-and-why-is-it-significant/. (Accessed: 10 May 2025)

Xu, G. *et al.* (2017) 'Effects of screenhouse cultivation and organic materials incorporation on global warming potential in rice fields', *Environmental Science and Pollution Research*, 24(7), pp. 6581–6591. Available at: https://doi.org/10.1007/s11356-017-8397-7

Zainol Abidin, M.A., Mahyuddin, M.N. and Mohd Zainuri, M.A.A. (2021) ‘Solar Photovoltaic Architecture and Agronomic Management in Agrivoltaic System: A Review’, *Sustainability*, 13(14), p. 7846. Available at: https://doi.org/10.3390/su13147846

APPENDICES

Appendix A: Foundation of PV rack

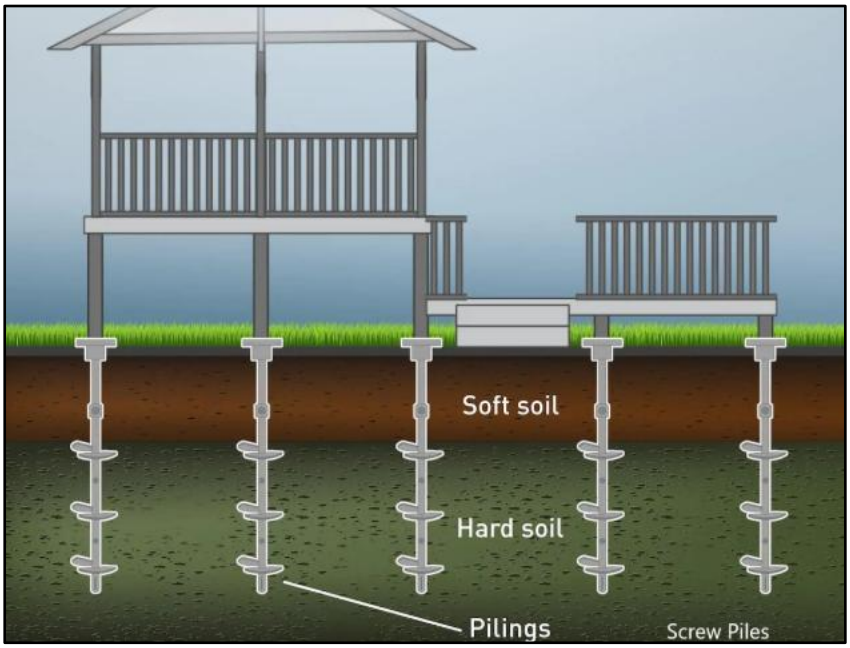

Figure A. 1: Herical Screw Pi;e as foundation of PV panels

Appendix B: Flowchart and Workflow

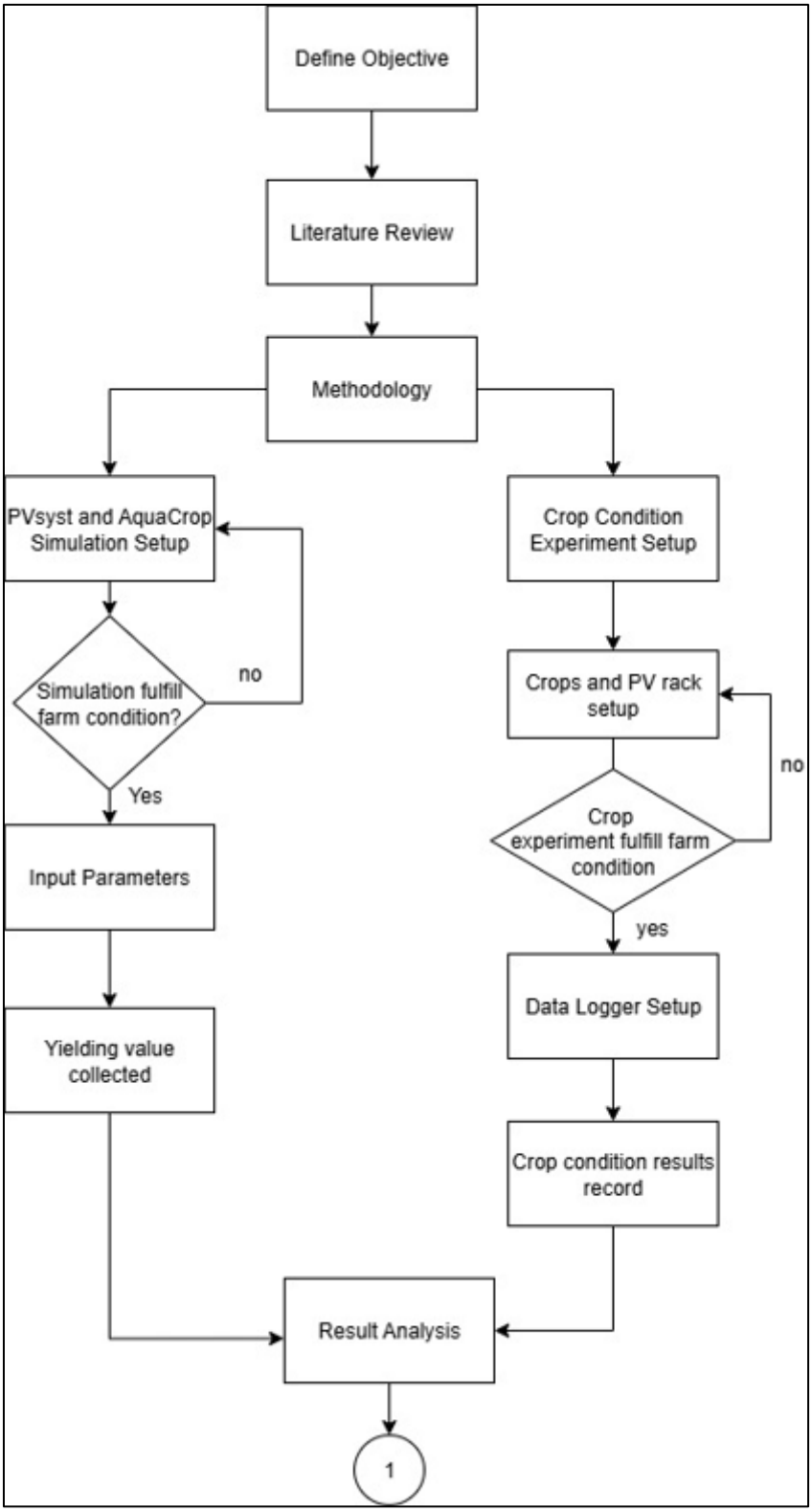

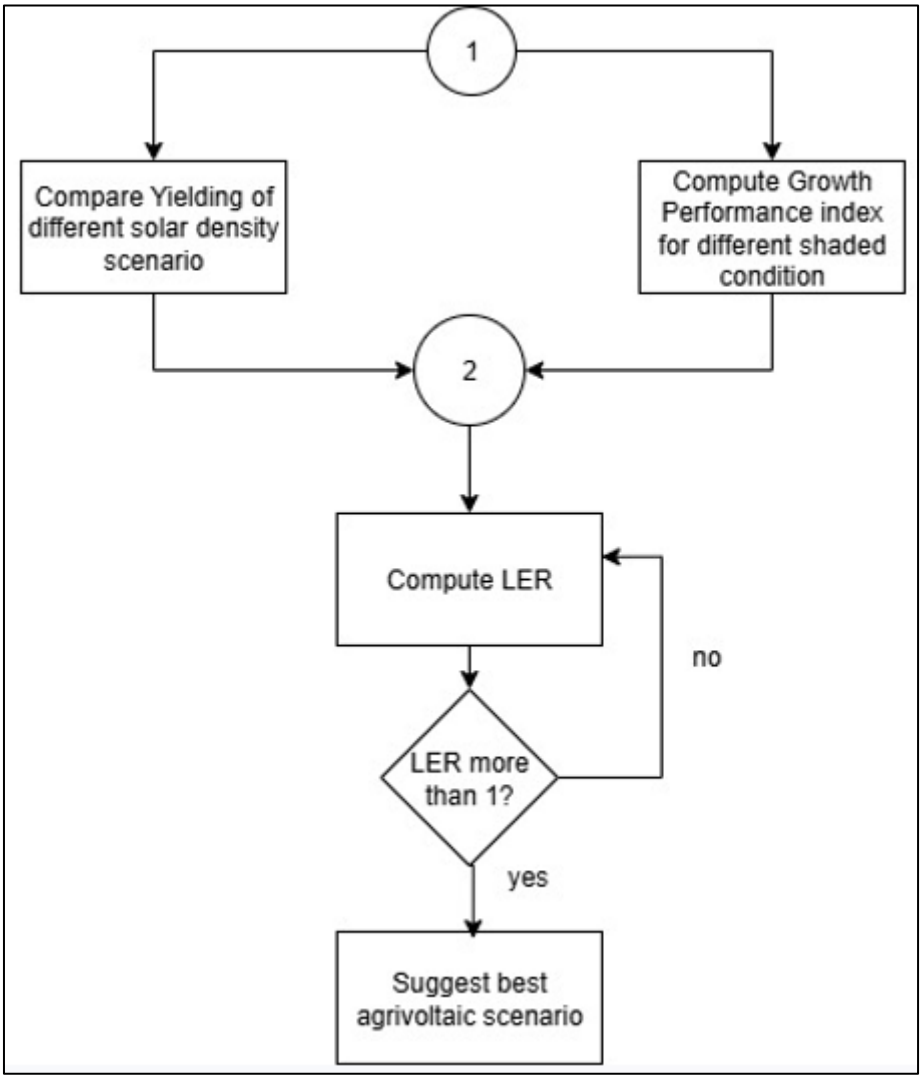

Figure B. 1: Workflow

No.	Project Activities	Planned Completion Date	W1	W2	W3	W4	W5	W6	W7	W8	W9	W10	W11	W12	W13	W14	W15	W16	W17
1.	1.Project Briefing 2. Planning with supervisor	2025-02-21																	
2.	1. Identify Research Gaps 2. Identify Methodology 3. Installation of PV syst and DSSAT	2025-03-08																	
3.	1. Review the research nature 2. Evaluation of Existing Data and Information 3. Experience in operating software 4. Preparation of report	2025-03-22																	
4.	1. Evaluation of Existing Data and Information 2. Data Gathering 3. Analyze Crop Yielding data 4. Design Module Layout 5. Preparation of report	2025-04-12																	
5.	1. Data Analyze for crop yielding 2. Design of PV layout 3. Preparation of report and completion of report	2025-05-03																	
6.	1. Preparation of presentation	2025-05-10																	

Figure B. 2: Gantt Chart for FYP1

No.	Project Activities	Planned Completion Date	W1	W2	W3	W4	W5	W6	W7	W8	W9	W10	W11	W12	W13	W14	W15	W16	W17
1.	Experiment Planning Stage - Choosing the suitable plant for experiment purpose - Design the configuration of the shading effect - Determine the location of the experiment	2025-06-12																	
2.	Setup the experiment - Construct the PV rack for creating shading effect - Purchase plant - Correct orientation (azimuth and tilt angle) - Setup PAR Sensor	2025-06-19																	
3.	-Monitoring the crop growth -Measuring the sun intensity level of the plant receive -measure the growth condition of plant for different shading condition	2025-09-13																	
4.	Solar Panel output simulation - Construct shading condition - Construct actual scenario - Input values (Panel and Inverter Info) - Construct simulation - Compare output	2025-09-13																	
5.	Report Writing - Correction for FYP 1 Report - Presentation slide	2025-09-21																	

Figure B. 3: Gantt Chart for FYP 2

Appendix C: Mounting Point of PV panels

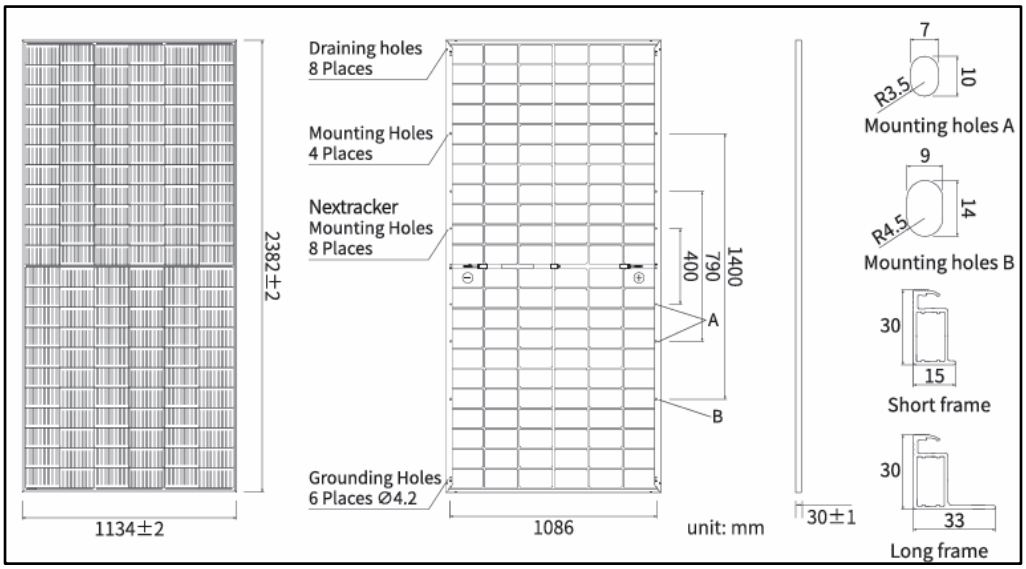

Figure C. 1: Mounting Point of JAM66D45 620W

Appendix D: Python Code for PAR values record

```
# -*- coding: utf-8 -*-
import minimalmodbus                                    #communication with RS485
Sensor
import time                                  #for timing and schedule
from datetime import datetime, timedelta             #for timing and schedule
import os
#import gc                                   #Control memory clean up
#import psutil

# Configuration for PAR sensors
par_sensors = [
    {'address': 1, 'name': 'PAR_Sensor_1'},
    {'address': 2, 'name': 'PAR_Sensor_2'},
    {'address': 3, 'name': 'PAR_Sensor_3'}
]

# Function to initialize sensors
def init_sensor(address):
    sensor = minimalmodbus.Instrument('/dev/ttyUSB0', address)        #
/dev/ttyUSB0 for Raspberry Pi, the com number should be according to which
pc port
    sensor.serial.baudrate = 4800 #speed of data trasfer (bits/second)
    sensor.serial.bytesize = 8  #number of bits per data unit
    sensor.serial.parity = minimalmodbus.serial.PARITY_NONE  #error
checking method, should match the sensor manual
    sensor.serial.stopbits = 1  #make end of each bits
    sensor.serial.timeout = 1  # Increased timeout to more seconds if needed,
wait time before giving up
    sensor.mode = minimalmodbus.MODE_RTU #remote terminal unit
    sensor.clear_buffers_before_each_transaction = True
```

```
    sensor.debug = True
    return sensor

# Initialize PAR
par_sensors_map = {sensor['name']: init_sensor(sensor['address']) for sensor in
par_sensors}

# Function to get the current date's filename
def get_daily_filename(directory):
    current_date = datetime.now().date()
    return os.path.join(directory, f"{current_date}_sensor_values.txt")

# Function to create a new text file with only PAR sensor headers
def create_text_file(filename, par_sensor_names):
    with open(filename, 'w') as file:
        headers = ['Timestamp'] + [name for name in par_sensor_names]
        file.write(','.join(headers) + '\n')

def main():
    directory = r'/home/simyanghong/Desktop/par_data'  # Change to your
directory
    os.makedirs(directory, exist_ok=True)

    start_hour = 7
    end_hour = 19  # 7 PM

    while True:
        now = datetime.now()
        current_time = now.time()
        start_time = datetime.combine(now.date(), datetime.min.time()) +
timedelta(hours=start_hour)
        end_time = datetime.combine(now.date(), datetime.min.time()) +
timedelta(hours=end_hour)
```

```
        filename = get_daily_filename(directory)
        if not os.path.exists(filename):
            create_text_file(filename, [sensor['name'] for sensor in par_sensors])

        if start_time.time() <= current_time < end_time.time():
            try:
                timestamp = datetime.now().strftime("%Y-%m-%d %H:%M:%S")
                row = [timestamp]
                start_logging_time = time.time()

                # Reading PAR sensors
                for sensor_name, sensor in par_sensors_map.items():
                    success = False
                    attempts = 3
                    for attempt in range(attempts):
                        try:
                            data = sensor.read_registers(0, 1, functioncode=3)
                            data_value = data[0]  # Extracting the first register value
                            print(f"{sensor_name} PAR value: {data_value} \u00B5mol/m\u00B2\u00B7s")
                            row.append(str(data_value))
                            success = True
                            break
                        except Exception as e:
                            print(f"Error reading data from {sensor_name} (attempt {attempt + 1}): {e}")

                    if not success:
                        row.append("None")

                # Log data into file
                with open(filename, 'a') as file:
```

```
                file.write('\t'.join(row) + '\n')

            print(f"Logged: {row}")

            elapsed_time = time.time() - start_logging_time
            sleep_time = max(60 - elapsed_time, 0)
            time.sleep(sleep_time)

            # Memory management
#             monitor_memory()
#             gc.collect()
        except Exception as e:
            print(f"Error logging data: {e}")
            time.sleep(60)
    else:
        print(f"Outside recording hours at {now}")
        time.sleep(60)

if __name__ == "__main__":
    main()
```

Appendix E: PV panels simulation result for different tilt angle

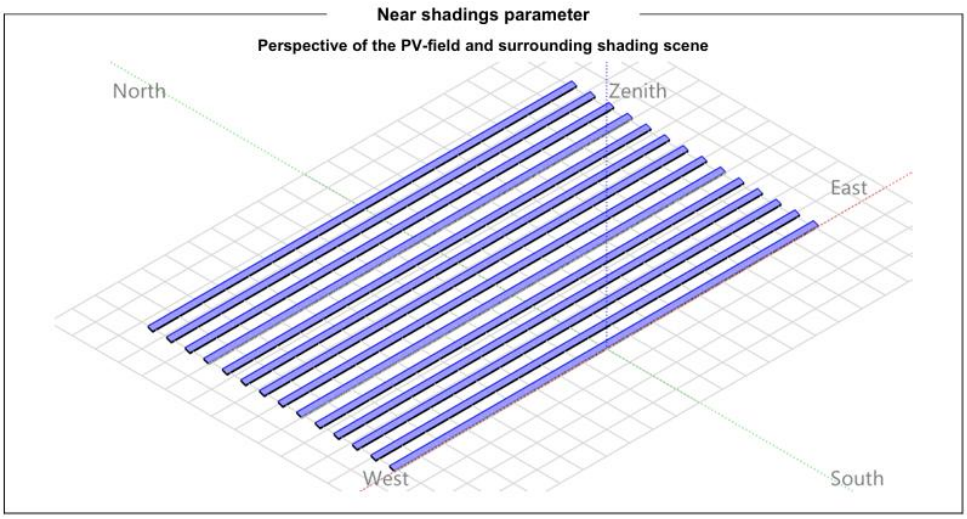

Figure E. 1: PV layout for different tilt angle

Main results

System Production

Produced Energy	424346 kWh/year	Specific production	1358 kWh/kWp/year
		Perf. Ratio PR	75.50 %

Normalized productions (per installed kWp)

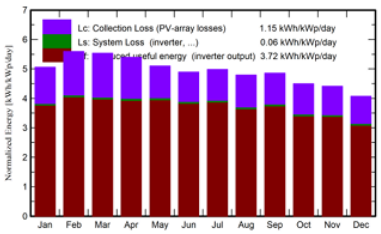

Performance Ratio PR

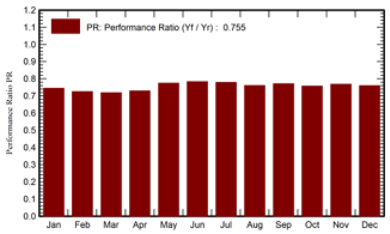

Balances and main results

	GlobHor kWh/m²	DiffHor kWh/m²	T_Amb °C	GlobInc kWh/m²	GlobEff kWh/m²	EArray kWh	E_Grid kWh	PR ratio
January	157.0	73.07	26.79	156.9	151.4	37092	36505	0.745
February	156.7	72.07	27.37	156.6	151.8	36036	35483	0.725
March	171.6	85.14	27.81	171.5	166.5	39144	38524	0.719
April	162.0	81.17	27.63	161.9	157.3	37514	36907	0.729
May	158.3	90.46	28.20	158.2	153.2	38938	38308	0.775
June	147.0	84.34	27.62	146.9	142.1	36535	35935	0.783
July	154.5	87.01	27.64	154.4	149.4	38177	37556	0.778
August	148.7	85.01	27.48	148.6	144.0	35905	35309	0.760
September	145.8	86.31	26.90	145.7	140.9	35723	35134	0.771
October	139.4	79.15	27.06	139.4	134.9	33585	32999	0.758
November	132.3	74.56	26.51	132.3	127.9	32295	31733	0.768
December	126.4	63.91	26.87	126.3	121.7	30508	29952	0.759
Year	1799.7	962.21	27.33	1798.7	1741.3	431453	424346	0.755

Legends

GlobHor	Global horizontal irradiation	EArray	Effective energy at the output of the array
DiffHor	Horizontal diffuse irradiation	E_Grid	Energy injected into grid
T_Amb	Ambient Temperature	PR	Performance Ratio
GlobInc	Global incident in coll. plane		
GlobEff	Effective Global, corr. for IAM and shadings		

Figure E. 2: Balance and Main results when tilt angle is 0°

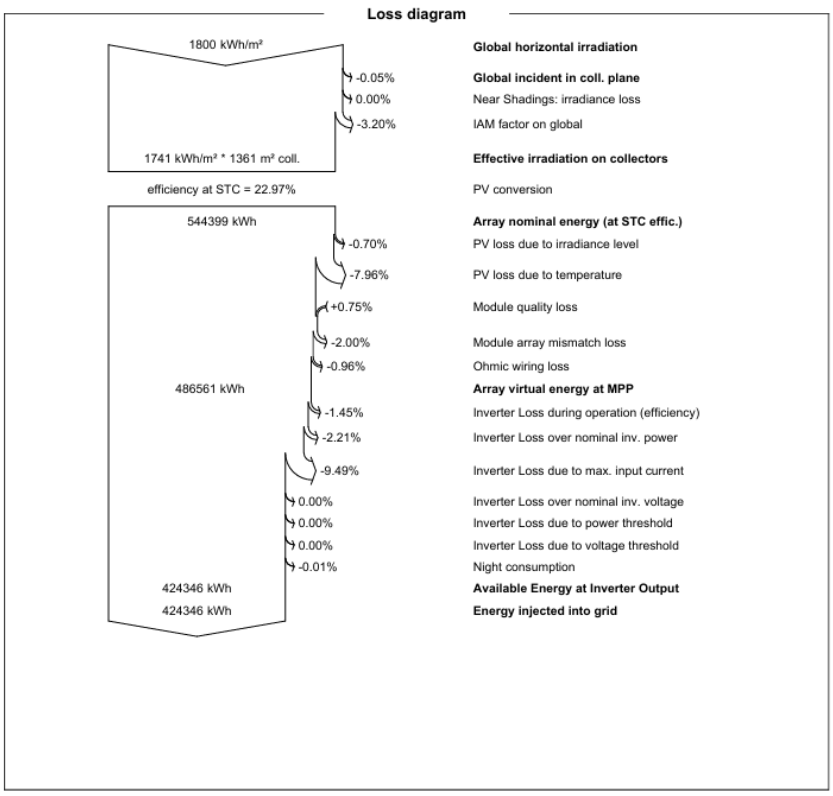

Figure E. 3: Loss Diagram when tilt angle is 0º

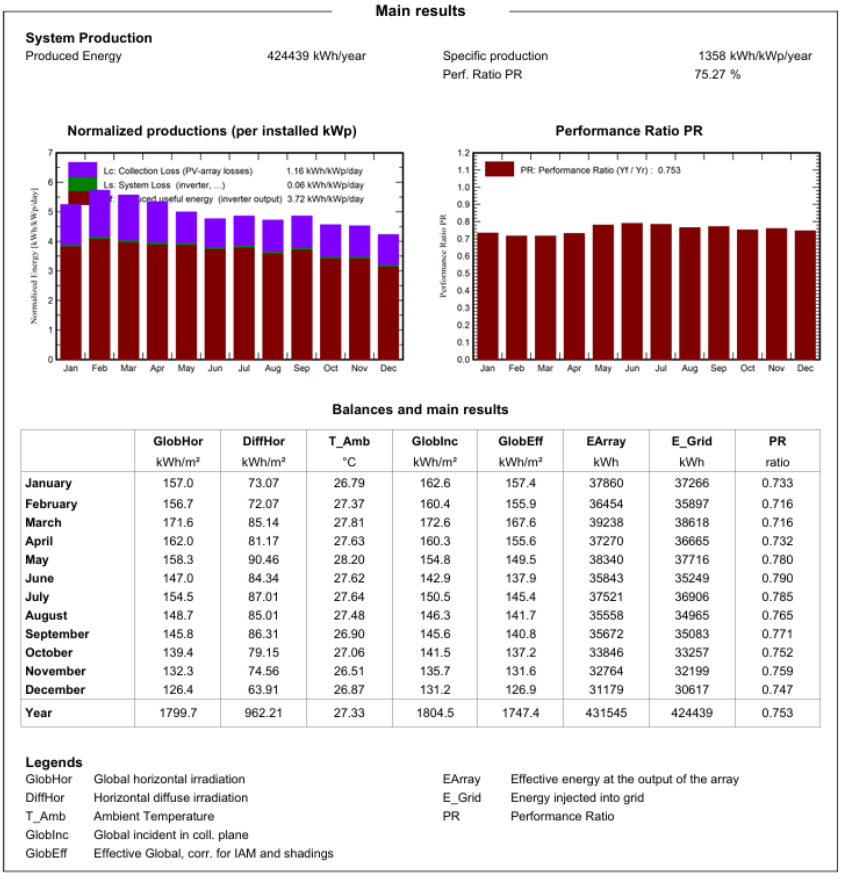

Balances and main results

	GlobHor kWh/m²	DiffHor kWh/m²	T_Amb °C	GlobInc kWh/m²	GlobEff kWh/m²	EArray kWh	E_Grid kWh	PR ratio
January	157.0	73.07	26.79	162.6	157.4	37860	37266	0.733
February	156.7	72.07	27.37	160.4	155.9	36454	35897	0.716
March	171.6	85.14	27.81	172.6	167.6	39238	38618	0.716
April	162.0	81.17	27.63	160.3	155.6	37270	36665	0.732
May	158.3	90.46	28.20	154.8	149.5	38340	37716	0.780
June	147.0	84.34	27.62	142.9	137.9	35843	35249	0.790
July	154.5	87.01	27.64	150.5	145.4	37521	36906	0.785
August	148.7	85.01	27.48	146.3	141.7	35558	34965	0.765
September	145.8	86.31	26.90	145.6	140.8	35672	35083	0.771
October	139.4	79.15	27.06	141.5	137.2	33846	33257	0.752
November	132.3	74.56	26.51	135.7	131.6	32764	32199	0.759
December	126.4	63.91	26.87	131.2	126.9	31179	30617	0.747
Year	1799.7	962.21	27.33	1804.5	1747.4	431545	424439	0.753

Legends

GlobHor	Global horizontal irradiation	EArray	Effective energy at the output of the array
DiffHor	Horizontal diffuse irradiation	E_Grid	Energy injected into grid
T_Amb	Ambient Temperature	PR	Performance Ratio
GlobInc	Global incident in coll. plane		
GlobEff	Effective Global, corr. for IAM and shadings		

Figure E. 4: Balance and Main results when tilt angle is 5º

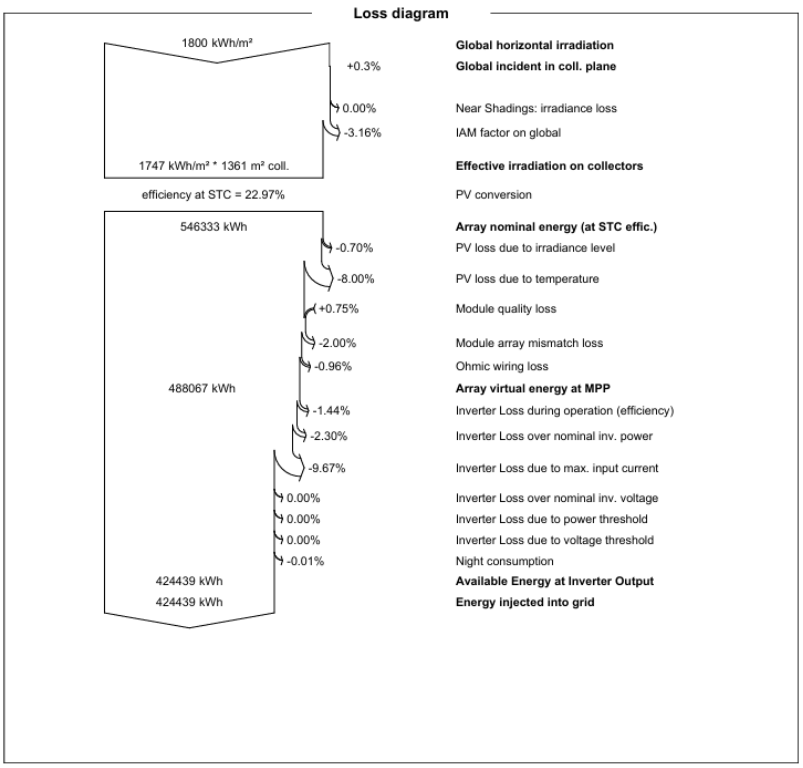

Figure E. 5: Loss Diagram when tilt angle is 5º

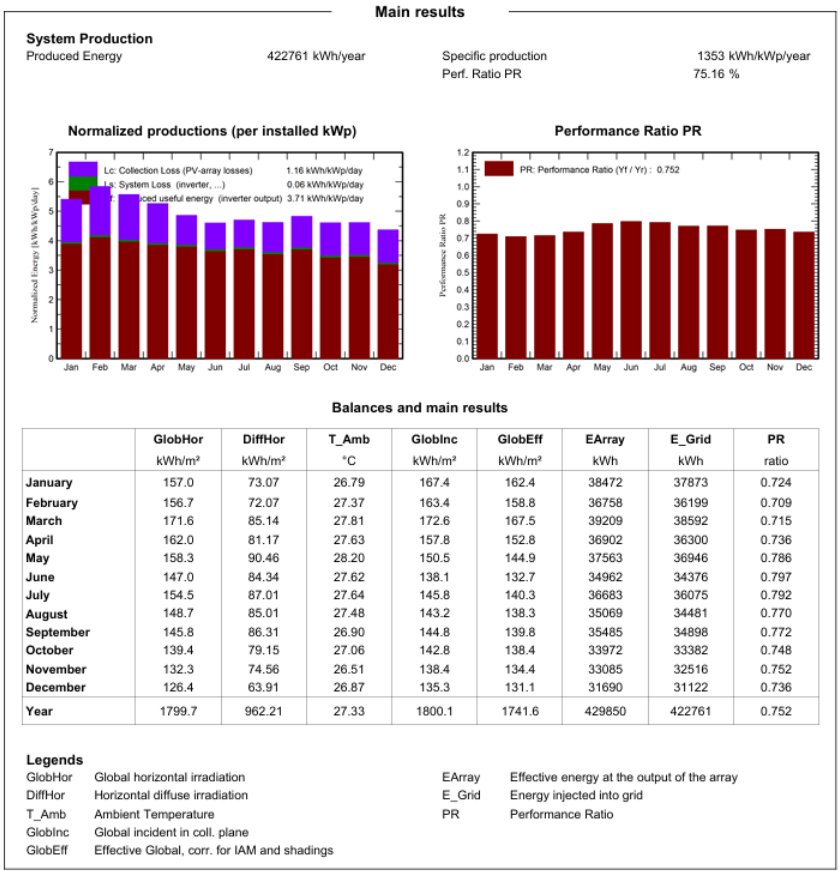

	GlobHor kWh/m²	DiffHor kWh/m²	T_Amb °C	GlobInc kWh/m²	GlobEff kWh/m²	EArray kWh	E_Grid kWh	PR ratio
January	157.0	73.07	26.79	167.4	162.4	38472	37873	0.724
February	156.7	72.07	27.37	163.4	158.8	36758	36199	0.709
March	171.6	85.14	27.81	172.6	167.5	39209	38592	0.715
April	162.0	81.17	27.63	157.8	152.8	36902	36300	0.736
May	158.3	90.46	28.20	150.5	144.9	37563	36946	0.786
June	147.0	84.34	27.62	138.1	132.7	34962	34376	0.797
July	154.5	87.01	27.64	145.8	140.3	36683	36075	0.792
August	148.7	85.01	27.48	143.2	138.3	35069	34481	0.770
September	145.8	86.31	26.90	144.8	139.8	35485	34898	0.772
October	139.4	79.15	27.06	142.8	138.4	33972	33382	0.748
November	132.3	74.56	26.51	138.4	134.4	33085	32516	0.752
December	126.4	63.91	26.87	135.3	131.1	31690	31122	0.736
Year	1799.7	962.21	27.33	1800.1	1741.6	429850	422761	0.752

Legends

GlobHor	Global horizontal irradiation	EArray	Effective energy at the output of the array
DiffHor	Horizontal diffuse irradiation	E_Grid	Energy injected into grid
T_Amb	Ambient Temperature	PR	Performance Ratio
GlobInc	Global incident in coll. plane		
GlobEff	Effective Global, corr. for IAM and shadings		

Figure E. 6: Balance and Main results when tilt angle is 10º

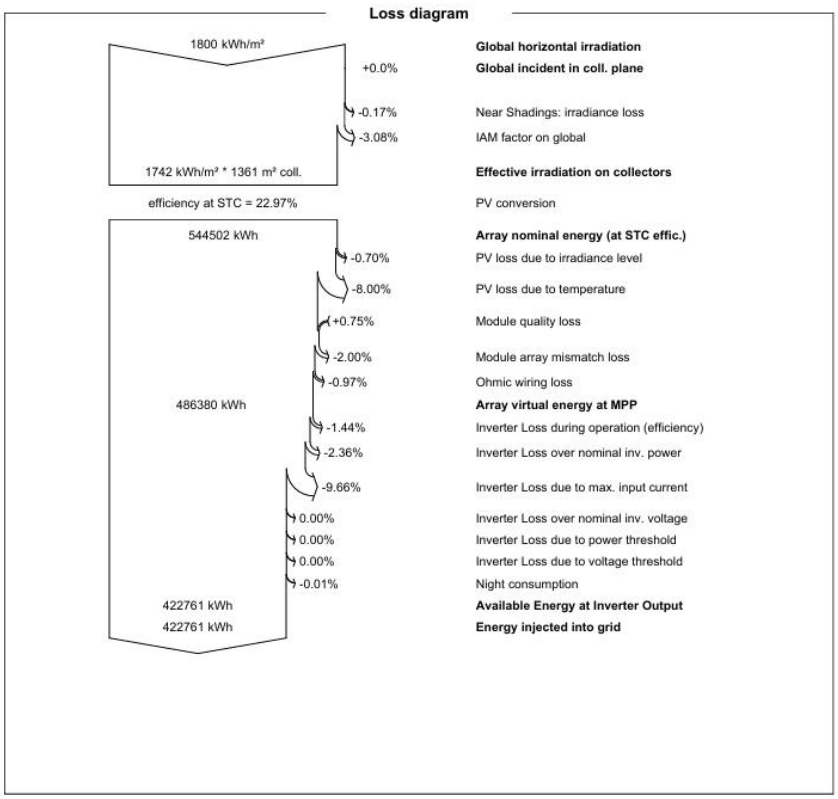

Figure E. 7: Loss Diagram when tilt angle is 10º

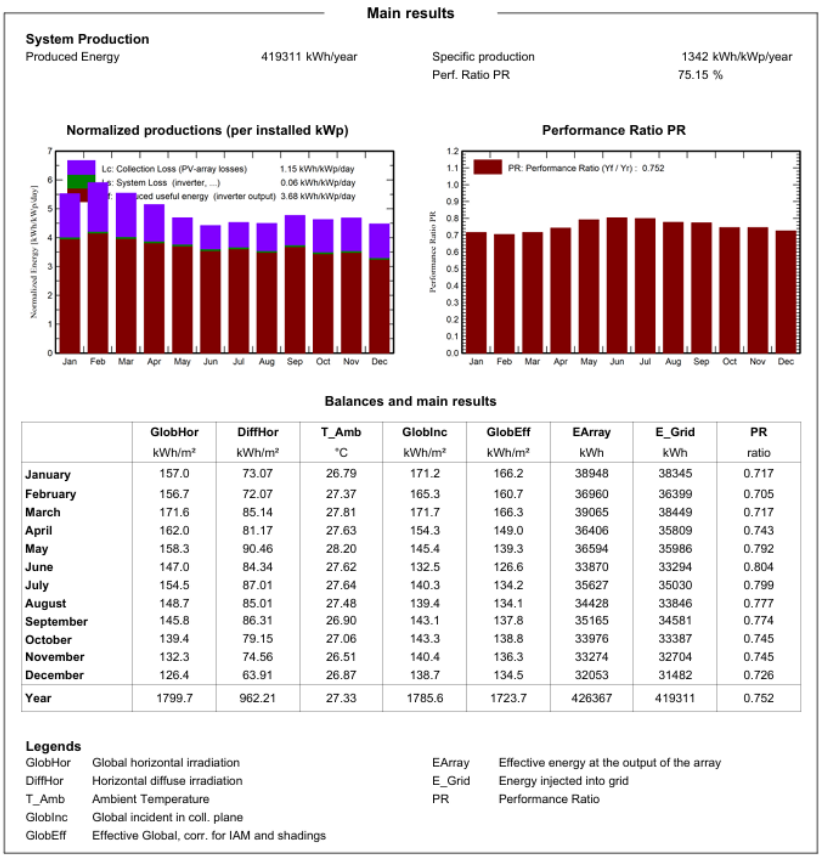

Balances and main results

	GlobHor kWh/m²	DiffHor kWh/m²	T_Amb °C	GlobInc kWh/m²	GlobEff kWh/m²	EArray kWh	E_Grid kWh	PR ratio
January	157.0	73.07	26.79	171.2	166.2	38948	38345	0.717
February	156.7	72.07	27.37	165.3	160.7	36960	36399	0.705
March	171.6	85.14	27.81	171.7	166.3	39065	38449	0.717
April	162.0	81.17	27.63	154.3	149.0	36406	35809	0.743
May	158.3	90.46	28.20	145.4	139.3	36594	35986	0.792
June	147.0	84.34	27.62	132.5	126.6	33870	33294	0.804
July	154.5	87.01	27.64	140.3	134.2	35627	35030	0.799
August	148.7	85.01	27.48	139.4	134.1	34428	33846	0.777
September	145.8	86.31	26.90	143.1	137.8	35165	34581	0.774
October	139.4	79.15	27.06	143.3	138.8	33976	33387	0.745
November	132.3	74.56	26.51	140.4	136.3	33274	32704	0.745
December	126.4	63.91	26.87	138.7	134.5	32053	31482	0.726
Year	1799.7	962.21	27.33	1785.6	1723.7	426367	419311	0.752

Legends

GlobHor	Global horizontal irradiation	EArray	Effective energy at the output of the array
DiffHor	Horizontal diffuse irradiation	E_Grid	Energy injected into grid
T_Amb	Ambient Temperature	PR	Performance Ratio
GlobInc	Global incident in coll. plane		
GlobEff	Effective Global, corr. for IAM and shadings		

Figure E. 8: Balance and Main results when tilt angle is 15º

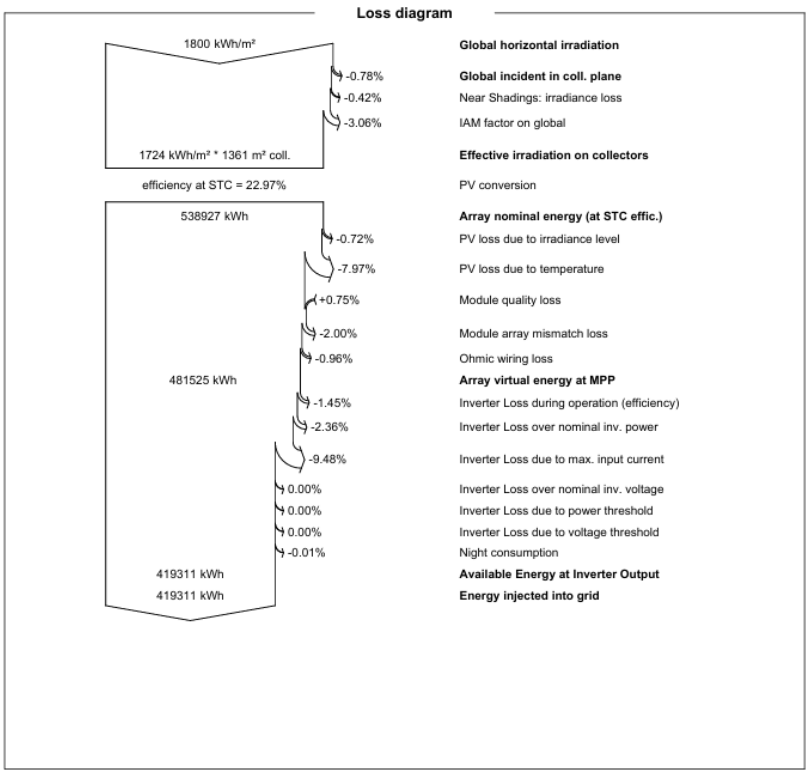

Figure E. 9: Loss Diagram when tilt angle is 15°

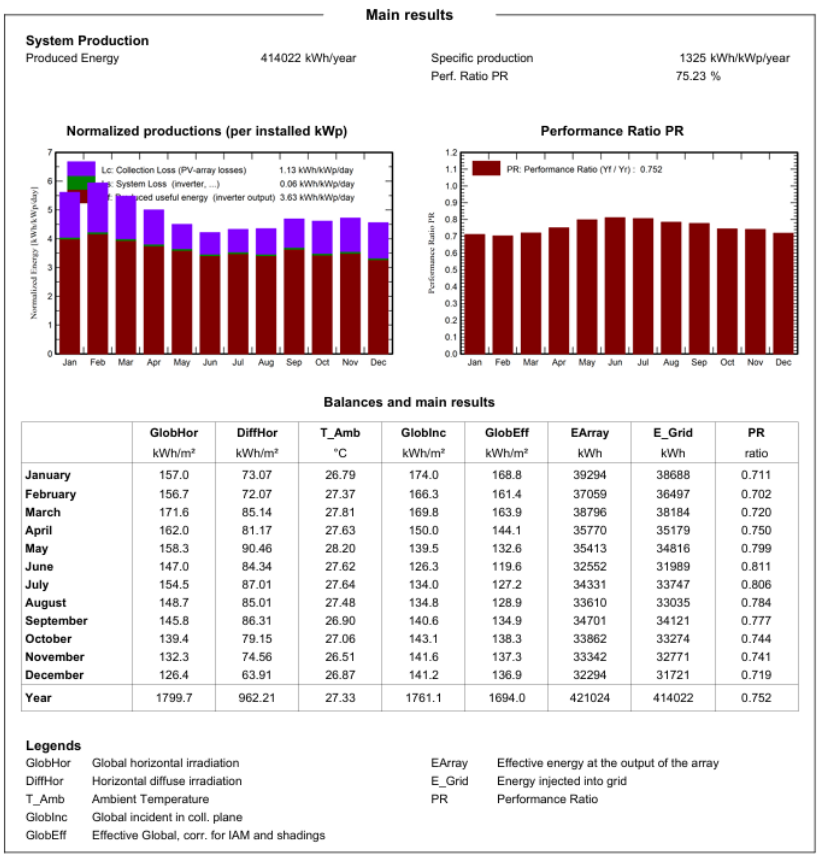

Balances and main results

	GlobHor kWh/m²	DiffHor kWh/m²	T_Amb °C	GlobInc kWh/m²	GlobEff kWh/m²	EArray kWh	E_Grid kWh	PR ratio
January	157.0	73.07	26.79	174.0	168.8	39294	38688	0.711
February	156.7	72.07	27.37	166.3	161.4	37059	36497	0.702
March	171.6	85.14	27.81	169.8	163.9	38796	38184	0.720
April	162.0	81.17	27.63	150.0	144.1	35770	35179	0.750
May	158.3	90.46	28.20	139.5	132.6	35413	34816	0.799
June	147.0	84.34	27.62	126.3	119.6	32552	31989	0.811
July	154.5	87.01	27.64	134.0	127.2	34331	33747	0.806
August	148.7	85.01	27.48	134.8	128.9	33610	33035	0.784
September	145.8	86.31	26.90	140.6	134.9	34701	34121	0.777
October	139.4	79.15	27.06	143.1	138.3	33862	33274	0.744
November	132.3	74.56	26.51	141.6	137.3	33342	32771	0.741
December	126.4	63.91	26.87	141.2	136.9	32294	31721	0.719
Year	1799.7	962.21	27.33	1761.1	1694.0	421024	414022	0.752

Legends

GlobHor	Global horizontal irradiation	EArray	Effective energy at the output of the array
DiffHor	Horizontal diffuse irradiation	E_Grid	Energy injected into grid
T_Amb	Ambient Temperature	PR	Performance Ratio
GlobInc	Global incident in coll. plane		
GlobEff	Effective Global, corr. for IAM and shadings		

Figure E. 10: Balance and Main results when tilt angle is 20°

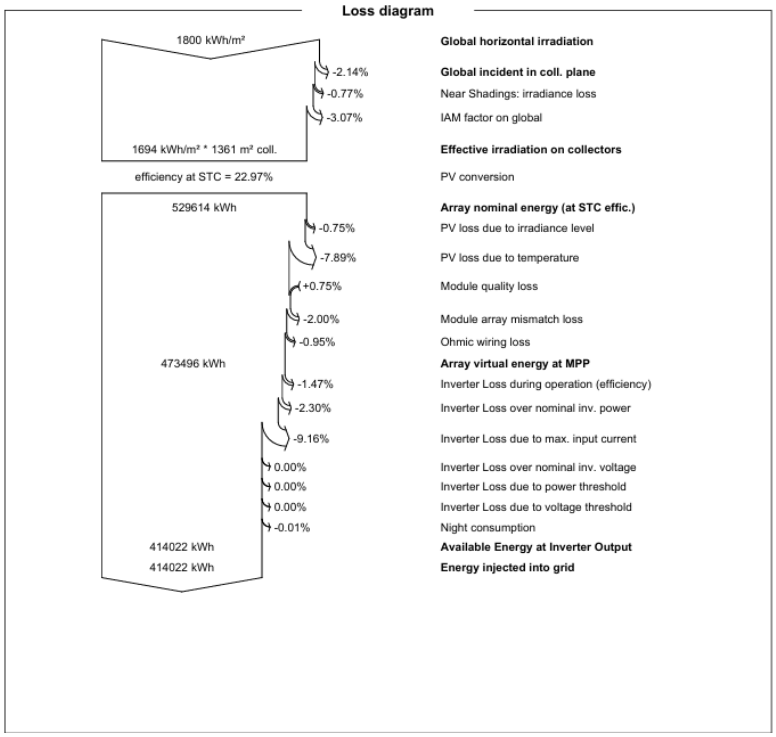

Figure E. 11: Loss Diagram when tilt angle is 20º

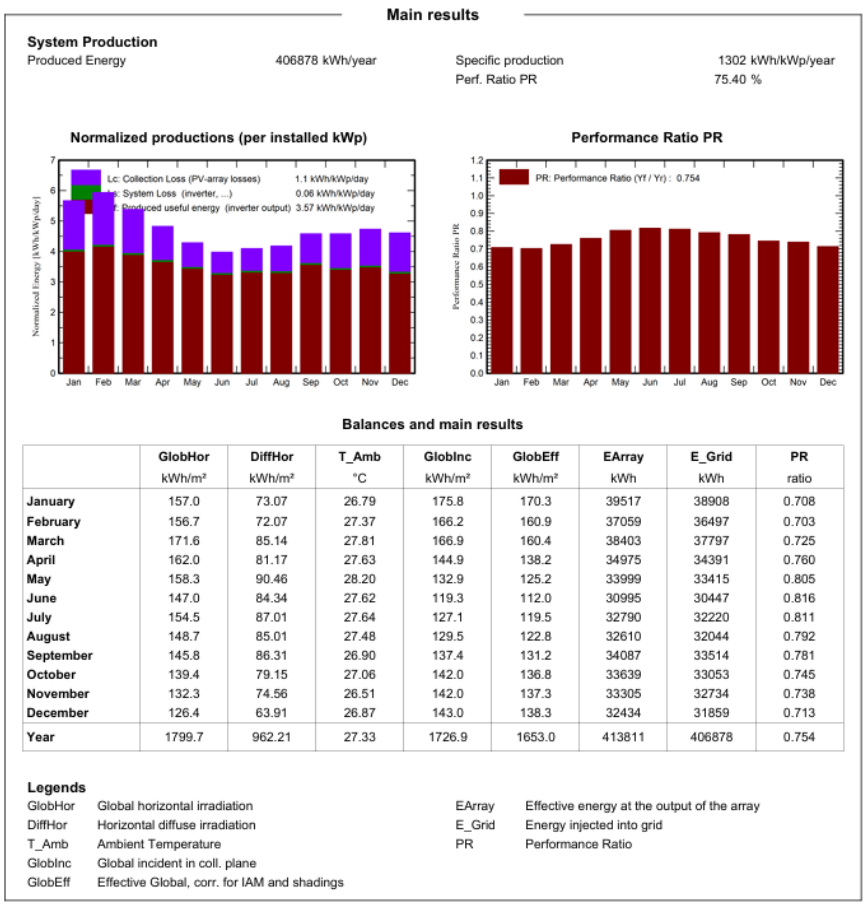

	GlobHor kWh/m²	DiffHor kWh/m²	T_Amb °C	GlobInc kWh/m²	GlobEff kWh/m²	EArray kWh	E_Grid kWh	PR ratio
January	157.0	73.07	26.79	175.8	170.3	39517	38908	0.708
February	156.7	72.07	27.37	166.2	160.9	37059	36497	0.703
March	171.6	85.14	27.81	166.9	160.4	38403	37797	0.725
April	162.0	81.17	27.63	144.9	138.2	34975	34391	0.760
May	158.3	90.46	28.20	132.9	125.2	33999	33415	0.805
June	147.0	84.34	27.62	119.3	112.0	30995	30447	0.816
July	154.5	87.01	27.64	127.1	119.5	32790	32220	0.811
August	148.7	85.01	27.48	129.5	122.8	32610	32044	0.792
September	145.8	86.31	26.90	137.4	131.2	34087	33514	0.781
October	139.4	79.15	27.06	142.0	136.8	33639	33053	0.745
November	132.3	74.56	26.51	142.0	137.3	33305	32734	0.738
December	126.4	63.91	26.87	143.0	138.3	32434	31859	0.713
Year	1799.7	962.21	27.33	1726.9	1653.0	413811	406878	0.754

Legends

GlobHor	Global horizontal irradiation	EArray	Effective energy at the output of the array
DiffHor	Horizontal diffuse irradiation	E_Grid	Energy injected into grid
T_Amb	Ambient Temperature	PR	Performance Ratio
GlobInc	Global incident in coll. plane		
GlobEff	Effective Global, corr. for IAM and shadings		

Figure E. 12: Balance and Main results when tilt angle is 25º

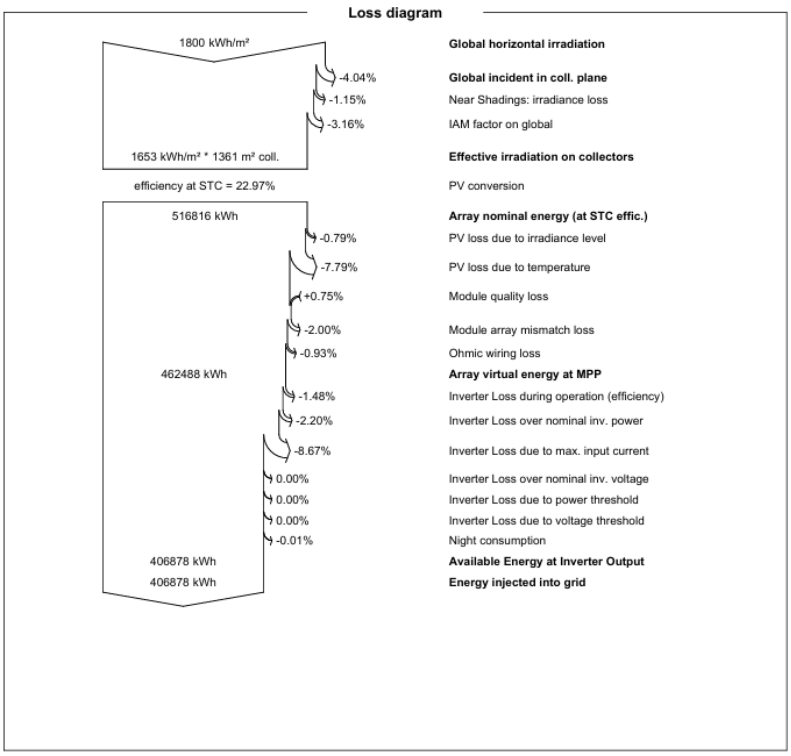

Figure E. 13: Loss Diagram when tilt angle is 25º

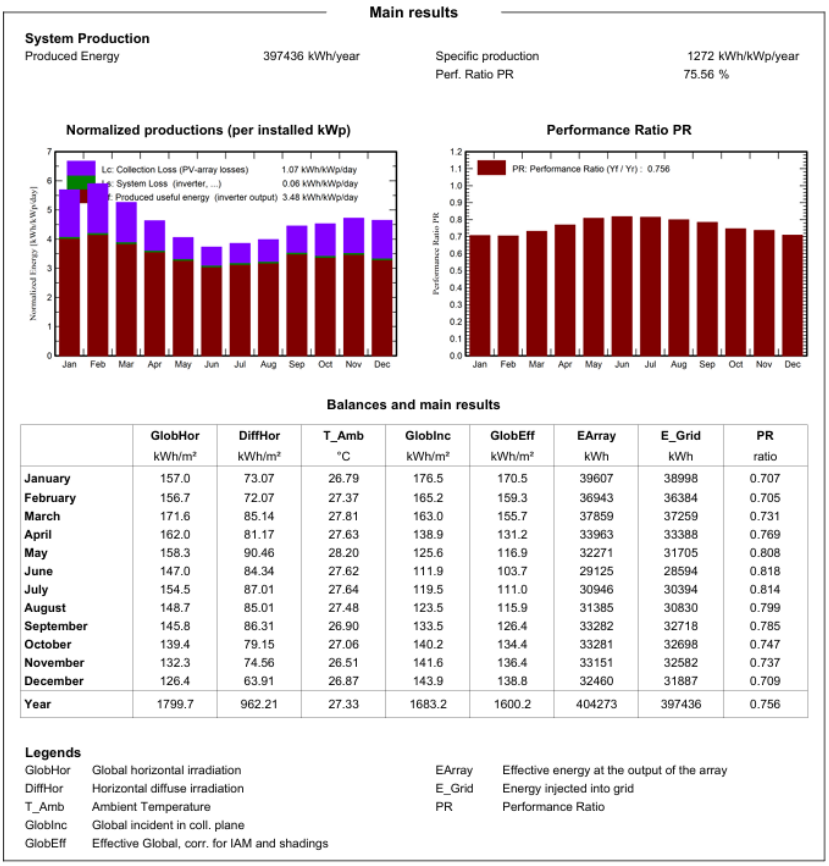

	GlobHor kWh/m²	DiffHor kWh/m²	T_Amb °C	GlobInc kWh/m²	GlobEff kWh/m²	EArray kWh	E_Grid kWh	PR ratio
January	157.0	73.07	26.79	176.5	170.5	39607	38998	0.707
February	156.7	72.07	27.37	165.2	159.3	36943	36384	0.705
March	171.6	85.14	27.81	163.0	155.7	37859	37259	0.731
April	162.0	81.17	27.63	138.9	131.2	33963	33388	0.769
May	158.3	90.46	28.20	125.6	116.9	32271	31705	0.808
June	147.0	84.34	27.62	111.9	103.7	29125	28594	0.818
July	154.5	87.01	27.64	119.5	111.0	30946	30394	0.814
August	148.7	85.01	27.48	123.5	115.9	31385	30830	0.799
September	145.8	86.31	26.90	133.5	126.4	33282	32718	0.785
October	139.4	79.15	27.06	140.2	134.4	33281	32698	0.747
November	132.3	74.56	26.51	141.6	136.4	33151	32582	0.737
December	126.4	63.91	26.87	143.9	138.8	32460	31887	0.709
Year	1799.7	962.21	27.33	1683.2	1600.2	404273	397436	0.756

Figure E. 14: Balance and Main results when tilt angle is 30º

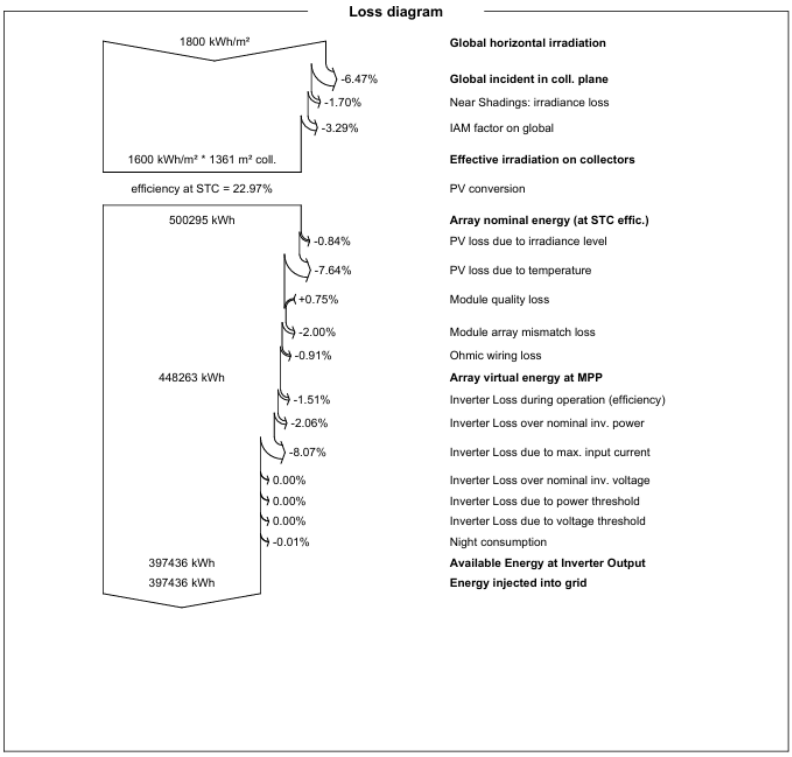

Figure E. 15: Loss Diagram when tilt angle is 30º

Appendix F: Plants's Growth Condition for 7 weeks

Table F. 1: Growth Conditions for plant 1

Plant 1					
Week	Height	Leaf	Fruit	Ave Fruit Diameter	
3	0.92	45	12	19.38	
4	0.93	27	12	20.04	
5	0.95	28	13	20.04	
6	0.945	22	13	21.44	
7	0.92	15	13	22.392	
8	0.92	14	13	23.136	
9	0.94	0	13	24.46	

Table F. 2: Growth Conditions for Plant 2

Plant 2					
Week	Height	Leaf	Fruit	Ave Fruit Diameter	
3	0.85	36	4	24.95	
4	0.845	39	4	25.775	
5	0.84	0	4	27.025	
6	0.84	22	4	27.975	
7	0.83	71	4	28.45	
8	0.83	66	3	28.4	
9	0.85	51	3	29.87	

Table F. 3: Growth Conditions for Plant 3

Plant 3					
Week	Height	Leaf	Fruit	Ave Fruit Diameter	
3	0.94	16	5	24.26	
4	0.91	27	6	24.3	
5	0.915	8	6	25.02	
6	0.92	10	6	23.74	
7	0.915	15	6	23.96	
8	0.91	0	6	24.42	
9	0.91	10	6	25.48	

Table F. 4: Growth Conditions for Plant 4

Plant 4					
Week	Height	Leaf	Fruit	Ave Fruit Diameter	
3	0.86	30	2	24.2	
4	0.87	0	2	25.2	
5	0.858	0	2	26.1	
6	0.86	6	2	26.75	
7	0.855	11	2	26.75	
8	0.85	3	2	28.05	
9	0.86	3	2	29.45	

Table F. 5: Growth Conditions for Plant 5

Plant 5					
Week	Height	Leaf	Fruit	Ave Fruit Diameter	
3	0.85	9	7	26.18	
4	0.84	45	6	26.74	
5	0.82	10	5	27.12	
6	0.8	0	5	27.4	
7	0.79	39	5	28.07	
8	0.8	49	5	28.18	
9	0.8	36	5	29.17	

Table F. 6: Growth Conditions for Plant 6

Plant 6					
Week	Height	Leaf	Fruit	Ave Fruit Diameter	
3	1	41	10	20.06	
4	1.01	43	11	20.5	
5	0.98	22	11	21.06	
6	1	0	9	23.14	
7	1.01	9	8	23.54	
8	1.03	0	7	23.4	
9	1	8	7	24.18	

Table F. 7: Plant Growing Photo Record for plant 1

Week 4	Week 5	Week 6
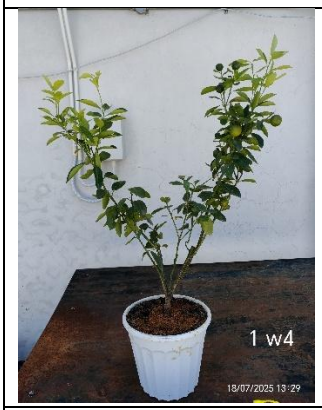		
Week 7	**Week 8**	**Week 9**
	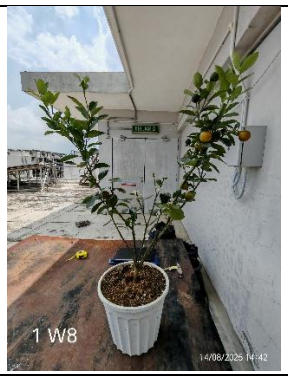	

Table F. 8: Plant Growing Photo Record for plant 2

Week 4	Week 5	Week 6
		
Week 7	**Week 8**	**Week 9**
		

Table F. 9: Plant Growing Photo Record for plant 3

Week 4	Week 5	Week 6
		
Week 7	**Week 8**	**Week 9**
		

Table F. 10: Plant Growing Photo Record for plant 4

Week 4	Week 5	Week 6
		
Week 7	**Week 8**	**Week 9**
		

Table F. 11: Plant Growing Photo Record for plant 5

Week 4	Week 5	Week 6
		
Week 7	**Week 8**	**Week 9**
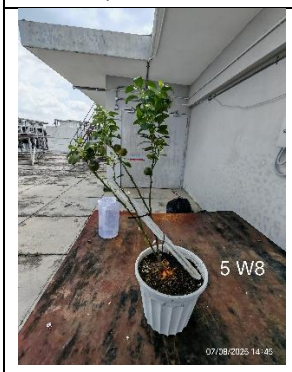		

Table F. 12: Plant Growing Photo Record for plant 6

Week 4	Week 5	Week 6
		
Week 7	**Week 8**	**Week 9**
		

Appendix G: TOPSIS Calculation

Table G. 1: AUC for each parameter for plant 1

Plant 1								
Week	Height	AOC Heigh	Leaf	AOC Leaf	Fruit	AOC Fruit	Ave Fruit l	AOC FD
3	0.92	0	45	0	12	0	19.38	0
4	0.93	0.925	27	36	12	12	20.04	19.71
5	0.95	0.94	28	27.5	13	12.5	20.04	20.04
6	0.945	0.9475	22	25	13	13	21.44	20.74
7	0.92	0.9325	15	18.5	13	13	22.392	21.916
8	0.92	0.92	14	14.5	13	13	23.136	22.764
9	0.94	0.93	0	7	13	13	24.24	23.688
		5.595		128.5		76.5		128.858

Table G. 2: AUC for each parameter for plant 2

Plant 2								
Week	Height	AOC Heigh	Leaf	AOC Leaf	Fruit	AOC Fruit	Ave Fruit l	AOC FD
3	0.85	0	36	0	4	0	24.95	0
4	0.845	0.8475	39	37.5	4	4	25.775	25.3625
5	0.84	0.8425	0	19.5	4	4	27.025	26.4
6	0.84	0.84	22	11	4	4	27.975	27.5
7	0.83	0.835	71	46.5	4	4	28.45	28.2125
8	0.83	0.83	66	68.5	3	3.5	28.4	28.425
9	0.85	0.84	51	58.5	3	3	29.87	29.135
		5.035		241.5		22.5		165.035

Table G. 3: AUC for each parameter for plant 3

Plant 3								
Week	Height	AOC Heigh	Leaf	AOC Leaf	Fruit	AOC	Ave Fruit l	AOC
3	0.94	0	16	0	5	0	24.26	0
4	0.91	0.925	27	21.5	6	5.5	24.3	24.28
5	0.915	0.9125	8	17.5	6	6	25.02	24.66
6	0.92	0.9175	10	9	6	6	23.74	24.38
7	0.915	0.9175	15	12.5	6	6	23.96	23.85
8	0.91	0.9125	0	7.5	6	6	24.42	24.19
9	0.91	0.91	10	5	6	6	25.48	24.95
		5.495		73		35.5		146.31

Table G. 4: AUC for each parameter for plant 4

Plant 4								
Week	Height	AOC	Leaf	AOC	Fruit	AOC	Ave Fruit l	AOC
3	0.86	0	30	0	2	0	24.2	0
4	0.87	0.865	0	15	2	2	25.2	24.7
5	0.858	0.864	0	0	2	2	26.1	25.65
6	0.86	0.859	6	3	2	2	26.75	26.425
7	0.855	0.8575	11	8.5	2	2	26.75	26.75
8	0.85	0.8525	3	7	2	2	28.05	27.4
9	0.86	0.855	3	3	2	2	29.45	28.75
		5.153		36.5		12		159.675

Table G. 5: AUC for each parameter for plant 5

Plant 5								
Week	Height	AOC	Leaf	AOC	Fruit	AOC	Ave Fruit l	AOC
3	0.85	0	59	0	7	0	26.18	0
4	0.84	0.845	45	52	6	6.5	26.74	26.46
5	0.82	0.83	10	27.5	5	5.5	27.12	26.93
6	0.8	0.81	0	5	5	5	27.4	27.26
7	0.79	0.795	39	19.5	5	5	28.07	27.735
8	0.8	0.795	49	44	5	5	28.18	28.125
9	0.8	0.8	36	42.5	5	5	29.17	28.68
		4.875		190.5		32		165.19

Table G. 6: AUC for each parameter for plant 6

Plant 6								
Week	Height	AOC	Leaf	AOC	Fruit	AOC	Ave Fruit l	AOC
3	1	0	41	0	10	0	20.06	0
4	1.01	1.005	43	42	11	10.5	20.5	20.28
5	0.98	0.995	22	32.5	11	11	21.06	20.78
6	1	0.99	0	11	9	10	23.14	22.1
7	1.01	1.005	9	4.5	8	8.5	23.54	23.34
8	1.03	1.02	0	4.5	7	7.5	23.4	23.47
9	1	1.015	8	4	7	7	24.18	23.79
		6.03		98.5		54.5		133.76

Sample calculations for the height norm and the norm factor of plant 1:

$$Height\ Norm = \sqrt{5.595^2 + 5.035^2 + 5.495^2 + 5.153^2 + 4.875^2 + 6.03^2}$$

$$Height\ Norm = 13.17$$

$$Norm\ factor\ for\ height\ of\ plant\ 1 = \frac{5.595}{13.17} = 0.42473$$

Positive ideal solution (A^*) and negative ideal solution (A^-):

$$A^* \ (positive\ ideal\ solution) = \ [0.1144, 0.1691, 0.1764, 0.1120]$$
$$A^- \ (negative\ ideal\ solution) = \ [0.0925, 0.0256, 0.0277, 0.0874]$$

Sample calculation of S_i^* and S_i^- for plant 1:

$$S_i^* = \sqrt{(0.1062 - 0.1144)^2 + (0.0900 - 0.1691)^2 + (0.1764 - 0.1764)^2 + (0.0874 - 0.1120)^2}$$
$$S_i^* = 0.083277$$

$$S_i^- = \sqrt{(0.1062 - 0.0925)^2 + (0.0900 - 0.0256)^2 + (0.1764 - 0.0277)^2 + (0.0874 - 0.0874)^2}$$
$$S_i^- = 0.16264$$

Sample calculation of TOPSIS value for plant 1:

$$TOPSIS\ Score\ of\ Plant\ 1 = \frac{0.16264}{0.083277 + 0.16264}$$
$$= 0.661363$$

Sample calculation of TOPSIS value for partially shaded:

$$Average\ TOPSIS\ value\ for\ partially\ shaded = \frac{0.661363 + 0.539693}{2}$$
$$= 0.600528$$

Appendix H: Shading Level of each shaded conditions

$$Shading\ of\ Partial\ Shaded = \left(1 - \frac{AVG\ PAR\ Partial\ Shaded}{AVG\ PAR\ Open\ Area}\right) \times 100\%$$

$$= \left(1 - \frac{586.29}{624.73}\right) \times 100\%$$

$$= 6.15\%$$

$$Shading\ of\ Heavy\ Shaded = \left(1 - \frac{AVG\ PAR\ Partial\ Shaded}{AVG\ PAR\ Open\ Area}\right) \times 100\%$$

$$= \left(1 - \frac{139.45}{624.73}\right) \times 100\%$$

$$= 77.68\%$$

$$Shading\ of\ Open\ Condition = \left(1 - \frac{AVG\ PAR\ Open\ condition}{AVG\ PAR\ Open\ condition}\right) \times 100\%$$

$$= \left(1 - \frac{624.73}{624.73}\right) \times 100\%$$

$$= 0\%$$

Appendix I: Simulated Crop Yielding using AquaCrop

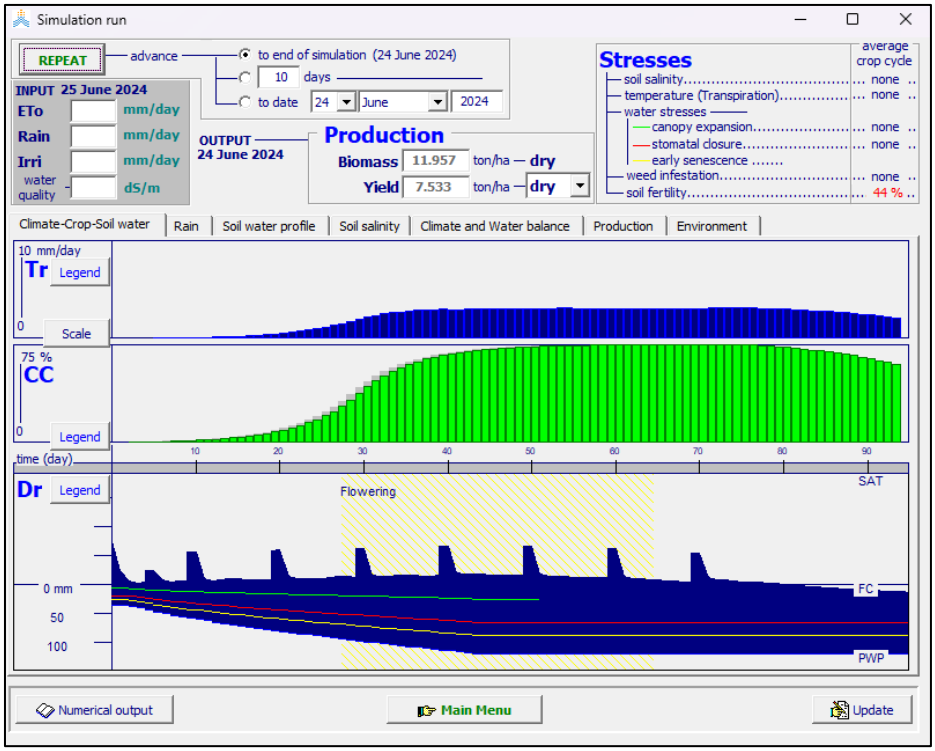

Figure I. 1: Simulated crop results for open condition

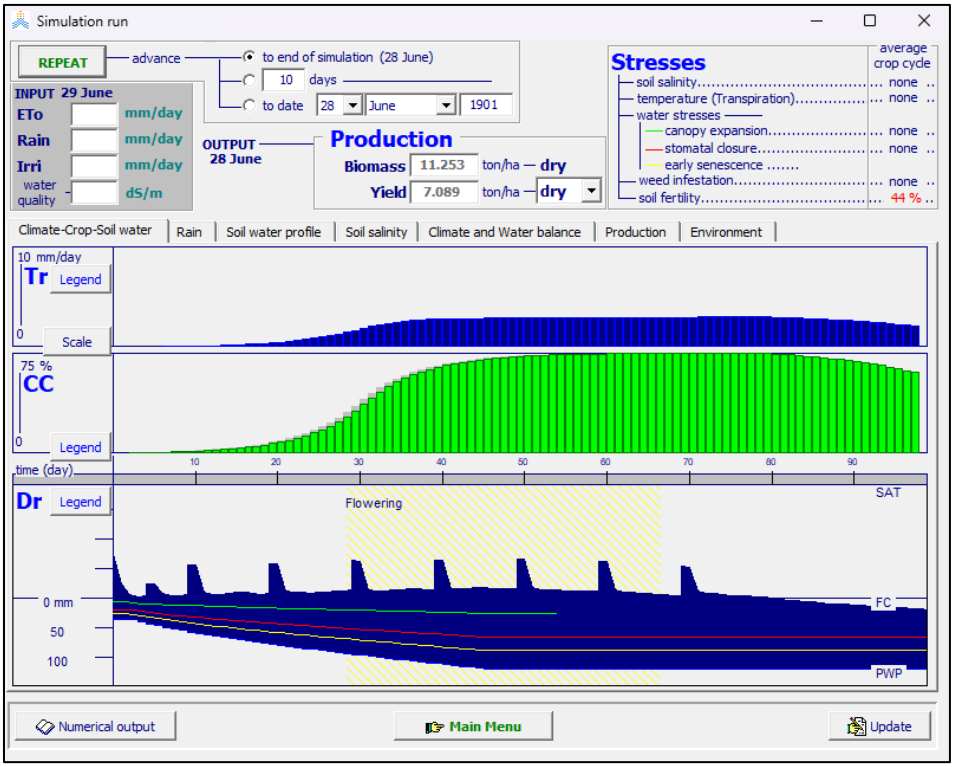

Figure I. 2: Simulated crop results for partially shaded condition

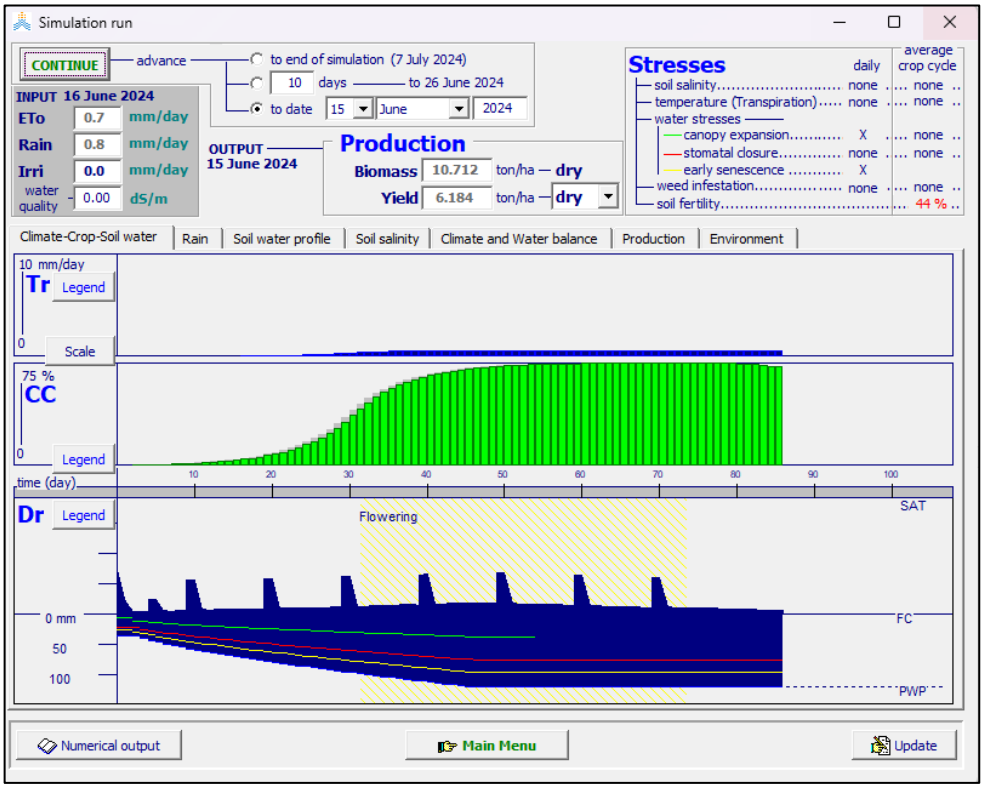

Figure I. 3: Simulated crop results for heavy shaded condition

Appendix J: LER Calculation

LER Caculation fo Full Solar Density Scenario:

$$LER\ of\ Full\ Solar\ Density$$

$$= \frac{Growth\ Performance\ of\ Crop\ - HS}{Growth\ Performance\ of\ Crop - OC} + \frac{Y_{PV}}{Y_{PV}}$$

$$= \frac{0.192202}{0.504395} + \frac{702.930 MWh/year}{702.930 MWh/year}$$

$$= 1.38$$

LER Caculation fo Half Solar Density Scenario:

$$LER\ of\ Half\ Solar\ Density$$

$$= \frac{Growth\ Performance\ of\ Crop\ - HS}{Growth\ Performance\ of\ Crop - OC} + \frac{Y_{PV-APV}}{Y_{PV}}$$

$$= \frac{0.60058}{0.504395} + \frac{330.402 MWh/year}{702.930 MWh/year}$$

$$= 1.64$$

Appendix K: Economic Calculation

Monetary return for both full solar and half solar density scenario of Solar Energy yielding:

$$Full\ Density\ PV\ revenue = 702930kWh\ x\ RM0.50$$
$$= RM351{,}465\ per\ year$$

$$Half\ Density\ PV\ revenue = 3304402kWh\ x\ RM0.50$$
$$= RM165{,}201\ per\ year$$

Passion fruits output for both full solar and half solar density scenario:

$$Partially\ Shaded\ Condition\ Revenue = RM\ 14868\ \times 0.60058$$
$$= RM\ 8929.42\ per\ year$$

$$Heavy\ Shaded\ Condition\ Revenue = RM14868\ \times 0.192202$$
$$= RM2857.66\ per\ year$$

Total revenue for full solar and half solar density scenario:

$$Revenue\ for\ full\ solar\ density$$
$$= Heavy\ Shaded\ Revenue + Full\ Density\ Revenue$$
$$= RM2857.66\ per\ year + RM351{,}465\ per\ year$$
$$= RM354{,}322.66\ per\ year$$

$$Revenue\ for\ half\ solar\ density$$
$$= Partially\ Shaded\ Revenue + Half\ Density\ Revenue$$
$$= RM\ 8929.42\ per\ year + RM165{,}201\ per\ year$$
$$= RM174{,}130.42\ per\ year$$

Appendix L: Open Access To Image Rights

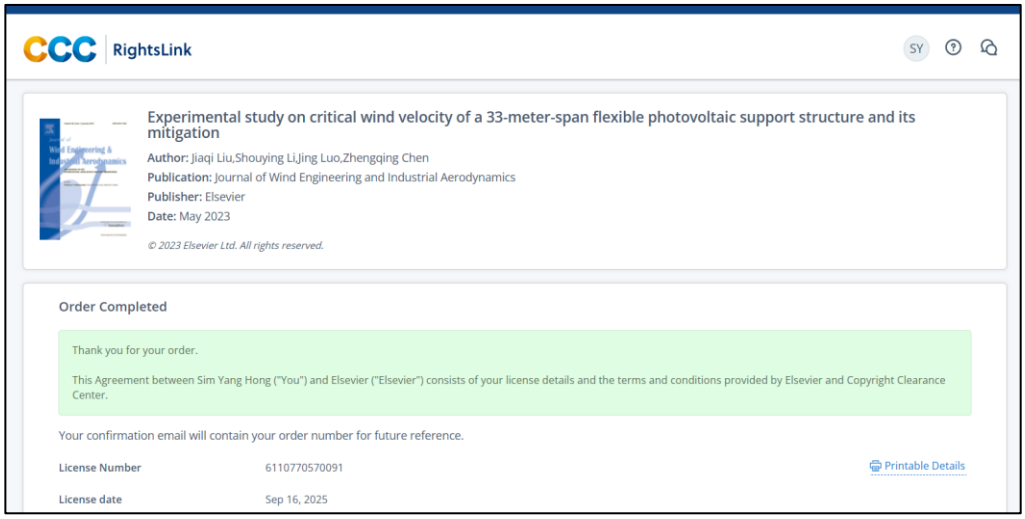

Figure L. 1: Reprinted with Permission from Copyright 2023 Elsevier to Experiment study on Critical wind load on PV structures (Liu *et al.,* 2023) in Figure 2.6 and Figure 2.7

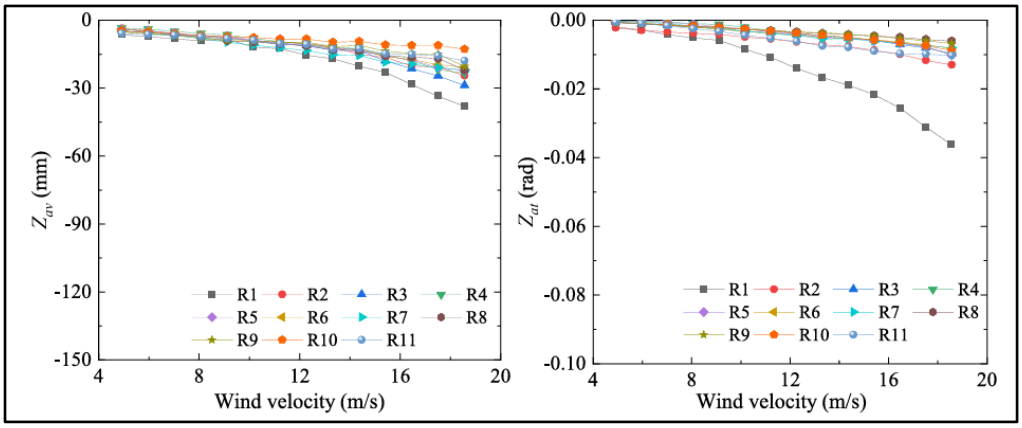

Figure 2.6: Average vertical and torsional displacement at different wind speed. (Liu *et al.*, 2023). Reprinted with permission from Copyright 2023 Elsevier.

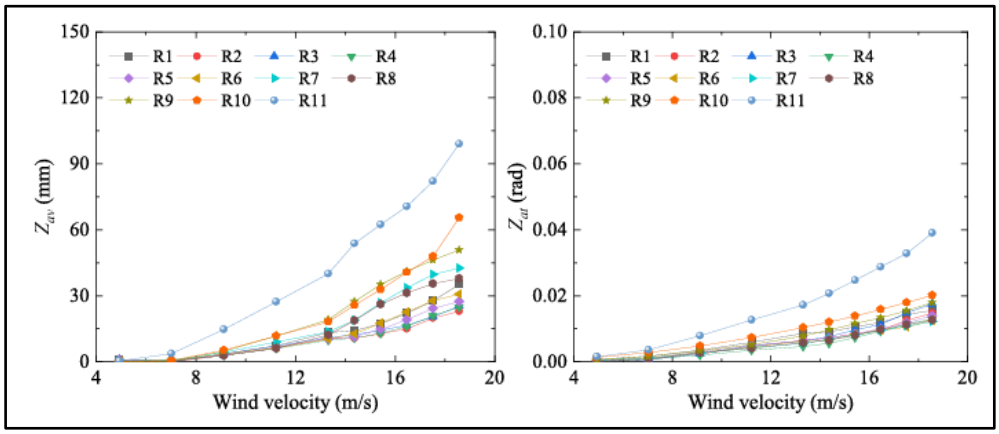

Figure 2.7: Average vertical and torsional displacement with different wind speed when wind direction equal to 180° (Liu *et al.*, 2023). Reprinted with permission from Copyright 2023 Elsevier.

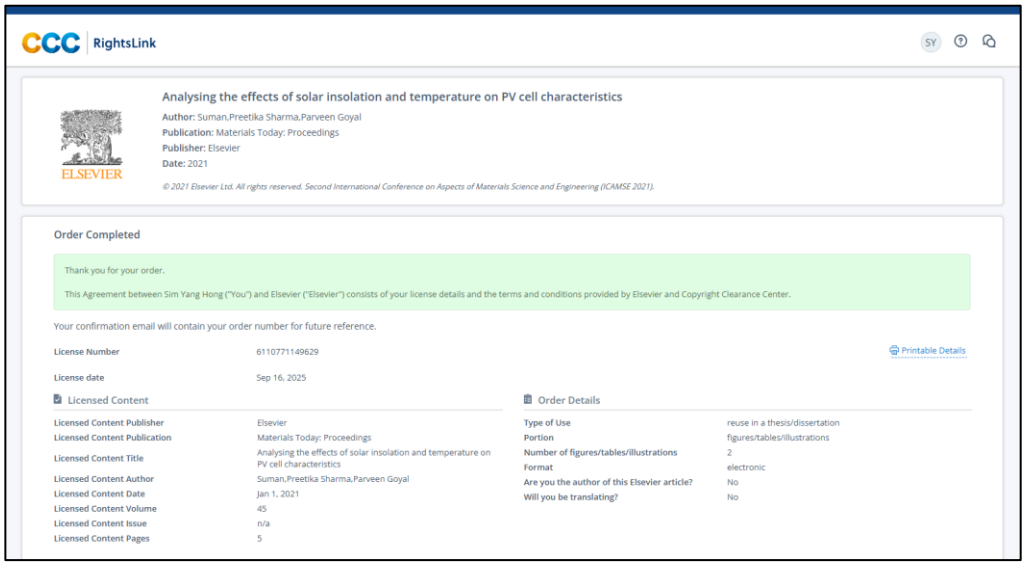

Figure L. 2: Reprinted with Permission from Copyright 2021 Elsevier to Reuse Analyzing the effect of solar irradiation and temperature on PV cell characteristics. (Suman *et al.*, 2021). Image in Figure 2.9 and Figure 3.1

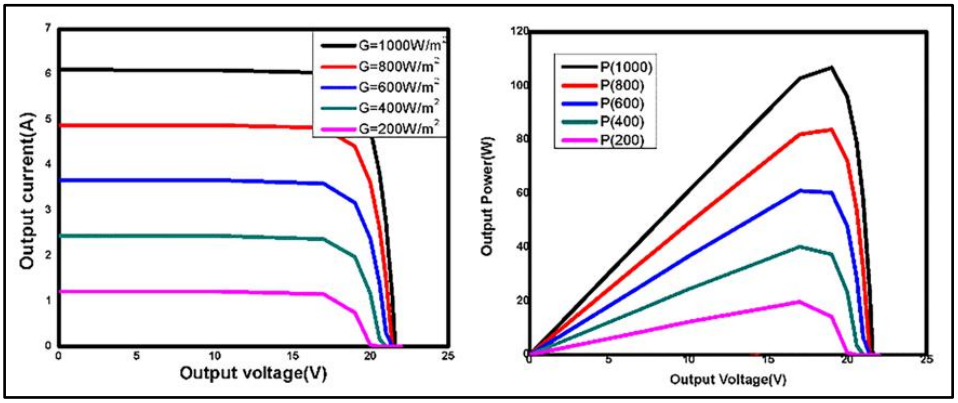

Figure 2.9: Load Current and Output Power at different irradiance (Suman et al. 2021). Reprinted with permission from Copyright 2021 Elsevier.

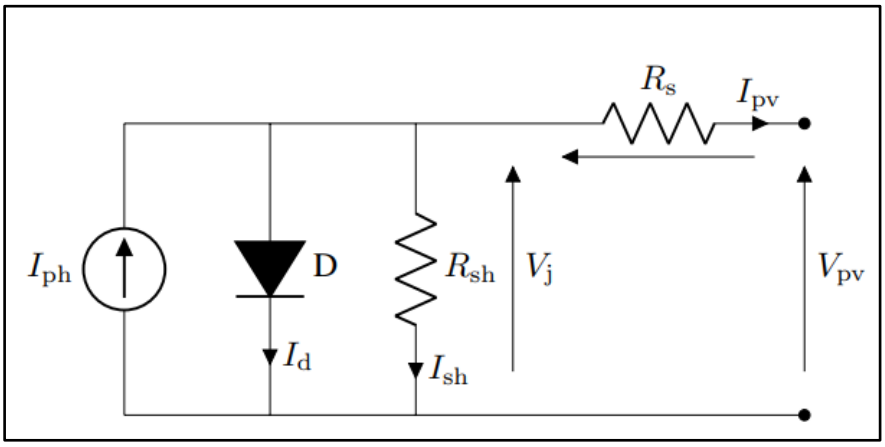

Figure 3.1: Electrical diagram of sigle-diode model (Suman et al,2021). Reprinted with permission from Copyright 2021 Elsevier.

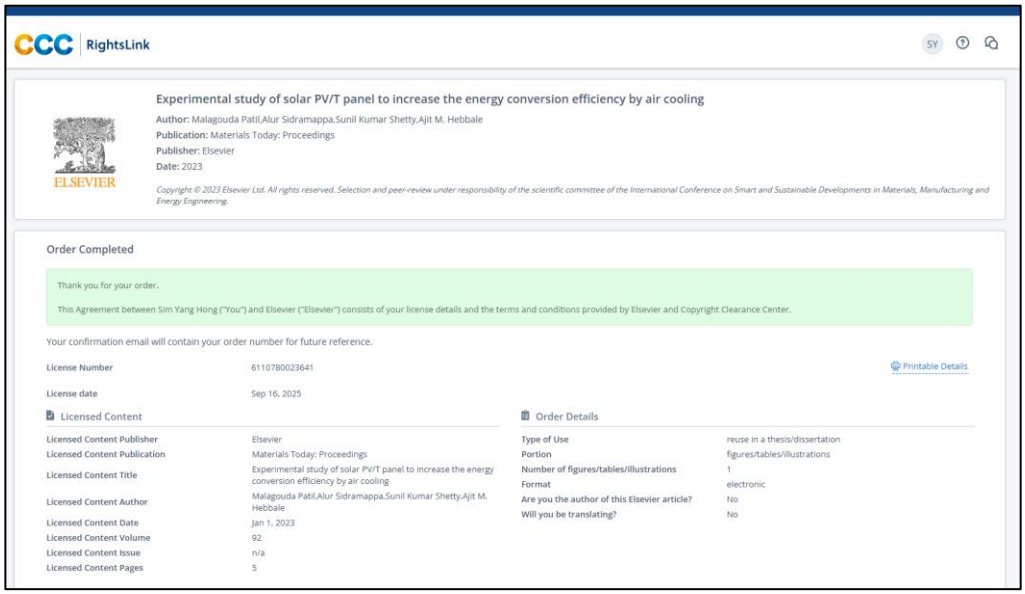

CCC RightsLink

Experimental study of solar PV/T panel to increase the energy conversion efficiency by air cooling

Author: Malagouda Patil,Alur Sidramappa,Sunil Kumar Shetty,Ajit M. Hebbale
Publication: Materials Today: Proceedings
Publisher: Elsevier
Date: 2023

Order Completed

Thank you for your order.

This Agreement between Sim Yang Hong ("You") and Elsevier ("Elsevier") consists of your license details and the terms and conditions provided by Elsevier and Copyright Clearance Center.

Your confirmation email will contain your order number for future reference.

License Number	6110780023641
License date	Sep 16, 2025

Printable Details

Licensed Content

Licensed Content Publisher	Elsevier
Licensed Content Publication	Materials Today: Proceedings
Licensed Content Title	Experimental study of solar PV/T panel to increase the energy conversion efficiency by air cooling
Licensed Content Author	Malagouda Patil,Alur Sidramappa,Sunil Kumar Shetty,Ajit M. Hebbale
Licensed Content Date	Jan 1, 2023
Licensed Content Volume	92
Licensed Content Issue	n/a
Licensed Content Pages	5

Order Details

Type of Use	reuse in a thesis/dissertation
Portion	figures/tables/illustrations
Number of figures/tables/illustrations	1
Format	electronic
Are you the author of this Elsevier article?	No
Will you be translating?	No

Figure L. 3: Reprinted with Permission from Copyright 2023 Elsevier to Reuse Experiment stdy os solar PV/T panels to increase the energy conversion efficiency by air cooling. (Patil *et al.*, 2023) Image in Figure 2.14

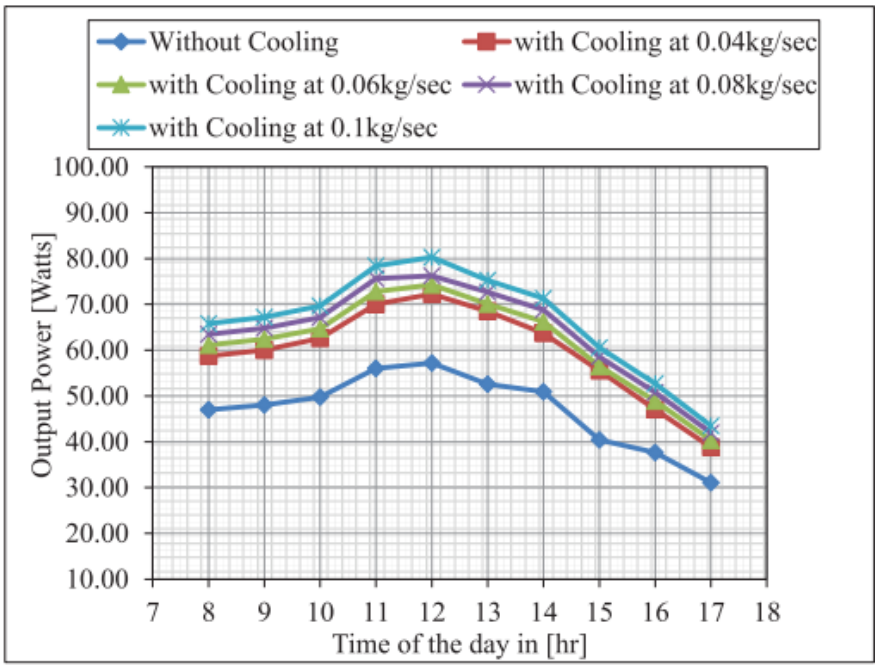

Figure 2.14: Output power versus time of day at various mass flow rates (Patil et al, 2023). Reprinted with permission from Copyright 2023 Elsevier.

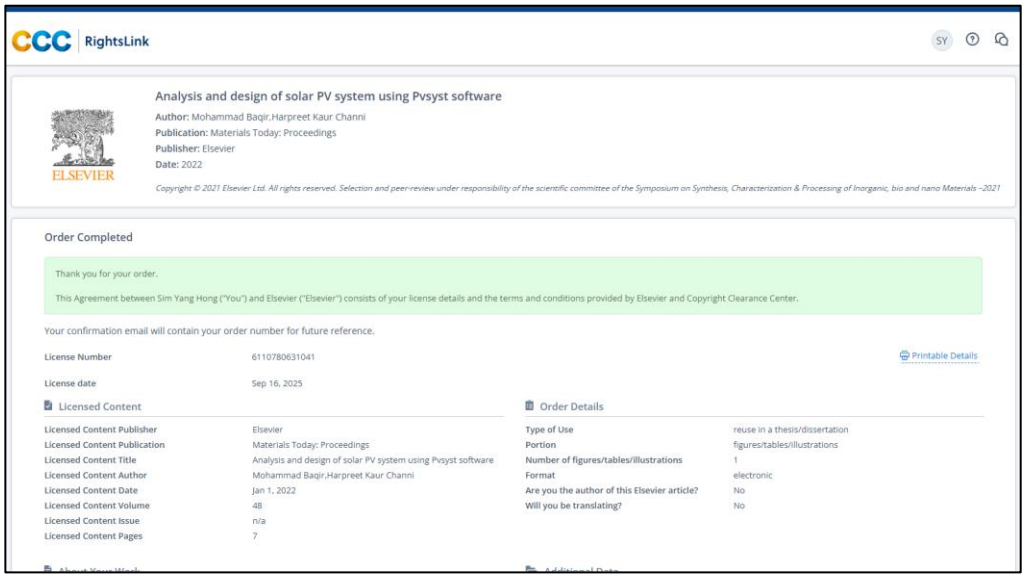

Figure L. 4: Reprinted with Permission from Copyright 2022 Elsevier to Analysis and design os solar PV system using PVsyst software (Patil *et al.*, 2022) Image in Figure 2.15 and Table 2.1

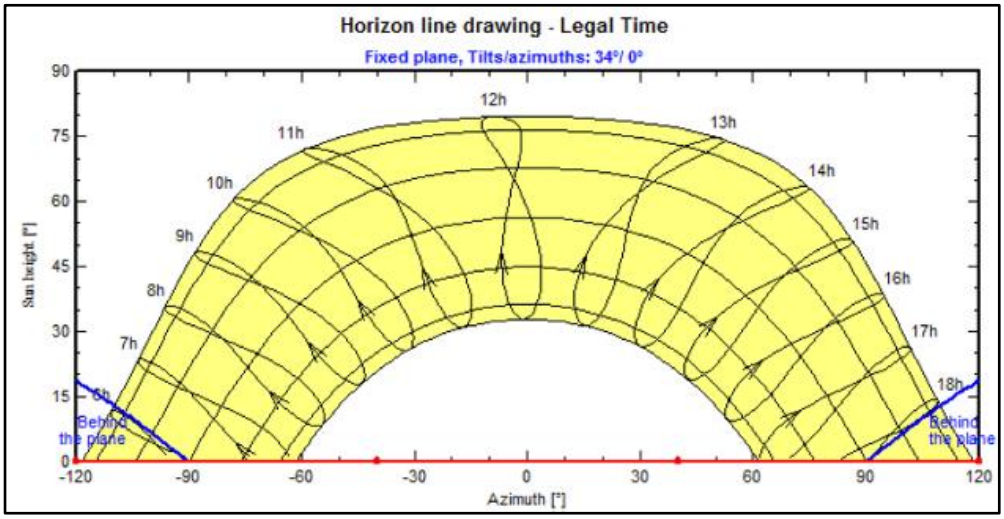

Figure 2.15: Sun Path in Arghanistan (Baqir & Channi, 2022). Reprinted with permission from Copyright 2022 Elsevier.

Month	GlobHor kWh/m^2	DiffHor kWh/m^2	T_Amb °C	GlobInc kWh/m^2	GlobEff kWh/m^2	EArray MWh	E_Grid MWh	PR Ratio
January	87.8	33.23	1.98	136.0	127.3	83.7	81.9	0.859
February	105.3	39.69	5.04	145.0	136.2	88.6	86.8	0.853
March	141.6	54.60	10.34	167.5	156.6	98.4	96.4	0.820
April	170.6	63.69	15.41	177.7	165.3	101.5	99.5	0.798
May	217.8	62.30	20.76	202.3	187.9	111.8	109.6	0.772
June	242.8	56.28	22.83	212.6	197.2	116.2	113.9	0.763
July	249.4	53.29	22.93	224.5	208.6	122.6	120.1	0.762
August	219.1	52.81	21.81	218.2	203.4	119.8	117.5	0.767
September	201.2	43.87	18.88	231.6	217.1	127.5	125.1	0.769
October	160.5	34.48	14.18	221.4	209.1	126.0	123.6	0.796
November	108.0	30.06	7.55	169.2	159.0	100.0	98.1	0.826
December	93.7	25.50	3.44	158.3	148.3	95.3	93.4	0.840
Year	1997.8	549.80	13.81	2264.1	2116.0	1291.4	1266.1	0.797

Table 2.1: Solar Irradiation and power output data (Baqir & Channi, 2022). Reprinted with permission from Copyright 2022 Elsevier.

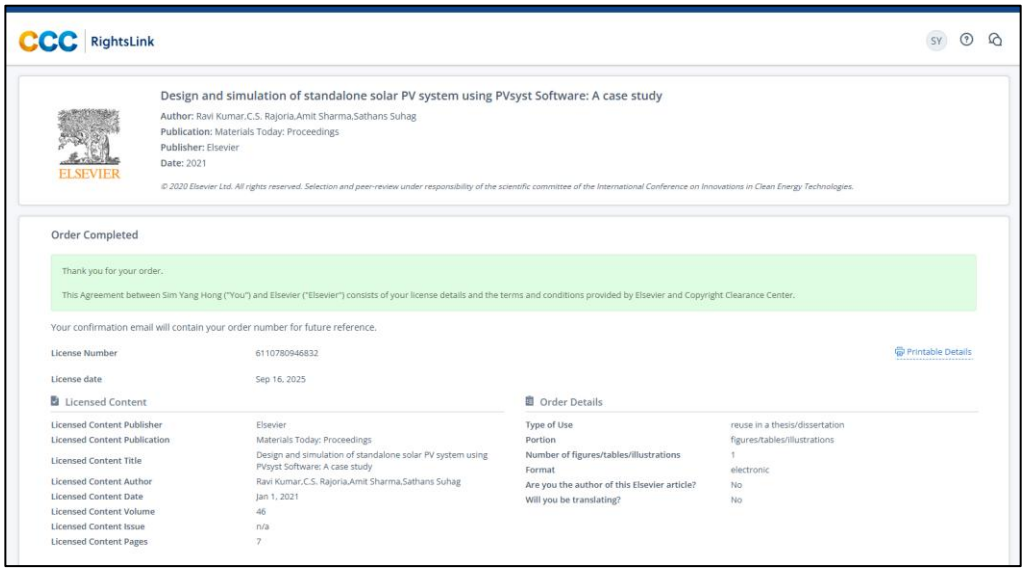

Figure L. 5: Reprinted with Permission from Copyright 2021 Elsevier to Design and simulation of standalone solar PV system using PVsyst Software: A case study (Kumar *et al.*, 2021) Image in Figure 2.16

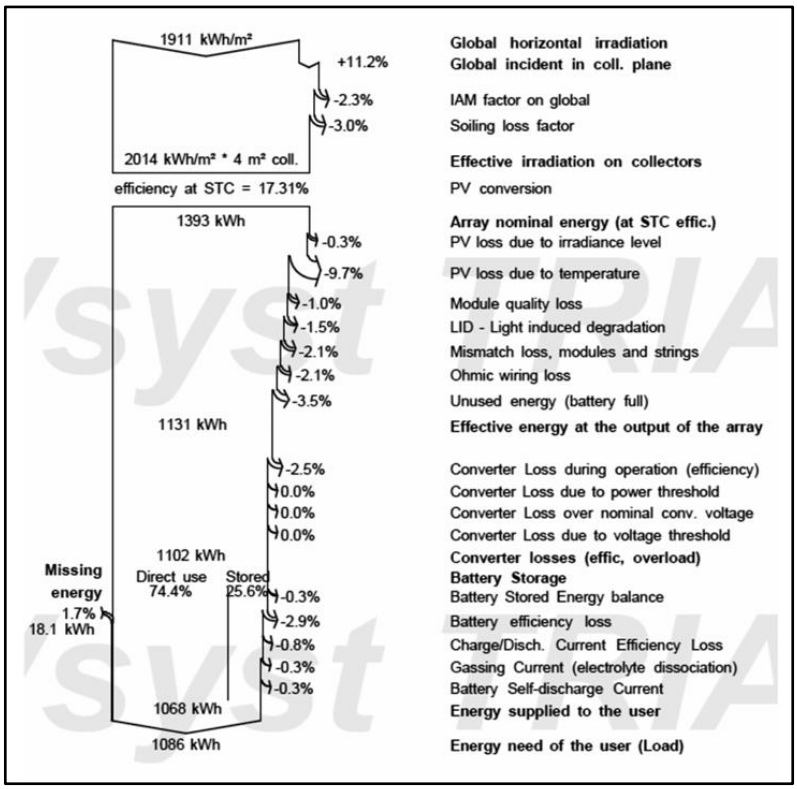

Figure 2.16: Loss Diagram (Kumar *et al*, 2021). Reprinted with permission from Copyright 2021 Elsevier.

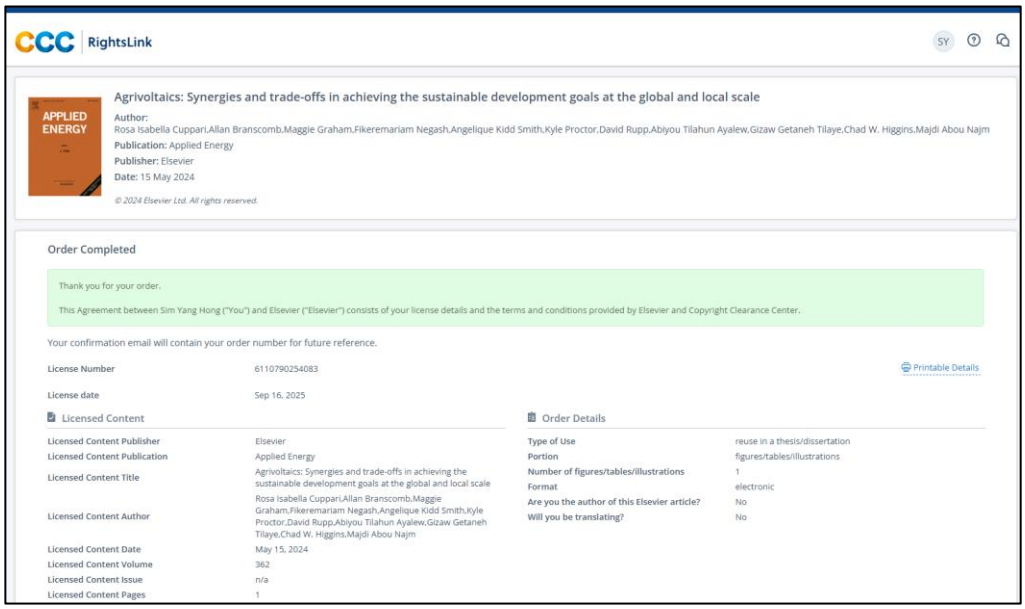

Figure L. 6: Reprinted with Permission from Copyright 2024 Elsevier to Agrivoltaics: Synergies and trade-offs in achieving the sustainable development goals at the global and local scale (Cuppari *et al.*, 2024) Image in Figure 2.23

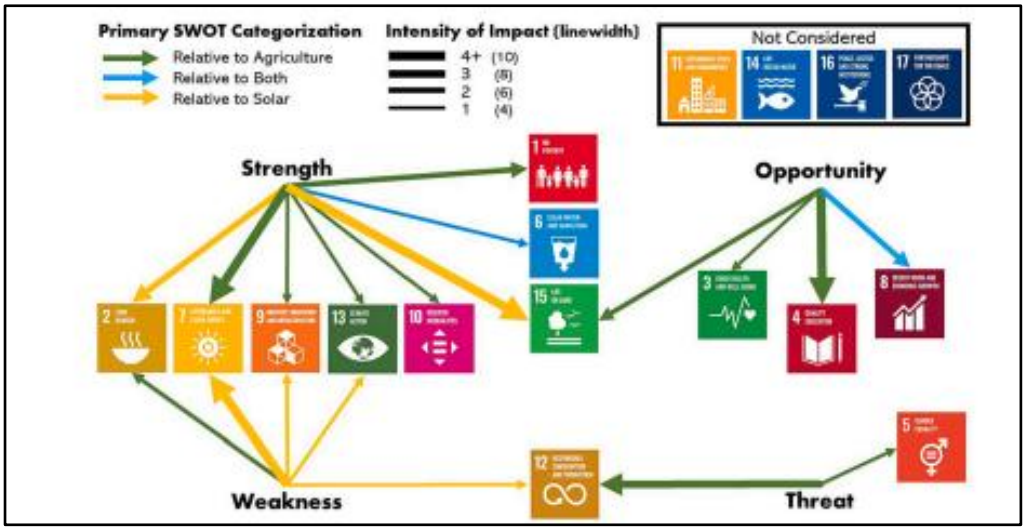

Figure 2.23: SWOT analysis for agrivoltaincs (Cuppari *et al*, 2024). Reprinted with permission from Copyright 2024 Elsevier.

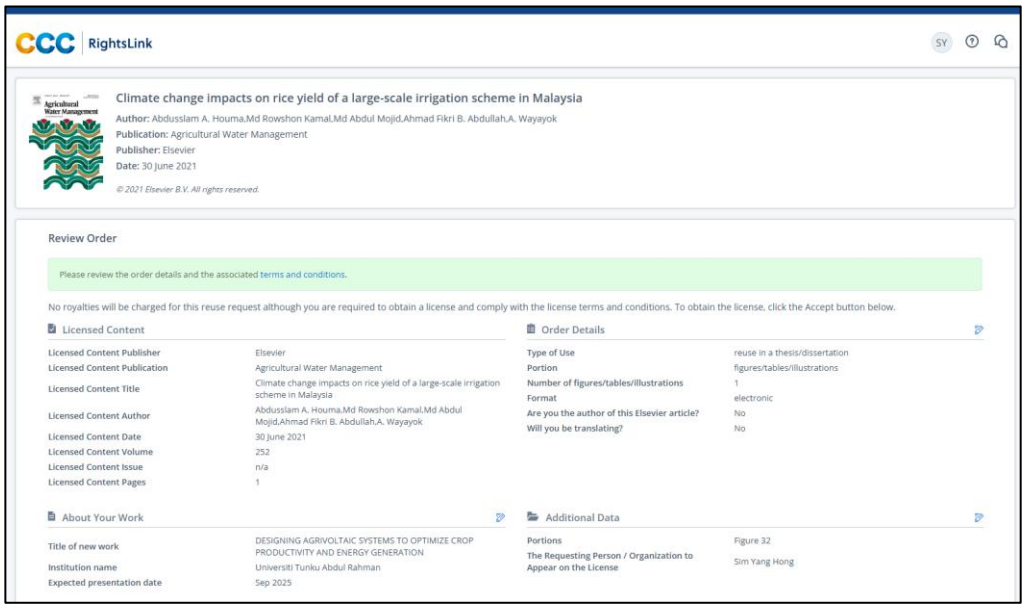

Figure L. 7: Reprinted with Permission from Copyright 2021 Elsevier to Climate change impacts on rice yield of a large scale Irrigation scheme in Malaysia (Houma *et al.*, 2021) Image in Figure 3.2

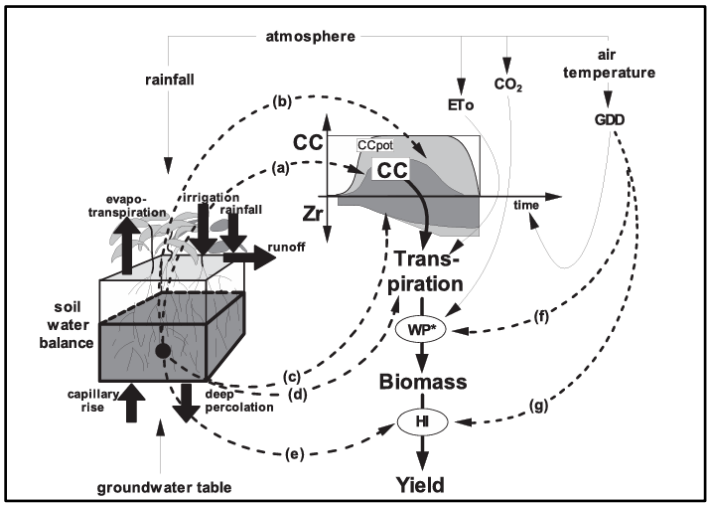

Figure 3.2: Calculation scheme for AquaCrop (Houma et al, 2021). Reprinted with permission from Copyright 2021 Elsevier.